

REVIEW

# Recent advances in developing small-molecule inhibitors against SARS-CoV-2



Rong Xiang<sup>a,†</sup>, Zhengsen Yu<sup>a,†</sup>, Yang Wang<sup>a,†</sup>, Lili Wang<sup>b</sup>,  
Shanshan Huo<sup>a</sup>, Yanbai Li<sup>a</sup>, Ruiying Liang<sup>a</sup>, Qinghong Hao<sup>a</sup>,  
Tianlei Ying<sup>c</sup>, Yaning Gao<sup>d,\*</sup>, Fei Yu<sup>a,\*</sup>, Shibo Jiang<sup>c,\*</sup>

<sup>a</sup>College of Life Sciences, Hebei Agricultural University, Baoding 071001, China

<sup>b</sup>Research Center of Chinese Jujube, Hebei Agricultural University, Baoding 071001, China

<sup>c</sup>Key Laboratory of Medical Molecular Virology (MOE/NHC/CAMS), School of Basic Medical Sciences, Shanghai Institute of Infectious Diseases and Biosecurity, Fudan University, Shanghai 200032, China

<sup>d</sup>Beijing Pharma and Biotech Center, Beijing 100176, China

Received 20 March 2021; received in revised form 13 June 2021; accepted 23 June 2021

## KEY WORDS

SARS-CoV-2;  
COVID-19;  
Therapeutic;  
Prophylactic;  
Small-molecule inhibitors

**Abstract** The COVID-19 pandemic caused by the novel SARS-CoV-2 virus has caused havoc across the entire world. Even though several COVID-19 vaccines are currently in distribution worldwide, with others in the pipeline, treatment modalities lag behind. Accordingly, researchers have been working hard to understand the nature of the virus, its mutant strains, and the pathogenesis of the disease in order to uncover possible drug targets and effective therapeutic agents. As the research continues, we now know the genome structure, epidemiological and clinical features, and pathogenic mechanism of SARS-CoV-2. Here, we summarized the potential therapeutic targets involved in the life cycle of the virus. On the basis of these targets, small-molecule prophylactic and therapeutic agents have been or are being developed for prevention and treatment of SARS-CoV-2 infection.

© 2022 Chinese Pharmaceutical Association and Institute of Materia Medica, Chinese Academy of Medical Sciences. Production and hosting by Elsevier B.V. This is an open access article under the CC BY-NC-ND license (<http://creativecommons.org/licenses/by-nc-nd/4.0/>).

\*Corresponding authors. Tel.: +86 21 54237673, fax: +86 21 54237465 (Shibo Jiang); Tel.: +86 312 7528935, fax: +86 312 7521283 (Fei Yu); Tel.: +86 10 62896868; fax: +86 10 62899978, (Yanning Gao).

E-mail addresses: [gyn9225@bjmu.edu.cn](mailto:gyn9225@bjmu.edu.cn) (Yanning Gao), [shmyf@hebau.edu.cn](mailto:shmyf@hebau.edu.cn) (Fei Yu), [shibojiang@fudan.edu.cn](mailto:shibojiang@fudan.edu.cn) (Shibo Jiang).

†These authors made equal contributions to this work.

Peer review under responsibility of Chinese Pharmaceutical Association and Institute of Materia Medica, Chinese Academy of Medical Sciences.

## 1. Introduction

In 2019, a new infectious respiratory disease emerged. A novel coronavirus was identified as the pathogen causing the outbreak of atypical pneumonia<sup>1,2</sup> and given a nomenclature of 2019 novel coronavirus (2019-nCoV) by the World Health Organization (WHO). The International Committee on Taxonomy of Viruses (ICTV) renamed the virus as severe acute respiratory syndrome coronavirus-2 (SARS-CoV-2) and the disease as coronavirus disease 2019 (COVID-19)<sup>7</sup>. Some virologists suggested changing the name to human coronavirus 2019 (HCoV-19) to avoid confusion with SARS-CoV that emerged in 2002<sup>3</sup>.

SARS-CoV-2 belongs to the genus betacoronavirus, together with SARS-CoV and Middle East respiratory syndrome coronavirus (MERS-CoV, with 82% and 50% homology, respectively)<sup>4–6</sup>. The main symptoms of COVID-19 include fever, fatigue, dry cough, upper chest discomfort and dyspnea. Severe cases are reported to show sepsis, secondary infections and organ failure. By 22 June 2021, COVID-19 had spread to more than 223 countries with more than 178,360,849 confirmed cases reported globally, including more than 3,869,384 deaths (<https://www.who.int/emergencies/diseases/novel-coronavirus-2019>). On 30 January 2020, WHO declared the COVID-19 outbreak to be a global public health emergency, and on 11 March 2020, WHO characterized COVID-19 as a pandemic<sup>1</sup>. While several COVID-19 vaccines have been approved for general or emergency use, no specific antiviral drugs are now available for prophylaxis or treatment of SARS-CoV-2<sup>19,244</sup>. Therefore, it is still urgently needed to develop effective prophylactics and therapeutics against SARS-CoV-2 infection. Here, we summarized the potential therapeutic targets involved in the life cycle of the virus, treatments now in clinical use, the progress of candidate drugs, and potential prophylactic and therapeutic drugs based on these targets to treat COVID-19 in the future.

## 2. Viral structure

SARS-CoV-2 is an enveloped virus with a positive-sense, single-stranded RNA [(+)-ssRNA] genome of ~30 kb<sup>8</sup> (Fig. 1). Upon cell entry, genomic RNA is translated as either ORF1a or ORF1ab owing to a frame shift, which is then cleaved into nonstructural proteins (nsps) by viral proteinases. These nsps are mainly responsible for the replication and transcription of genomic RNA. A series of subgenomic RNAs (sgRNAs) are discontinuously transcribed and finally translated into structural proteins [spike protein (S), envelope protein (E), membrane protein (M), and nucleocapsid protein (N)], and several accessory proteins (3a, 3b, 6, 7a, 7 b, 8, 9b, 9c and 10)<sup>8,9</sup>. A lipid bilayer comprising the S protein, the M protein and the E protein cloaks the helical nucleocapsids, consisting of the N protein that is associated with the viral RNA (Fig. 1).

## 3. SARS-CoV-2 life cycle and potential targets for the development of small-molecule inhibitors against SARS-CoV-2 infection

SARS-CoV-2 enters the target cell through two different ways, either plasma or endosomal membrane fusion (Fig. 2). The S protein of SARS-CoV-2 mediates the attachment of virus to the membrane of the host cell through its interaction with angiotensin-converting enzyme 2 (ACE2) and cellular heparan sulfate as the entry receptors, respectively<sup>10,11</sup>. For plasma

membrane fusion, the S protein can be activated by transmembrane protease serine 2 (TMPRSS2) in close proximity to the ACE2 receptor, which initiates fusion between the viral membrane and the plasma membrane. In the absence of TMPRSS2, SARS-CoV-2 can be internalized *via* endocytosis<sup>10</sup>. After the virus enters the cell *via* the endocytic pathway, a lysosome-mediated drop in pH occurs in the endosome. The low pH environment activates endosomal proteinases, such as cathepsin B/L, which activate the S protein and prepares the virus for subsequent steps of fusion<sup>10,12</sup>.

After membrane fusion, either with the host cell membrane or the endosome membrane, the viral (+)-sense genomic RNA [(+)-gRNA] is released into the cytoplasm to allow translation of the two polyproteins, pp1a and 1 ab. Autoproteolytic cleavage of polyproteins produces more than a dozen nsps<sup>13</sup>, including papain-like protease (PLpro), 3C-like protease (3CLpro), RNA-dependent RNA polymerase (RdRp) and helicase. Of these, PLpro and 3CLpro are responsible for polyprotein cleavage. And some nsps use (+) gRNA as a template to form a replicase-transcriptase complex.

After generating (−)-sense genomic RNA [(-) gRNA], it can serve as the template for the synthesis of (+) gRNA, which becomes the genome of the new virus particle<sup>13,14</sup>. Transmembrane structural proteins (S, M and E) undergo a series of steps in the endoplasmic reticulum (ER) including being synthesized, inserted and folded, and finally transported to the ER-Golgi intermediate compartment (ERGIC)<sup>15</sup>. The N proteins are translated in the cytoplasm and encapsulate (+) gRNA to form nucleocapsids<sup>16</sup>. Virion assembly occurs in the ERGIC, and virions are then transported from the ERGIC through the Golgi apparatus to the cell surface *via* small vesicles<sup>16</sup>.

Potential small-molecule anti-SARS-CoV-2 drugs can be divided into two categories, depending on the targets. The first class of inhibitors target the viral proteins, such as S protein, viral enzymes (PLpro, 3CLpro, RdRp and helicase)<sup>17–20</sup>, and some structural proteins<sup>21,22</sup> (Fig. 2 and Table 2). The second class of inhibitors can interact with the host proteins, such as the receptor ACE2 or heparan sulfate, the serine protease TMPRSS2, or the endosomal acid protease cathepsin L to prevent viral entry<sup>10,23,24</sup>, as well as some regulators of the human immune system signaling pathways required for virus replication and infection<sup>25,26</sup> (Fig. 2 and Table 3).

## 4. Strategies for developing small-molecule SARS-CoV-2 inhibitors

Based on individual approaches used for the discovery of anti-SARS-CoV-2 agents, strategies can be divided into three major categories. The first one is virtual screening. Cryo-electron microscopy, X-ray crystallography, as well as homology modeling, could provide various efficacious protein structures, promoting molecular docking for rapid identification of hit or lead compounds through screening free or commercially accessible databases, such as ZINC, DrugBank, or ChemDiv. This approach is effective, economical, and time-saving. The second approach is the experiment-based high-throughput screening (HTS). Similar to virtual screening, the first objective of HTS is to identify active small molecules within compound libraries, including approved drugs, clinical trial drug candidates and even in-house compound databases. This method, which screens a large number of compounds against a known drug target, is also a time-consuming and expensive process with no guarantee of success. The third strategy

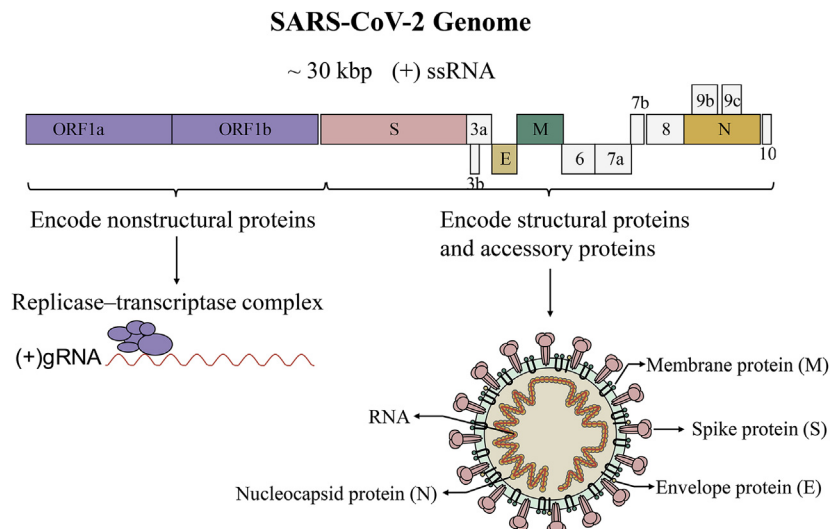


**Figure 1** Schematic diagram of genome composition and particle structure of SARS-CoV-2. SARS-CoV-2 genome consists of open reading frames (ORFs) expressing structural proteins including spike protein (S), envelope protein (E), membrane protein (M), and nucleocapsid protein (N), and ORFs1a, 1 b, etc. Expressing non-structural and accessory proteins. Among them, N protein and (+) ssRNA form nucleocapsids with three other structural proteins to form mature viral particles.

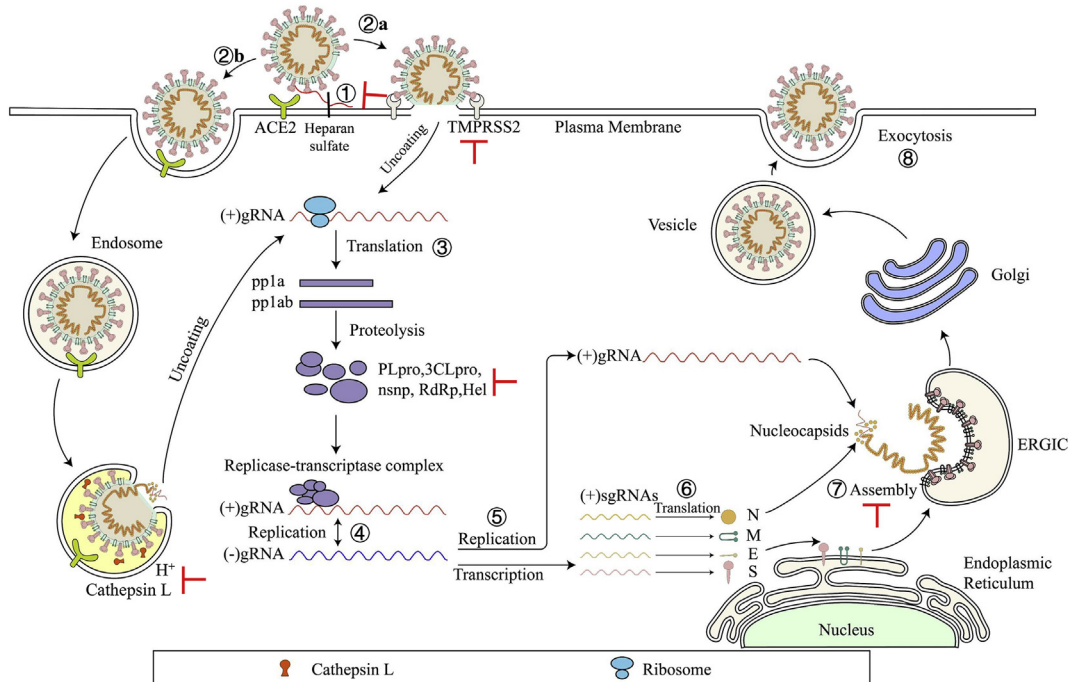


**Figure 2** Life cycle of SARS-CoV-2. SARS-CoV-2 first binds, *via* its S protein, to the receptor ACE2 on the target cell (①). Then, the virus must gain access to the host cell cytosol through plasma (②a) or endosomal membrane fusion (②b). This is assisted by activation of S protein by TMPRSS2 (②a) or cathepsin B/L (②b), followed by fusion of the viral and cellular membranes. The viral genome is released, uncoated and translated into viral replicase polyproteins pp1a and 1 ab (③), which are then cleaved into nonstructural proteins (nsps) by viral proteinases as papain-like protease (PLpro) and 3C-like protease (3CLpro). Many of these nsps are RNA-dependent RNA polymerase (RdRp) or Helicase (Hel) which then assemble into the replicase-transcriptase complex which replicates the (+)-sense genomic RNA ((+) gRNA). (−)-sense genomic RNA ((-) gRNA) is synthesized and used as a template to form (+) gRNA and subgenomic RNAs (sgRNAs) (⑤). The viral structural proteins, S, E, and M are translated from sgRNAs (⑥) and inserted into the endoplasmic reticulum (ER), from where they are transported to the ER–Golgi intermediate compartment (ERGIC) to interact with the (+) gRNA-encapsulated N proteins and assemble into viral particles (⑦). The budded vesicles containing mature viral particles are then transported to the cell surface for release after maturation in the Golgi bodies (⑧). Possible targets for inhibitors are marked in red.

**Table 1** Summary of peptide-based SARS-CoV-2 inhibitors.

Peptide	Sequence	Testing model	Activity IC <sub>50</sub> (μmol/L)	Toxicity CC <sub>50</sub> (μmol/L)	Clinical information	Ref.
EK1	SLDQINVTFLDLEYEMKKLEEA IKKLEESYIDLKEL	<i>In vitro</i>	2.468	—	Preclinical	45
EK1C4	SLDQINVTFLDLEYEMKKLEEA IKKLEESYIDLKELGSGSG-PEG4 (cholesterol)	<i>In vitro</i>	0.0365	≥5	Preclinical	45
IPB02	ISGINASVVNIQKEIDRLNEVAKNLNE SLIDLQELK (cholesterol)	<i>In vitro</i> (pseudovirus)	0.08 ± 0.017	—	Preclinical	49
SARS-CoV-2-HR2P (aa 1168–1203)	DISGINASVVNIQKEIDRLNEVAKNLN ESLIDLQEL	<i>In vitro</i> (pseudovirus)	0.98	—	Preclinical	50
[SARS <sub>HRC</sub> -PEG <sub>4</sub> ] <sub>2</sub> -chol	[DISGINASWNIQKEIDRLNEVAKNLNE SLIDLQEL-PEG4]2-chol	<i>In vivo</i>	~0.005	>100	Preclinical	51
SBP1	IEEQAKTFLDKFNHEADLFYQS	—	—	—	Preclinical	52
AHB1	DEDLEELERLYRKAEEVAKEAKDASRR GDDERAKEQMERAMRLFDQVFEL AQELQEKTQDGQRQKATHLDKAVKE AADELYQRVRELEEQVMHVLDQVSELAH ELLHKLGEELERAAYFNWWATEMMLEL IKSSDEREIREIEEARRILEHLEELARK	<i>In vitro</i>	0.035	—	Preclinical	53
AHB2	ELEEQVMHVLDQVSELAHLLHKLTGEELE RAAYFNWWATEMMLELIKSDDEREIR EIEEEARRILEHLEELARK	<i>In vitro</i>	0.016	—	Preclinical	53
LCB1	DKEWLQKIYEIMRLDELGHAEASMRVSD LIYEFMKGDERLLEEAERLLEEVER	<i>In vitro</i>	0.000024	—	Preclinical	53
LCB3	NDDELHMLMTDLVYEAHLFAKDEEIKKRVF QLFELADKAYKNNDRQKLEKVVEEL KELLERLLS	<i>In vitro</i>	0.000048	—	Preclinical	53
ATN-161	Ac-PHSCN-NH2	<i>In vitro</i>	3.16	>1000	Preclinical	54
SARS-BLOCK Peptide 5	Unknown	<i>In vitro</i> (pseudovirus)	Sub-micromolar	<20	Preclinical	57
P9	NGAICWGCPCTAFRQIGNCGHFKVRCCKIR	<i>In vitro</i>	2.4 μg/mL	—	Preclinical	184
P9R	NGAICWGCPCTAFRQIGNCGRFRVRCCRIR	<i>In vitro</i>	0.9 μg/mL	≥300 μg/mL	Preclinical	184
8P9R	(NGAICWGCPCTAFRQIGNCGRFRVRCCRIR)*8	<i>In vivo</i>	0.3 μg/mL	≥200 μg/mL	Preclinical	185

**Table 2** Small-molecule SARS-CoV-2 inhibitors targeting viral proteins.

Number of chemical structures in Fig.	Inhibitor	Testing model	Activity IC <sub>50</sub> (μmol/L)	Toxicity CC <sub>50</sub> (μmol/L)	Clinical information	Ref.
Entry inhibitor						
<b>Fig. 4 (1)</b>	Salvianolic acid C (Sal-C)	<i>In vitro</i>	3.41	≥100	Preclinical	58
<b>Fig. 4 (2)</b>	Arbidol	<i>In vitro</i>	4.11	31.79	ChiCTR2000029573 NCT04252885	60,64
<b>Fig. 4 (3)</b>	DRI-C23041	<i>In vitro</i> (pseudovirus)	5.6	≥135	Preclinical	65
<b>Fig. 4 (4)</b>	Cepharanthine	<i>In vitro</i>	1.41	11.22	Preclinical	66
		<i>In vitro</i>	0.13	—	Preclinical	78
		<i>In vitro</i>	2.8	12.9	Preclinical	94
<b>Fig. 4 (5)</b>	Abemaciclib	<i>In vitro</i>	3.16	7.08	Preclinical	66
<b>Fig. 4 (6)</b>	Osimertinib	<i>In vitro</i>	3.98	10.00	Preclinical	66
<b>Fig. 4 (7)</b>	Trimipramine	<i>In vitro</i>	20.52	≥20	Preclinical	66
		<i>In vitro</i>	1.5	—	Preclinical	78
<b>Fig. 4 (8)</b>	Colforsin	<i>In vitro</i>	23.06	25.2	Preclinical	66
<b>Fig. 4 (9)</b>	Ingenol	<i>In vitro</i>	0.06	≥20	Preclinical	66
<b>Fig. 4 (10)</b>	Clofazimine	<i>In vitro</i>	0.31	—	Preclinical	68
Replication inhibitors						
Target 3CLpro						
<b>Fig. 5 (11)</b>	Tafenoquine	<i>In vitro</i>	2.5	—	Preclinical	72
		<i>In vitro</i>	~ 2.6	≥50	Preclinical	73
<b>Fig. 5 (12)</b>	<b>12</b>	<i>In vitro</i>	0.25 ± 0.15	≥100	Preclinical	74
<b>Fig. 5 (13)</b>	<b>13</b>	<i>In vitro</i>	0.15 ± 0.14	63.3 ± 2.3	Preclinical	74
<b>Fig. 5 (14)</b>	<b>14</b>	<i>In vitro</i>	0.9 ± 0.8	≥100	Preclinical	74
<b>Fig. 5 (15)</b>	<b>15</b>	<i>In vitro</i>	0.8 ± 0.7	≥100	Preclinical	74
<b>Fig. 5 (16)</b>	Baicalin	<i>In vitro</i>	10.27	≥200	Preclinical	75
<b>Fig. 5 (17)</b>	Baicalein	<i>In vitro</i>	1.69	≥200	Preclinical	75
		<i>In vitro</i>	10	≥100	Preclinical	76
		<i>In vitro</i>	2.9	>500	Preclinical	77
<b>Fig. 5 (18)</b>	Masitinib	<i>In vitro</i>	3.2	—	Preclinical	78
<b>Fig. 5 (19)</b>	Ebselen	<i>In vitro</i>	4.67 ± 0.80	—	Preclinical	79
<b>Fig. 5 (20)</b>	N3	<i>In vitro</i>	16.77 ± 1.70	—	Preclinical	79
<b>Fig. 5 (21)</b>	Cinanserin	<i>In vitro</i>	20.61 ± 0.97	≥200	Preclinical	79
<b>Fig. 5 (22)</b>	<b>22</b>	<i>In vitro</i>	0.53 ± 0.01	≥100	Preclinical	82
<b>Fig. 5 (23)</b>	<b>23</b>	<i>In vitro</i>	0.72 ± 0.09	≥100	Preclinical	82
<b>Fig. 5 (24)</b>	<b>24</b>	<i>In vitro</i>	4–5	—	Preclinical	83
<b>Fig. 5 (25)</b>	GC373	<i>In vitro</i>	1.5	≥200	Preclinical	84
<b>Fig. 5 (26)</b>	GC376	<i>In vitro</i>	0.92	≥200	Preclinical	84
		<i>In vitro</i>	3.37 ± 1.68	≥100	Preclinical	86
		<i>In vitro</i>	0.70	≥200	Preclinical	87
		<i>In vitro</i>	2.189 ± 0.092	≥100	Preclinical	85
<b>Fig. 5 (27)</b>	<b>27</b>	<i>In vitro</i>	2.883 ± 0.227	≥100	Preclinical	85
<b>Fig. 5 (28)</b>	Boceprevir	<i>In vitro</i>	1.31 ± 0.58	≥100	Preclinical	86
		<i>In vitro</i>	15.57	≥200	Preclinical	87
		<i>In vitro</i>	50.1	>10	Preclinical	94
<b>Fig. 5 (29)</b>	Calpain inhibitors II	<i>In vitro</i>	2.07 ± 0.76	≥100	Preclinical	86
<b>Fig. 5 (30)</b>	Calpain inhibitors XII	<i>In vitro</i>	0.49 ± 0.18	≥100	Preclinical	86
<b>Fig. 5 (31)</b>	Bepridil	<i>In vitro</i>	0.86	>25	Preclinical	92
<b>Fig. 5 (32)</b>	MPI5	<i>In vitro</i>	2.5–5	—	Preclinical	93
<b>Fig. 5 (33)</b>	MPI8	<i>In vitro</i>	1.25–2.5	—	Preclinical	93
<b>Fig. 5 (34)</b>	Nelfinavir mesylate	<i>In vivo</i>	3.3	12.3	Preclinical	94
		<i>In vitro</i>	1.13	24.32	Preclinical	152
<b>Fig. 5 (35)</b>	Z-FA-FMK	<i>In vitro</i>	0.13	≥50	Preclinical	95
<b>Fig. 5 (36)</b>	DA-3003-1	<i>In vitro</i>	4.47	7.74	Preclinical	95
<b>Fig. 5 (37)</b>	MG-115	<i>In vitro</i>	0.023	1.13	Preclinical	95
<b>Fig. 5 (38)</b>	MK0893	<i>In vitro</i>	3.16	12.59	Preclinical	95
<b>Fig. 5 (39)</b>	Suramin	<i>In vitro</i>	~20	≥5000	Preclinical	96
<b>Fig. 5 (40)</b>	Lopinavir	<i>In vitro</i>	26.63	49.75	Phase 2 (NCT04276688, NCT04315948)	99,104,124
<b>Fig. 5 (41)</b>	Ritonavir	<i>In vitro</i>	≥100	48.91	Phase 2 NCT04276688	99,104

(continued on next page)

**Table 2 (continued)**

Number of chemical structures in Fig.	Inhibitor	Testing model	Activity IC <sub>50</sub> (μmol/L)	Toxicity CC <sub>50</sub> (μmol/L)	Clinical information	Ref.
Fig. 5 (42)	Dipyridamole (DIP)	<i>In vitro</i>	8.63	74.11		152
Fig. 5 (43)	GRL-0920	<i>In vitro</i>	0.1	—	Preclinical	106
Fig. 5 (44)	MI-09	<i>In vivo</i>	2.8	≥100	Preclinical	107
Fig. 5 (45)	MI-30	<i>In vivo</i>	0.86	—	Preclinical	108
Target PLpro						
Fig. 5 (46)	Dasatinib	—	—	—	Clinical cases	114
Fig. 5 (47)	Dronedarone	<i>In vitro</i>	4.5	12.1	Preclinical	94
Fig. 5 (48)	48	<i>In vitro</i>	21.0	≥80	Preclinical	109
Fig. 5 (49)	GRL-0617	<i>In vitro</i>	2.1	≥100	Preclinical	117
Target RdRp						
Fig. 5 (50)	Remdesivir	<i>In vivo</i>	0.77	≥100	Phase 4 (NCT04252664, NCT04257656, NCT04315948,	19,124,119,125
Fig. 5 (51)	Favipiravir	<i>In vitro</i>	61.88	>400	ChiCTR 2000029600 ChiCTR 2000030254	19
Fig. 5 (52)	β-D-N4-Hydroxycytidine (EIDD-1931)	<i>In vitro</i>	0.3	>10	Preclinical	120
Fig. 5 (53)	Dolutegravir	<i>In vitro</i>	22.04	≥40	Preclinical	146
Other small-molecule inhibitor						
Fig. 6 (54)	Tipranavir	<i>In vitro</i>	13.34	76.80	Preclinical	152
Fig. 6 (55)	Saquinavir	<i>In vitro</i>	8.83	44.43	Preclinical	152
Fig. 6 (56)	Atazanavir	<i>In vitro</i>	9.36	>81	Preclinical	152
Fig. 6 (57)	Azithromycin	<i>In vitro</i>	2.12	>40	Phase 2 NCT04329832	146
Fig. 6 (58)	Spiperone	<i>In vitro</i>	2.49	>40	Preclinical	146
Fig. 6 (59)	Opipramol dihydrochloride	<i>In vitro</i>	5.05	>40	Preclinical	146
Fig. 6 (60)	Quinidine hydrochloride	<i>In vitro</i>	5.11	>40	Preclinical	146
Fig. 6 (61)	Alprostadil	<i>In vitro</i>	5.39	>40	Preclinical	146
Fig. 6 (62)	Ivermectin	<i>In vitro</i>	~2	—	Preclinical	157
		<i>In vitro</i>	4.1	13.2	Preclinical	94
Fig. 6 (63)	Penciclovir	<i>In vitro</i>	95.96	>400	Preclinical	19

is to repurpose the application of clinical and preclinical drugs. Given the available knowledge on their safety profiles, these methods could be easily implemented to rapidly identify effective drugs for use in clinics or clinical trials to treat patients based on emergency use authorization.

Other methods of computer-aided drug design are used much less frequently than virtual screening. Structure- and fragment-based drug designs are iterative processes for designing new small-molecule inhibitors. For example, molecular docking, *de novo* drug design, pharmacophore modeling and quantitative structure–activity relationship models are commonly used for guiding inhibitor screening and optimization. Compared with repurposing old drugs for new indications, other strategies mentioned above are generally limited by long processing time and high cost, making them unsuited for the development of drugs for emergency use, such as COVID-19. However, we propose that computer-aided, small-molecule drug discovery will be one of the most important strategies for research and development of COVID-19 therapeutics and prophylactics in the future.

The development of antiviral agents against SARS-CoV-2 infection calls for the use of human disease-related cells to create novel models to study the biological characteristics of SARS-CoV-2 and to promote drug screening. Given that SARS-CoV-2 mainly infects the respiratory tract, researchers have used human pluripotent stem cells (hPSCs) to develop a lung organoid model (hPSC-LO) for SARS-CoV-2 infection<sup>27</sup>. hPSC-LOs, especially alveolar type II-like cells, could be easily infected by SARS-CoV-2, displaying strong induction of chemokines upon SARS-CoV-2 infection, consistent with the phenomenon observed in COVID-19 patients. At the same time, as a supplement to hPSC-LOs, these researchers also used hPSCs to construct colon organoids (hPSC-COs) to explore the response of colon cells to SARS-CoV-2 infection. Using hPSC-LOs, they conducted HTS of drugs approved by FDA and identified several SARS-CoV-2 entry inhibitors, including imatinib mesylate [Fig. 10B (127)], myco-phenolic acid and quinacrine dihydrochloride [Fig. 10C (159, 160)]. These three drugs were proven to be blockers of SARS-CoV-2 infection in a toxicity-independent manner in Vero E6 cells with

**Table 3** Small-molecule SARS-CoV-2 inhibitors targeting host cell proteins.

Number of chemical structures in Fig.	Inhibitor	Testing model	Activity IC <sub>50</sub> (μmol/L)	Toxicity CC <sub>50</sub> (μmol/L)	Clinical information	Ref.
Target ACE2						
Fig. 7 (64)	Candesartan	<i>In vitro</i>	—	—	Preclinical	160
Fig. 7 (65)	Olmesartan	<i>In vitro</i>	—	—	Preclinical	159
Fig. 7 (66)	Telmisartan	—	—	—	Phase 3 NCT04356495	
Fig. 7 (67)	Losartan	—	—	—	Phase 1 (NCT04312009, NCT04311177, NCT04328012, NCT04335123)	162–164
Target TMPRSS2						
Fig. 8 (68)	Camostat mesylate	<i>In vitro</i> (pseudovirus)	~1	≥500	Phase 2a/4 (NCT04321096, NCT04338906)	10
Fig. 8 (69)	Nafamostat	<i>In vitro</i>	22.50 0.01	≥100 —	NCT04352400	19 177
Fig. 8 (70)	MI-432	<i>In vitro</i>	≤10	≥50	Preclinical	180
Fig. 8 (71)	MI-1900	<i>In vitro</i>	≤50	≥50	Preclinical	180
Target cathepsin B/L						
Fig. 9 (72)	Amantadine	<i>In vitro</i>	≥100	≥100	Preclinical	187
Fig. 9 (73)	Chlorpromazine	<i>In vitro</i>	≥100	≥100	Preclinical	187
Fig. 9 (74)	E64-d	<i>In vitro</i>	~4.487	≥0	Preclinical	187
Fig. 9 (75)	Chloroquine	<i>In vitro</i>	2.71	273.20	Several clinical trials (ChiCTR2000029609 et al.)	97,188,189
Fig. 9 (76)	Hydroxychloroquine	<i>In vitro</i> <i>In vivo</i> (macaques)	2.01 4.51	>30 249.50	Several clinical trials (ChiCTR2000029803, ChiCTR2000029868, ChiCTR2000029898, ChiCTR2000029899, ChiCTR2000029992, ChiCTR2000030054, NCT04315948)	212 124,146,188,189,191
Fig. 9 (77)	Apilimod	<i>In vitro</i> <i>In vitro</i>	4.47 0.023	>30 —	Preclinical	212 68
Fig. 9 (78)	MDL-28170	<i>In vitro</i>	~0.01	—	Preclinical	197
Fig. 9 (79)	Z LVG CHN2	<i>In vitro</i>	0.22	—	Preclinical	68
Fig. 9 (80)	VBY-825	<i>In vitro</i>	0.19	—	Preclinical	68
Fig. 9 (81)	ONO 5334	<i>In vitro</i>	0.3	—	Preclinical	68
Fig. 9 (82)	Teicoplanin	<i>In vitro</i>	0.41	—	Preclinical	201
Fig. 9 (83)	Omeprazole	<i>In vitro</i>	1.66	—	Preclinical	146

(continued on next page)

**Table 3** (continued)

Number of chemical structures in Fig.	Inhibitor	Testing model	Activity IC <sub>50</sub> (μmol/L)	Toxicity CC <sub>50</sub> (μmol/L)	Clinical information	Ref.
Dual inhibitors: Target cathepsin L and 3CLpro						
Fig. 5 (29)	Calpain inhibitors II	<i>In vitro</i>	2.07 ± 0.76	≥100	Preclinical	86,88
Fig. 5 (30)	Calpain inhibitors XII	<i>In vitro</i>	0.49 ± 0.18	≥100	Preclinical	86,88
Other small-molecule inhibitor						
Fig. 10 (84)	Thalidomide	—	—	—	Phase 2 (NCT04273581, NCT04273529)	205
Fig. 10 (85)	Fingolimod	—	—	—	NCT04280588	205,207
Fig. 10 (86)	Teriflunomide	<i>In vitro</i>	6	—	Small patient cohort	208
		<i>In vitro</i>	26.06	850.5		210
Fig. 10 (87)	Leflunomide	<i>In vitro</i>	41.49	879.0	Preclinical	210
Fig. 10 (88)	Brequinar	<i>In vitro</i>	0.123	231.3	Preclinical	210
Fig. 10 (89)	S312	<i>In vitro</i>	1.56	158.2	Preclinical	210
Fig. 10 (90)	S416	<i>In vitro</i>	0.017	178.6	Preclinical	210
Fig. 10 (91)	ROC-325	<i>In vitro</i>	3.28 ± 0.57	>30	Preclinical	212
Fig. 10 (92)	Clomipramine	<i>In vitro</i>	13.6 ± 2.96	>30	Preclinical	212
Fig. 10 (93)	Hycanthone	<i>In vitro</i>	5.79 ± 0.26	14.2	Preclinical	212
Fig. 10 (94)	Mefloquine	<i>In vitro</i>	3.85 ± 0.24	8.78	Preclinical	212
		<i>In vitro</i>	8.06	18.53	Preclinical	244
		<i>In vivo</i>	3.2	≥10	Preclinical	94
Fig. 10 (95)	Dithioerythritol thiosulfonate 16 GNS561	<i>In vitro</i>	50	≥500	Preclinical	214
		<i>In vitro</i>	0.006 for USA-WA1/2020; 0.03 for IHU MI6	2.0 for USA-WA1/2020; 6.7 for IHU MI6	Preclinical	215
Fig. 10 (96)	VPS34-IN1	<i>In vitro</i>	0.55	≥50	Preclinical	218
Fig. 10 (97)	PIK-III	<i>In vitro</i>	0.12	≥50	Preclinical	218
Fig. 10 (98)	Orlistat	<i>In vitro</i>	21.25	≥1000	Preclinical	218
Fig. 10 (99)	Triacsin C	<i>In vitro</i>	0.04	≥50	Preclinical	218
Fig. 10 (100)	MI-1851	<i>In vitro</i>	≤10	≥50	Preclinical	180
Fig. 10 (101)	Decanoyl-RVKR-chloromethylketone (dec-RVKR-cmk)	<i>In vitro</i>	0.057	318.2	Preclinical	221
Fig. 10 (102)	Homoharringtonine	<i>In vitro</i>	2.55	59.75	Preclinical	99
Fig. 10 (103)	Emetine	<i>In vitro</i>	0.46	56.46	Preclinical	99
		<i>In vitro</i>	0.0004	>10	Preclinical	94
Fig. 10 (104)	2-Deoxy-D-glucose (2-DG)	<i>In vitro</i>	9090	—	Preclinical	228,229
Fig. 10 (105)	Pladienolide B	<i>In vitro</i>	0.007	—	Preclinical	228
Fig. 10 (106)	Ribavirin	<i>In vitro</i>	70	—	NCT04356677	228
Fig. 10 (107)	NMS-873	<i>In vitro</i>	0.025	—	Preclinical	140,228
Fig. 10 (108)	Cycloheximide	<i>In vitro</i>	0.17	—	Preclinical	228
Fig. 10 (109)	Baricitinib	—	—	—	Phase 2,3,4 (2020-001854-23, 2020-001354-22, NCT04358614)	232

<a href="#">Fig. 10 (110)</a>	Nitazoxanide	<i>In vitro</i>	2.12	>35.53	Phase 2, 3 (NCT04341493, NCT01056380, NCT04348409)	<a href="#">19,238</a>
		<i>In vitro</i>	4.90	>300		<a href="#">237</a>
<a href="#">Fig. 10 (111)</a>	JIB-04	<i>In vitro</i>	0.695	>300	Preclinical	<a href="#">237</a>
<a href="#">Fig. 10 (112)</a>	Fenofibrate	<i>In vitro</i>	20	>100	Preclinical	<a href="#">187</a>
<a href="#">Fig. 10 (113)</a>	Plitidepsin	<i>In vitro</i>	0.70 nmol/L for Vero E6; 0.73 nmol/L for hACE2-293 T; 1.62 nmol/L for human lung cells	1.99 nmol/L in Vero E6; ≥200 nmol/L for hACE2-293 T; 65.43 nmol/L for human lung cells	Phase 1/2 (NCT04382066)	<a href="#">187,239</a>
<a href="#">Fig. 10 (114)</a>	Clemizole hydrochloride	<i>In vitro</i>	23.94	≥40	Preclinical	<a href="#">146</a>
<a href="#">Fig. 10 (115)</a>	Benztropine mesylate	<i>In vitro</i>	17.79	>>50	Preclinical	<a href="#">244</a>
		<i>In vitro</i>	1.8	—	Preclinical	<a href="#">78</a>
<a href="#">Fig. 10 (116)</a>	Fluphenazine dihydrochloride	<i>In vitro</i>	8.98	20.02	Preclinical	<a href="#">244</a>
<a href="#">Fig. 10 (117)</a>	Amodiaquine hydrochloride	<i>In vitro</i>	5.64	>38.63	Preclinical	<a href="#">244</a>
<a href="#">Fig. 10 (118)</a>	Amodiaquine dihydrochloride dihydrate	<i>In vitro</i>	4.94	34.42	Preclinical	<a href="#">244</a>
<a href="#">Fig. 10 (119)</a>	Thiethylperazine maleate	<i>In vitro</i>	8.02	18.37	Preclinical	<a href="#">244</a>
<a href="#">Fig. 10 (120)</a>	Triparanol	<i>In vitro</i>	6.41	21.21	Preclinical	<a href="#">244</a>
<a href="#">Fig. 10 (121)</a>	Terconazole	<i>In vitro</i>	16.14	41.46	Preclinical	<a href="#">244</a>
<a href="#">Fig. 10 (122)</a>	Fluspirilene	<i>In vitro</i>	5.32	30.33	Preclinical	<a href="#">244</a>
<a href="#">Fig. 10 (123)</a>	Clomipramine hydrochloride	<i>In vitro</i>	7.59	>29.68	Preclinical	<a href="#">244</a>
<a href="#">Fig. 10 (124)</a>	Promethazine hydrochloride	<i>In vitro</i>	10.44	>42.59	Preclinical	<a href="#">244</a>
<a href="#">Fig. 10 (125)</a>	Toremifene citrate	<i>In vitro</i>	11.3	20.51	Preclinical	<a href="#">244</a>
<a href="#">Fig. 10 (126)</a>	Tamoxifen citrate	<i>In vitro</i>	8.98	37.96	Preclinical	<a href="#">244</a>
<a href="#">Fig. 10 (127)</a>	Imatinib mesylate	<i>In vitro</i>	5.32	>30.86	Preclinical	<a href="#">244</a>
		<i>In vivo</i>	2.15	—	Preclinical	<a href="#">27</a>
			(humanized mice carrying hPSC-derived lung xenografts)			
<a href="#">Fig. 10 (128)</a>	Bruceine A	<i>In vitro</i>	0.011	31.4	Preclinical	<a href="#">246</a>
<a href="#">Fig. 10 (129)</a>	Bufalin	<i>In vitro</i>	0.018	>40	Preclinical	<a href="#">246</a>
<a href="#">Fig. 10 (130)</a>	Cinobufagin	<i>In vitro</i>	0.018	>40	Preclinical	<a href="#">246</a>
<a href="#">Fig. 10 (131)</a>	Bufotaline	<i>In vitro</i>	0.0259	>40	Preclinical	<a href="#">246</a>
<a href="#">Fig. 10 (132)</a>	Periplcoside	<i>In vitro</i>	0.0657	>40	Preclinical	<a href="#">246</a>
<a href="#">Fig. 10 (133)</a>	Brusatol	<i>In vitro</i>	0.0492	19	Preclinical	<a href="#">246</a>
<a href="#">Fig. 10 (134)</a>	Digoxin	<i>In vitro</i>	0.1541	>40	Preclinical	<a href="#">246</a>
<a href="#">Fig. 10 (135)</a>	Veratridine	<i>In vitro</i>	2.376	>100	Preclinical	<a href="#">246</a>
<a href="#">Fig. 10 (136)</a>	Oridonin	<i>In vitro</i>	1.462	>40	Preclinical	<a href="#">246</a>
<a href="#">Fig. 10 (137)</a>	Isoalantolactone	<i>In vitro</i>	1.483	>40	Preclinical	<a href="#">246</a>
<a href="#">Fig. 10 (138)</a>	Isoliensinine	<i>In vitro</i>	1.615	40	Preclinical	<a href="#">246</a>
<a href="#">Fig. 10 (139)</a>	Alantolactone	<i>In vitro</i>	1.724	36.7	Preclinical	<a href="#">246</a>
<a href="#">Fig. 10 (140)</a>	Cryptotanshinone	<i>In vitro</i>	5.024	>100	Preclinical	<a href="#">246</a>
<a href="#">Fig. 10 (141)</a>	Dehydrocostus lactone	<i>In vitro</i>	2.322	36.2	Preclinical	<a href="#">246</a>
<a href="#">Fig. 10 (142)</a>	Momordinic	<i>In vitro</i>	3.529	>40	Preclinical	<a href="#">246</a>

(continued on next page)

**Table 3** (continued)

Number of chemical structures in Fig.	Inhibitor	Testing model	Activity IC <sub>50</sub> (μmol/L)	Toxicity CC <sub>50</sub> (μmol/L)	Clinical information	Ref.
Fig. 10 (143)	Liensinine	<i>In vitro</i>	2.537	25.4	Preclinical	246
Fig. 10 (144)	Dehydrodiisoeugenol	<i>In vitro</i>	10.29	≥100	Preclinical	246
Fig. 10 (145)	Cornuside	<i>In vitro</i>	5.262	≥40	Preclinical	246
Fig. 10 (146)	Roburicacid	<i>In vitro</i>	5.267	≥40	Preclinical	246
Fig. 10 (147)	Coniferylaldehyde	<i>In vitro</i>	11.03	≥40	Preclinical	246
Fig. 10 (148)	Panduratin A	<i>In vitro</i>	0.81	14.71	Preclinical	247
Fig. 10 (149)	Thioguanine	<i>In vitro</i>	1.7	25.4	Preclinical	94
Fig. 10 (150)	Moxidectin	<i>In vitro</i>	3.1	6.9	Preclinical	94
Fig. 10 (151)	Ivacaftor	<i>In vitro</i>	3.7	12.9	Preclinical	94
Fig. 10 (152)	Azelnidipine	<i>In vitro</i>	5.3	12.9	Preclinical	94
Fig. 10 (153)	Penfluridol	<i>In vitro</i>	2.4	12.9	Preclinical	94
Fig. 10 (154)	Salinomycin	<i>In vitro</i>	0.00048	13.1	Preclinical	94
Fig. 10 (155)	Monensin	<i>In vitro</i>	6.4	6.6	Preclinical	94
Fig. 10 (156)	Maduramicin	<i>In vitro</i>	1.3	3.4	Preclinical	94
Fig. 10 (157)	Tilorone	<i>In vitro</i>	0.18	—	Preclinical	248
Fig. 10 (158)	Pyronaridine	<i>In vitro</i>	0.198	—	Preclinical	248
Fig. 10 (159)	Mycophenolic acid	<i>In vivo</i> (humanized mice carrying hPSC-derived lung xenografts)	0.9	—	Preclinical	27
Fig. 10 (160)	Quinacrine dihydrochloride	<i>In vivo</i> (humanized mice carrying hPSC-derived lung xenografts)	0.84	—	Preclinical	27

half maximal inhibitory concentrations ( $IC_{50}$ s) of 2.15, 0.9 and 0.84  $\mu\text{mol/L}$ , respectively (Table 3)<sup>27</sup>. Taken together, these data demonstrate that cell disease models provide valuable tools for drug screening to identify COVID-19 therapeutic candidates.

Traditional Chinese medicine (TCM) has been widely applied in clinics in China for COVID-19 patients. Ni et al.<sup>28</sup> have reported that after three patients with COVID-19 treated with Shuanghuanglian Oral Liquid, their symptoms improved, and the patients finally recovered without any adverse reactions. In addition, Lianhuaqingwen was proven to be effective in inhibiting SARS-CoV-2 infection in Vero E6 cells and attenuating the production of proinflammatory cytokines, suggesting that Lianhuaqingwen may have a potential inhibitory effect on the cytokine storm induced by SARS-CoV-2 infection<sup>29</sup>. From the above experience, researchers should also make some headway to screen and develop promising TCM compounds or extracts as efficacious COVID-19 therapeutics.

Some researchers have provided a novel drug discovery strategy to manage COVID-19 by systematically studying the molecular details of SARS-CoV-2<sup>30</sup>. They first successfully cloned, labeled, and expressed 26 of 29 viral proteins in human cells, and

then applied affinity purification mass spectrometry (AP-MS) for identification of human proteins, which could physically interact with each viral protein. In the end, they identified 332 high-confidence SARS-CoV-2-human protein–protein interactions. Sixty-six druggable human proteins, or host factors targeted by 69 existing FDA-approved drugs, are reported. The efficacy in live SARS-CoV-2 infection assays of 69 compounds is currently being evaluated<sup>30</sup>. Host-dependent factors that mediate viral infection may become effective molecular targets for the development of a broadly effective antiviral therapy against SARS-CoV-2 infection.

## 5. Small-molecule SARS-CoV-2 inhibitors targeting viral proteins

### 5.1. Entry inhibitors

Like SARS-CoV, SARS-CoV-2 uses a glycosylated, homotrimeric class I fusion S protein to gain entry into host cells<sup>31–33</sup>. The SARS-CoV-2 S gene denotes the functional components: signal

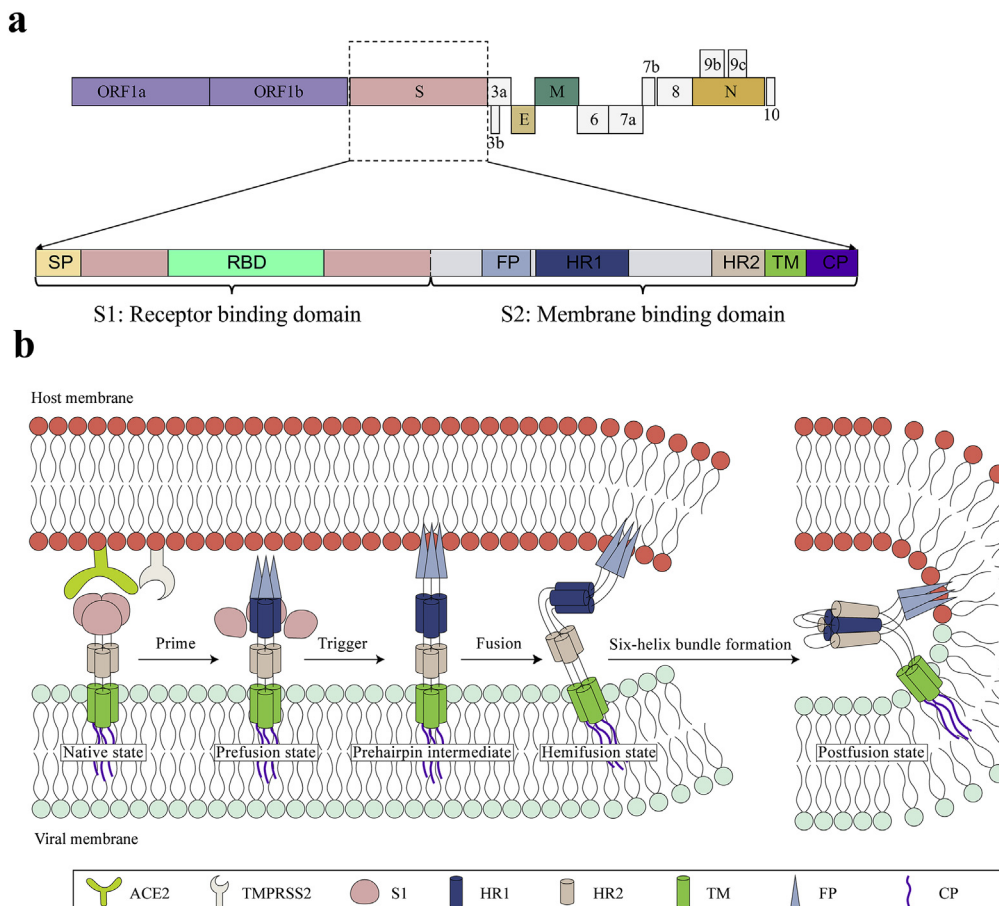


**Figure 3** Structural regions and fusion mechanism of SARS-CoV-2 S protein. (A) The functional regions in SARS-CoV-2 S protein include SP (signal peptide, light yellow), RBD (receptor-binding domain; light green), FP (fusion peptide; light blue), HR1 (heptad repeat 1; gray-blue), HR2 (heptad repeat 2; flesh), TM (transmembrane; grass green), and CP (cytoplasmic; purple). (B) SARS-CoV-2 S protein fusion pathway base on class I fusion protein. The S protein starts in the native state and undergoes priming of the S1 subunit by relevant proteases to achieve the prefusion state. Subsequent triggering by relevant proteases will enable the FP to insert in the host membrane and allow the S protein to form the prehairpin intermediate. The prehairpin begins to fold back on itself due to HR1 and HR2 interactions forming the 6-HB, and eventual postfusion stable states. During the S protein foldback, the two membranes will approach each other until the outer leaflets merge (hemifusion) and eventually the inner leaflets merge.

peptide (SP) and receptor-binding domain (RBD) in the S1 subunit and fusion peptide (FP), heptad repeat 1 (HR1), heptad repeat 2 (HR2), transmembrane (TM) and cytoplasm (CP) in the S2 subunit (Fig. 3A). Class I fusion proteins catalyze membrane fusion reaction through a sequence of states: (1) native state, (2) prefusion state, (3) prehairpin intermediate state, (4) hemifusion state, and (5) postfusion state (Fig. 3B). The S protein is comprised of S1 and S2 subunits and exists in a metastable pre-fusion conformation. Binding between the RBD of S1 and the receptor ACE2 triggers a conformational change of the S2 subunit, which destabilizes the prefusion trimer, and this results in shedding of the S1 subunit and activating the fusogenic activity of the S2 subunit<sup>34–36</sup>. During the fusion process, the FP is exposed and inserts into the host cell membrane, triggering the transient formation of a prehairpin intermediate that bridges the viral and cell membranes. Then, the HR1 and HR2 associate with each other to form a six-helix bundle (6-HB), drawing both viral and target cell membranes into close proximity in a manner that results in fusion between the viral and host cell membranes<sup>15</sup>.

#### 5.1.1. Peptides

Peptides derived from the HR1 and HR2 domains in the class I viral fusion protein block the viral 6-HB formation by binding to the pre-hairpin intermediate, thus showing antiviral activity<sup>37</sup>. This activity has been reported for emerging CoVs, including SARS-CoV and MERS-CoV<sup>35,38–40</sup>. In response to the outbreak of SARS-CoV, a group of HR2-based peptides that could effectively inhibit viral infection were developed<sup>35,40–43</sup>. A pan-CoV fusion inhibitor, designated EK1, was designed, which could inhibit the fusion of diverse HCoVs, including SARS-CoV, MERS-CoV, HCoV-229 E, HCoV-NL63, and HCoV-OC43<sup>44</sup>. More recent studies showed that EK1 is an effective peptide inhibitor against SARS-CoV-2 S protein-mediated membrane fusion and pseudovirus infection in a dose-dependent manner (Table 1)<sup>45</sup>. Recent studies have shown that conjugation of a lipid group to a peptide is a feasible strategy to enhance the antiviral activity and *in vivo* stability of the lipopeptide viral fusion inhibitor<sup>46–48</sup>. The lipopeptide EK1C4 derived from EK1 was found to be an effective inhibitor against S protein-mediated membrane fusion and pseudotyped SARS-CoV-2 infection, with IC<sub>50</sub>s of 1.3 and 15.8 nmol/L, respectively, which are about 241- and 149-fold more potent than that of the unmodified peptide EK1, respectively (Table 1)<sup>45</sup>. Similarly, Zhu et al.<sup>49</sup> designed an HR2 sequence-based lipopeptide fusion inhibitor, termed IPB02, which exhibited highly potent activity in inhibiting SARS-CoV-2 S protein-mediated cell–cell fusion and pseudovirus infection (Table 1).

The sequence alignment has shown that the S2 subunits of SARS-CoV-2 and SARS-CoV are highly conserved, and the overall identity of the HR1 and HR2 domains is 92.6% and 100%, respectively, while in the HR1 core region, eight of 21 residues showed mutations (about 38% difference)<sup>50</sup>. Therefore, it is necessary to design fusion inhibitory peptides based on the amino acid sequences of SARS-CoV-2 HR1 and HR2. Unlike EK1, SARS-CoV-2-HR1P (aa924–965) and SARS-CoV-2-HR2P (aa1168–1203) are derived from the HR1 and HR2 of SARS-CoV-2<sup>50</sup>. Results reveal that SARS-CoV-2-HR2P showed potent fusion-inhibitory activity with an IC<sub>50</sub> of 0.18 μmol/L, whereas SARS-CoV-2-HR1P exhibited no significant inhibition at concentrations up to 40 μmol/L (Table 1)<sup>50</sup>.

de Vries et al.<sup>51</sup> designed a dimeric lipopeptide fusion inhibitor, [SARS<sub>HRC</sub>-PEG<sub>4</sub>]<sub>2</sub>-chol, varying from SARS-CoV-2-HRP2 only in a single amino acid<sup>50</sup>. [SARS<sub>HRC</sub>-PEG<sub>4</sub>]<sub>2</sub>-chol inhibited

SARS-CoV-2 entry with an IC<sub>50</sub> of ~5 nmol/L in TMPRSS2-positive Vero E6 cells. While toxicity of [SARS<sub>HRC</sub>-PEG<sub>4</sub>]<sub>2</sub>-chol in human airway epithelium was minimal, even at the high concentrations tested (< 20% at 100 μmol/L, Table 1). It is worth noting that daily intranasal administration to SARS-CoV-2 ferrets can completely prevent SARS-CoV-2 direct-contact transmission<sup>51</sup>.

Peptides to disrupt SARS-CoV-2-RBD binding to ACE2 can also inhibit the virus which target the stage of viral attachment to prevent entry to host cells, a new modality for COVID-19 therapeutic intervention. For example, SBP1 (a 23-mer peptide fragment) consisting of amino acids in the α1 helix of the ACE2 peptidase domain (PD) was synthesized. The results of bio-layer interferometry revealed that SBP1 could specifically bind with SARS-CoV-2-RBD in low nanomolar concentration (Table 1)<sup>52</sup>, and block the interaction between SARS-CoV-2 S protein and ACE2, thereby preventing the virus from entering host cells and providing a new treatment and diagnostic strategy against COVID-19<sup>52</sup>.

To inhibit the viral attachment between S protein and ACE2, the peptides designed by Cao et al.<sup>53</sup> using two *de novo* design approaches, also known as minibinders, were either built around an ACE2 helix or based on RBD-binding motifs. AHB1 and AHB2 (Table 1), followed the first approach, exhibited strongly neutralization SARS-CoV-2 with IC<sub>50</sub>s of 35 and 15.5 nmol/L, respectively. Using the second approach, LCB1 and LCB3 neutralized SARS-CoV-2 with IC<sub>50</sub>s of 23.54 and 48.1 pmol/L, respectively (Table 1). These hyperstable minibinders provide new approaches for SARS-CoV-2 therapeutics.

Beddingfield and colleagues identified ATN-161, the fibronectin-derived anticancer peptide, that inhibited SARS-CoV-2 attachment through a hypothesized α5β1 integrin-based mechanism and indicated that ATN-161 could reduce SARS-CoV-2 infection with an IC<sub>50</sub> of 3.16 μmol/L<sup>54</sup> (Table 1). Integrins have been shown to bind to ACE2 and SARS-CoV-2 S protein<sup>55,56</sup>. The results of Beddingfield et al.<sup>54</sup> suggest that inhibiting S protein interaction with α5β1 integrin and the interaction between α5β1 integrin and ACE2 using ATN-161 represents a promising approach to treat COVID-19.

Watson et al.<sup>57</sup> designed peptides, SARS-BLOCK™, by mimicking the SARS-CoV-2 RBD that target the stage of viral attachment. They designed, simulated, synthesized, modeled epitopes, predicted peptide folding, and characterized behavior of synthetic peptides. Among of them, peptides **1**, **4**, **5** and **6** blocked SARS-CoV-2 pseudotyped virus infection in ACE2-HEK293 cells. And peptide **5** showed inhibitory activity with an IC<sub>50</sub> in the sub-micromolar concentrations and an IC<sub>95</sub> of ~2.22 μmol/L (Table 1).

#### 5.1.2. Small-molecule compounds

The SARS-CoV-2 S protein plays a key role in recognizing receptor and mediating virus-cell membrane fusion showing itself to be an efficient mediator of viral entry. The S protein is not only an important binding site for neutralizing antibodies, but it is also a major target for therapeutic drug development. Yang et al.<sup>58</sup> report that salvianolic acid C [Sal-C, Fig. 4 (1)], a hydrophilic compound from Danshen, a TCM, potent to inhibit SARS-CoV-2 infection in blocking the formation of 6-HB core of S protein. And Sal-C exhibited potent antiviral activity against authentic SARS-CoV-2 with an IC<sub>50</sub> of 3.41 μmol/L (Table 2)<sup>58</sup>. Their study advances a potential use of Sal-C for COVID-19 therapy or prophylaxis and

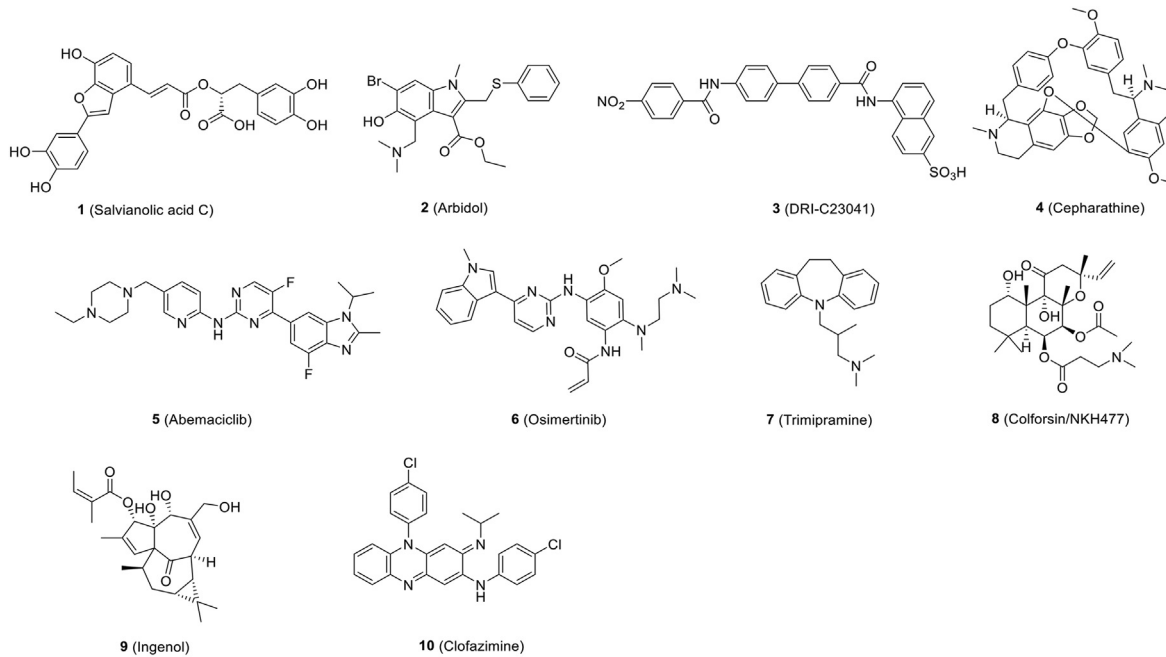


**Figure 4** Chemical structures of small-molecule inhibitors that inhibit SARS-CoV-2 entry.

provides a basis for the development of fusion inhibitors against SARS-CoV-2 infection.

Arbidol [umifenovor, Fig. 4 (2)], an anti-influenza drug approved in China and Russia, targets the SARS-CoV-2 S protein to impede S protein-mediated membrane fusion and, hence, the entry of virus into host cells<sup>59</sup>. It showed satisfactory activity against SARS-CoV-2 *in vitro*<sup>60</sup>. IC<sub>50</sub> and the 50% cytotoxic concentration (CC<sub>50</sub>) of Arbidol in cell-based assays were 4.11 and 31.79 μmol/L, respectively, and the selectivity index (SI = CC<sub>50</sub>/IC<sub>50</sub>) was 7.73 (Table 2)<sup>60</sup>. Several clinical trials were evaluated for the treatment of COVID-19, including arbidol monotherapy and arbidol combined with lopinavir/ritonavir<sup>61,62</sup>. According to clinical trials, post-exposure prophylaxis using arbidol could reduce infection exposed to confirmed cases of COVID-19<sup>63</sup>. Compared to a supportive care group, arbidol monotherapy presented little effect for patients hospitalized with mild and moderate COVID-19<sup>64</sup>.

Novel drug-like compounds, DRI-C23041, DRI-C91005, which targeted the viral attachment stage, inhibited the interaction of hACE2 with SARS-CoV-2 S protein in cell-free ELISA-type assays<sup>65</sup>. DRI-C23041 [Fig. 4 (3)] inhibited SARS-CoV-2-S pseudovirus with IC<sub>50</sub> of 5.6 μmol/L (Table 2)<sup>65</sup>.

Using the SARS-S and MERS-S pseudovirus infection assays, six compounds (cepharanthine, abemaciclib, osimertinib, trimipramine, colforsin, and ingenol) [Fig. 4 (4–9)], were identified as cell entry inhibitors from a HTS in approved drug libraries. The molecular mechanism of action of these small-molecule entry inhibitors has not been fully characterized. These inhibitors have been further confirmed to reduce (> 30%) cytopathic effect (CPE) caused by SARS-CoV-2 infection in Vero E6 cells with IC<sub>50</sub>s of 1.41, 3.16, 3.98, 20.52, 23.06 and 0.06 μmol/L, respectively (Table 2)<sup>66</sup>.

Clofazimine [Fig. 4 (10)], an FDA-approved molecule, was found to be an anti-tuberculosis drug, which was later used to treat leprosy<sup>67</sup> and then showed antiviral activity against SARS-CoV-2

with an IC<sub>50</sub> of 310 nmol/L *in vitro*<sup>68</sup>. Clofazimine, which has recently been identified as a broad-spectrum inhibitor of coronaviruses, may be a promising candidate for coronaviruses that have emerged and may emerge in the future. Because of its comparatively low manufacturing cost, clofazimine could significantly reduce the health burden, particularly in developing countries. In antiviral assays, clofazimine exhibited excellent antiviral activity against SARS-CoV-2 *in vitro* and *in vivo*. In addition, when combined with remdesivir, antiviral synergy was demonstrated against SARS-CoV-2 *in vitro* and *in vivo*. In mechanistic studies, clofazimine was shown to inhibit cell fusion between effector cells expressing SARS-CoV-2 S protein and Vero cells<sup>69</sup>.

## 5.2. Replication inhibitors

### 5.2.1. 3C-like protease inhibitors

Two large polyproteins, pp1a and pp1ab, are inactive until cleavage by virally encoded cysteine proteases, namely, 3CLpro and PLpro<sup>70</sup>, into different numbers of nsps in replication of SARS-CoV-2. The processing of pp1a and pp1ab is indispensable for viral life cycles. Thus, inhibition of cysteine proteases, is an effective therapeutic strategy for COVID-19.

3CLpro represents the most attractive target for the discovery of SARS-CoV-2 inhibitors. Previous studies demonstrate that amino residue Cys145 in the catalytic pocket of 3CLpro is an effective site for the development of covalent inhibitors against SARS-CoV and other coronaviruses<sup>71</sup>.

Chen and his colleagues<sup>72</sup> established a HTS platform based on fluorescence resonance energy transfer (FRET) to identify drugs targeting the SARS-CoV-2 3CLpro from compound libraries, especially FDA-approved drugs, to be used immediately to treat patients with COVID-19. Their findings indicate that the 8-aminoquinoline antimalarial drug tafenoquine [Fig. 5A-1 (11)] induced significant conformational change in SARS-CoV-2 3CLpro, exposing some hydrophobic residues and ultimately

leading to protein aggregation, diminishing its protease activity. Moreover, tafenoquine significantly repressed the yield of SARS-CoV-2 RNA in a cell culture system with an  $IC_{50}$  of around 2.5  $\mu\text{mol/L}$  (Table 2). In Vero E6 cells, another research team reported that tafenoquine has an  $IC_{50}$  of  $\sim 2.6 \mu\text{mol/L}$  for SARS-CoV-2 (Table 2), which is four times more potent than hydroxychloroquine<sup>73</sup>. Time-of-addition experiment is consistent with the different mechanism for tafenoquine *versus* hydroxychloroquine. Physiologically based pharmacokinetic models indicate that the unbound concentration of tafenoquine may exceed  $EC_{90}$  for at least 8 weeks after administration in the lungs of COVID-19 patients.

Some 3CLpro inhibitors synthesized by Rathnayake et al.<sup>74</sup> show activity against multiple coronaviruses in enzyme- and cell-based assays. Among compounds **12–15** (**6c**, **6e**, **6h** and **6j** in Ref. 74) [Fig. 5A-1 (12–15)], **13** showed the most potent antiviral activity against SARS-CoV-2 3CLpro in both fluorescence resonance energy transfer enzyme assay ( $IC_{50}$ , 0.17  $\mu\text{mol/L}$ ) and cell-based assay ( $IC_{50}$ , 0.15  $\mu\text{mol/L}$ , Table 2).

Baicalin and baicalein [Fig. 5A-1 (16, 17)], key components in TCM *Scutellaria* B., were reported as the first noncovalent, non-peptidomimetic inhibitors of SARS-CoV-2 3CLpro, which exhibited potent antiviral activity with  $IC_{50}$ s of 10.27 and 1.69  $\mu\text{mol/L}$ , respectively, in a cell-based system (Table 2)<sup>75</sup>. Crystal structure of 3CLpro in complex with baicalein shows that baicalein occupies the core of the substrate-binding pocket through interacting with the crucial S1/S2 subsites and the oxyanion loop, blocking substrates from approaching the active site<sup>75</sup>. This unique mode of action can be regarded as a completely different type of 3CLpro inhibitor. Another team reported that infection of SARS-CoV-2 and VSV were potently inhibited by baicalein with  $IC_{50}$ s around 10 and 15  $\mu\text{mol/L}$ , respectively<sup>76</sup>. Mechanistically, baicalein inhibits mitochondrial OXPHOS, which is reversibly related to mPTP activity in host cells. The virus changes mitochondrial metabolism by inactivating mPTP to promote its production, and the inhibition of OXPHOS attenuates viral replication. A recent research team also reported that the ethanol extract of *Scutellaria baicalensis* and baicalein, the major component, showed inhibition of SARS-CoV-2 replication in Vero cells with  $IC_{50}$ s of 0.74 and 2.9  $\mu\text{mol/L}$ , respectively<sup>77</sup>. Ethanol extract inhibits virus entry, whereas baicalein mainly acts on the post-entry stage of the virus.

To inhibit the replication of HCoV-OC43, Drayman's team<sup>78</sup> screened a library of 1900 clinically safe drugs, identified 26 top hits and further tested their antiviral activity against SARS-CoV-2. Of the 26 drugs tested, the compounds with the best antiviral activity against SARS-CoV-2 were cepharanthine ( $IC_{50} = 0.13 \mu\text{mol/L}$ ), flupenthixol ( $IC_{50} = 0.56 \mu\text{mol/L}$ ), desloratadine ( $IC_{50} = 0.9 \mu\text{mol/L}$ ), trimipramine ( $IC_{50} = 1.5 \mu\text{mol/L}$ ), lapatinib ( $IC_{50} = 1.6 \mu\text{mol/L}$ ), benztrpine ( $IC_{50} = 1.8 \mu\text{mol/L}$ ), bafetinib ( $IC_{50} = 2.2 \mu\text{mol/L}$ ), azelastine ( $IC_{50} = 2.4 \mu\text{mol/L}$ ) and masitinib [Fig. 5A-1 (18)] ( $IC_{50} = 3.2 \mu\text{mol/L}$ , Table 2). By studying the mechanism of action, they found that masitinib, a cancer treatment drug developed as a tyrosine-kinase inhibitor, inhibited the activity of the SARS-CoV-2 3CLpro.

To identify drug candidates for clinical trials, Jin and co-workers<sup>79</sup> initiated multiple strategies that combining structure-assisted drug design, virtual drug screening and HTS could rapidly discover novel lead compounds. This strategy resulted in the development of a FRET assay to test more than 10,000 compounds as inhibitors of 3CLpro. First, they identified a mechanism-based inhibitor, N3, by computer-aided drug design and then determined that N3 bound with 3CLpro of SARS-CoV-2

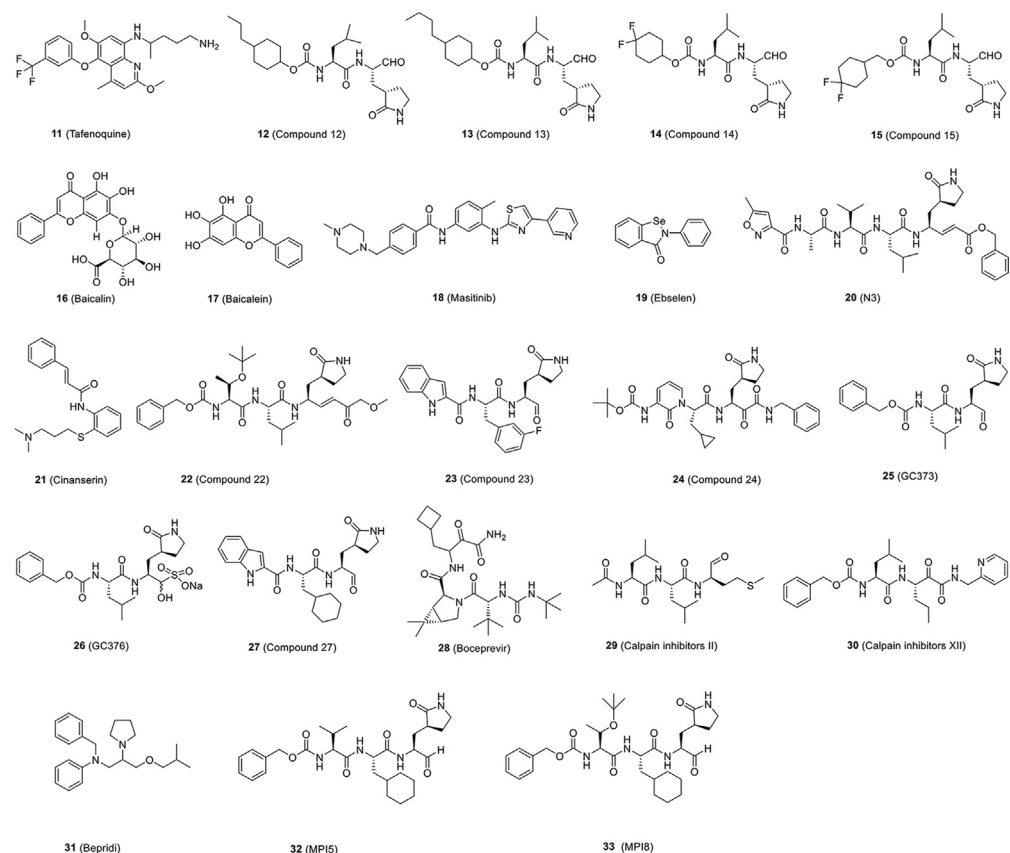
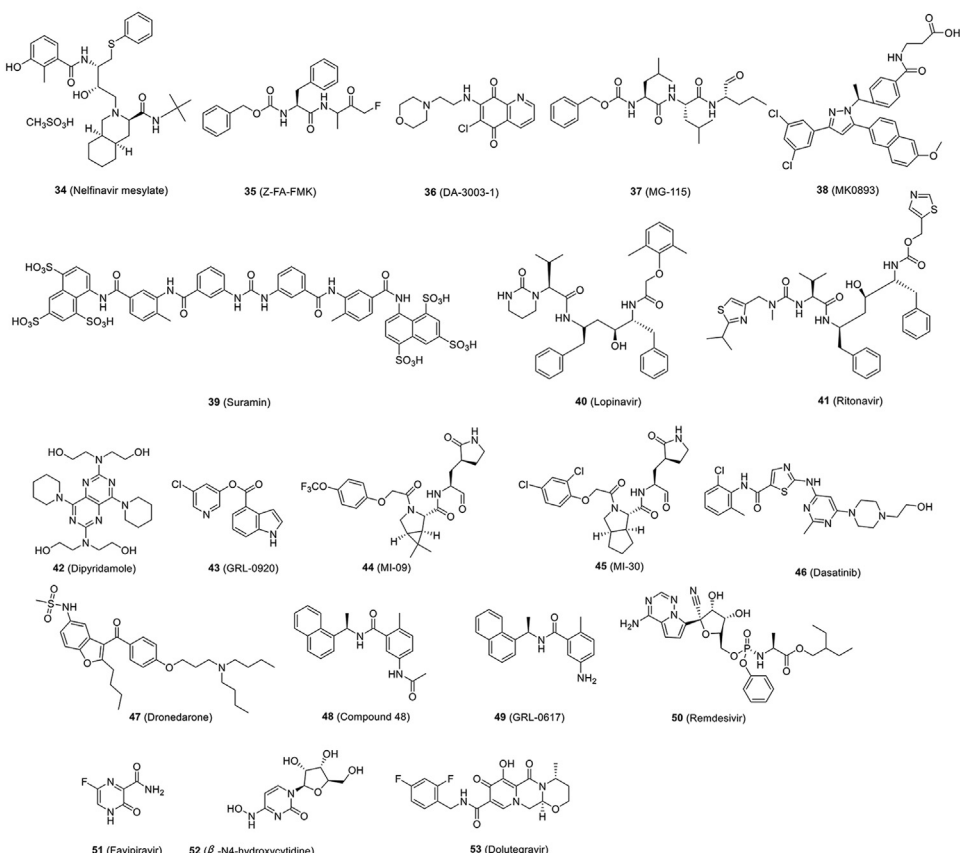
at a resolution of 2.1 Å (PDB code 7BQY) by measuring the crystal structure of 3CLpro in complex with N3. Finally, they found that seven FDA-approved or clinical drugs (ebselen, disulfiram, TDZD-8, tideglusib, carmofur, shikonin and PX-12) could inhibit 3CLpro using an enzymatic inhibition assay. However, it should be pointed out that the mechanism of action of six of them (ebselen, disulfiram, tideglusib, carmofur, shikonin and PX-12) remains to be elucidated. Ma et al.<sup>80</sup> proved that these six inhibitors were nonspecific inhibitors of 3CLpro. Among these compounds, ebselen and N3 [Fig. 5A-1 (19, 20)] showed the strongest inhibition against SARS-CoV-2 in a plaque-reduction assay with  $IC_{50}$ s of 4.67 and 16.77  $\mu\text{mol/L}$ , respectively (Table 2). They also identified cinanserin [Fig. 5A-1 (21)], a well-characterized serotonin antagonist, which displayed moderate inhibition against SARS-CoV-2 with an  $IC_{50}$  value of 20.61  $\mu\text{mol/L}$  (Table 2)<sup>79</sup>. Later, Yang and coworkers<sup>81</sup> presented the X-ray crystal structure of SARS-CoV-2 3CLpro in complex with carmofur at a resolution of 1.6 Å (PDB code 7BUY). The Yang and Liu groups<sup>82</sup> also co-published X-ray crystal structures of SARS-CoV-2 3CLpro in complex with peptidomimetic aldehyde compounds **22** and **23** (**11a** and **11b** in Ref. 82) [Fig. 5A-1 (22, 23)]. Both **22** and **23** exhibited good anti-SARS-CoV-2-infection activities in cells with  $IC_{50}$ s of  $0.53 \pm 0.01$  and  $0.72 \pm 0.09 \mu\text{mol/L}$ , respectively, using a plaque-reduction assay (Table 2). Cytotoxicity and pharmacokinetic experiments were carried out later, suggesting that the two compounds were promising drug candidates for further clinical studies<sup>82</sup>.

Zhang et al.<sup>83</sup> synthesized a series of peptidomimetic  $\alpha$ -ketoamides as broad-spectrum inhibitors of 3CLpro of alphacoronaviruses, betacoronaviruses and enteroviruses. Recently, they determined the crystal structure of 3CLpro of SARS-CoV-2 at 1.75 Å resolution (PDB code 6Y2E) and co-crystal structures bound with compound **24** (**13b** in Ref. 83) [PDB code 6Y2F, Fig. 5A-1 (24)] with  $\alpha$ -ketoamide as the warhead. **24** exhibited inhibition against SARS-CoV-2 infection in human Calu 3 cells with an  $IC_{50}$  of 4–5  $\mu\text{mol/L}$  (Table 2). The pharmacokinetic studies of **24**, given these favorable results, provide a promising framework for the development of new 3CLpro inhibitors for COVID-19.

Similarly, the dipeptide-based protease inhibitors GC373 and GC376 [Fig. 5A-1 (25, 26)] were effective inhibitors against 3CLpro of both SARS-CoV and SARS-CoV-2. GC373 is a peptide aldehyde metabolite of GC376. The binding mode of the inhibitors on SARS-CoV-2 3CLpro showed a covalent modification of the amino residue Cys145 in the catalytic site (PDB code 6WTK and 6WTJ). More importantly, both GC373 and GC376 were found to be potent inhibitors of SARS-CoV-2 replication in cells with  $IC_{50}$ s near 1  $\mu\text{mol/L}$  with little to no toxicity (Table 2), making them potent drug candidates for the treatment of COVID-19<sup>84</sup>. Structural comparison of reported 3CLpro–inhibitor complex reveals that all of the covalent inhibitor connected to the sulphur atom of amino residue Cys145 (Fig. 5B).

Iketani et al.<sup>85</sup> described three structurally diverse compounds—**27** (4 in Ref. 85) [Fig. 5A-1 (27)], GC376, and MAC-5576—with inhibitory activity against the SARS-CoV-2 3CLpro. Next, they tested these compounds for inhibition of SARS-CoV-2 viral replication. They found that **27** and GC376 could block SARS-CoV-2 infection with  $IC_{50}$  values of  $2.883 \pm 0.227$  and  $2.189 \pm 0.092 \mu\text{mol/L}$  (Table 2), respectively, whereas MAC-5576 did not.

Recently, four inhibitors targeting the 3CLpro of SARS-CoV-2, namely GC376, boceprevir, and calpain inhibitors II and XII [Fig. 5A-1 (26, 28–30)], were identified with  $IC_{50}$ s ranging from

**A-1****A-2**

**Figure 5** SARS-CoV-2 replication inhibitors. (A) Chemical structures of SARS-CoV-2 replication inhibitors. (B) Overall views of the 3CLpro-N3 (yellow) complex overlapped with carmofur (blue), 13 b (silver), GC373 (red) and GC376 (green) (PDB ID: 7BQY, 7BUY, 6Y2F, 6WTJ and 6WTK), and amino residue Cys145 was shown as cyan. (C) Overall views of the RdRp-suramin (cyan) complex overlapped with the remdesivir (magenta)-bound RdRp structure (PDB ID: 7D4F and 7BV2). nsp 12 was shown as yellow and accessory subunits nsp 7 and nsp 8 were shown as blue and pink.

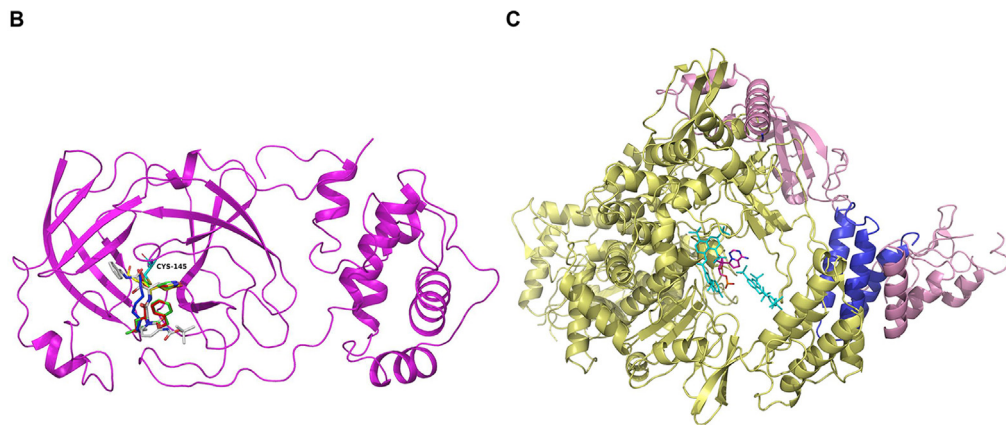


**Figure 5** (continued)

0.45 to 4.13  $\mu\text{mol/L}$  in the enzymatic assay<sup>86</sup>. Significantly, the four compounds exhibited inhibition against SARS-CoV-2 replication in cells with  $\text{IC}_{50}$ s ranging from 0.49 to 3.37  $\mu\text{mol/L}$  (Table 2). Especially, boceprevir and calpain inhibitors II and XII represent novel chemotypes, providing a starting point for the development of novel SARS-CoV-2 inhibitors<sup>86</sup>. Another article also reported that boceprevir and GC376 showed inhibitory effects against SARS-CoV-2 in Vero cells [multiplicity of infection (MOI) = 0.01] with  $\text{IC}_{50}$  values of 15.57 and 0.70  $\mu\text{mol/L}$ , respectively (Table 2)<sup>87</sup>. Moreover, combination of GC376 with remdesivir had a sterilizing additive effect<sup>87</sup>. In addition, some researchers found that the anti-3CLpro activity of calpain inhibitors II and XII was weaker than that of another 3CLpro inhibitor, GC376, in the SARS-CoV-2 3CLpro enzyme inhibition assay<sup>88</sup>. However, calpain inhibitors II and XII actually performed better than GC376 in reducing the replication of SARS-CoV-2 in cell culture<sup>86</sup>. They recently discovered that calpain inhibitors II and XII are also have inhibitory activity against human cathepsin L, which is a host-protease responsible for viral entry<sup>88</sup>. Calpain inhibitors II and XII are dual inhibitors that efficiently target viral protease 3CLpro and human protease cathepsin L, which may explain the excellent antiviral activity of them, despite having inferior affinity for 3CLpro when compared to the specific inhibitor GC376. Dual inhibitors can potentially inhibit drug resistance. Even if the viral protein changes, this type of inhibitor remains effective against unchanged human host proteins. In addition, Hu et al.<sup>89</sup> found that boceprevir, calpain inhibitors II and XII, and GC-376 showed broad-spectrum antiviral activity against SARS-CoV-2, SARS-CoV and MERS-CoV infection, as well as human coronaviruses (CoVs) 229 E, OC43, and NL63. In addition, Cáceres et al.<sup>90</sup> has reported that GC376 is effective in inhibiting SARS-CoV-2 infection *in vivo*. Treatment of SARS-CoV-2-infected K18-hACE2 mice with GC376 resulted in decreased viral loads and reduced inflammation. Recently, Shi et al.<sup>91</sup> reported that application of low-dose GC376 in combination with GS441524, a parent nucleotide analog of remdesivir, that targets the coronavirus RdRp, *via* intranasal or intranasal and intramuscular administration could effectively protect mice against challenge of mouse-adapted SARS-CoV-2.

Vatansever et al.<sup>92</sup> have reported that 6 small-molecule drugs (pimozide, ebastine, rupintrivir, bepridil, sertaconazole, and rimonabant) exhibited 50% inhibition of 3CLpro activity at concentration below 100  $\mu\text{mol/L}$  and that bepridil [Fig. 5A-1 (31)]

was the basic molecule that potentiates dual functions by raising endosomal pH to interfere with SARS-CoV-2 entry into the host cell, thereby inhibiting 3CLpro activity in infected cells. Their results revealed that bepridil inhibited CPE induced by SARS-CoV-2 infection in Vero E6 and A549/ACE2 cells with  $\text{IC}_{50}$  value of 0.86 and 0.46  $\mu\text{mol/L}$ , respectively.

Based on the previous medicinal chemistry studies about 3CLpro of SARS-CoV, Yang et al.<sup>93</sup> have designed and synthesized a series of SARS-CoV-2 3CLpro inhibitors that contain  $\beta$ -(S-2-oxopyrrolidin-3-yl)-alaninal (Opal) for the formation of a reversible covalent bond with the cysteine C145 in SARS-CoV-2 3CLpro active site. Among them, MPI5 and MPI8 [Fig. 5A-1 (32, 33)] completely inhibited CPE induced by SARS-CoV-2 infection in Vero E6 cells at 2.5–5  $\mu\text{mol/L}$  and A549 cells at 0.16–0.31  $\mu\text{mol/L}$ . In preclinical and clinical studies on COVID-19 treatment, their inhibitory potency was remarkably higher than that of some existing molecules.

Jan et al.<sup>94</sup> identified that boceprevir and nelfinavir mesylate [Fig. 5A (28, 34)] can inhibit SARS-CoV-2 infection and replication with  $\text{IC}_{50}$ s of 50.1 and 3.3  $\mu\text{mol/L}$ , respectively, by measuring viral-induced CPE (Table 2). Through target-based assay, they found that nelfinavir mesylate and boceprevir showed inhibitory activity against 3CL pro. Also, nelfinavir mesylate was selected to evaluate its anti-infective efficacy in female golden Syrian hamsters. Nelfinavir mesylate showed good antiviral effects *in vivo*, and the viral load in hamster lungs was significantly reduced.

Walrycin B, hydroxocobalamin, suramin sodium, Z-DEVD-FMK, LLL-12, and Z-FA-FMK were identified as the most potent 3CLpro inhibitors among 23 hits in a SARS-CoV-2 3CLpro enzyme assay<sup>95</sup>. The protease inhibitor Z-FA-FMK [Fig. 5A-2 (35)] inhibited CPE induced by SARS-CoV-2 infection with an  $\text{IC}_{50}$  of 0.13  $\mu\text{mol/L}$  with no apparent cytotoxicity (Table 2). However, hydroxocobalamin, suramin sodium, and Z-DEVP-FMK were invalidated in the CPE assay. Walrycin B and LLL-12 showed apparent toxicity to Vero E6 cells. Other compounds identified, including DA-3003-1, MG-115 and MK0893 [Fig. 5A-2 (36–38)], all exhibited antiviral activity, as well, with more or less cytotoxicity to Vero E6 cells (Table 2). Another research team reported that an antiparasitic drug suramin [Fig. 5A-2 (39)] inhibits SARS-CoV-2 replication and SARS-CoV-2 infection in Vero E6 cells with an  $\text{IC}_{50}$  of ~20  $\mu\text{mol/L}$ <sup>96</sup> (Table 2). And suramin could reduce the viral load by two–three logs

in Vero E6 cells or Calu-3 2B4 cells (the human lung epithelial cell line). Analysis of time-of-addition and plaque reduction assays performed on Vero E6 cells indicated that suramin acts in the early stages of the replication cycle and may prevent virus binding or entry.

Lopinavir/ritonavir [LPV/r, Fig. 5A-2 (40, 41)], a protease inhibitor used for HIV infection, showed inhibitory activity against the replication of SARS-CoV, MERS-CoV and SARS-CoV-2 *in vitro* (Table 2)<sup>97–99</sup>. Although these drugs were initially thought to inhibit SARS-CoV and MERS-CoV 3CLpro<sup>18,100,101</sup>, it should be pointed out that lopinavir and ritonavir failed to inhibit the activity of SARS-CoV-2 3CLpro<sup>86</sup>. In Korea, clinical administration of LPV/r reduced SARS-CoV-2 viral load rapidly, but no placebo-controlled trial was carried out, and the sample of patients was limited<sup>102</sup>. On the other hand, Cao et al.<sup>103</sup> carried out a randomized, controlled, open-label clinical trial for the treatment of severe COVID-19 with LPV/r (400 and 100 mg, respectively). The two sets of clinical results showed that LPV/r offered little clinical improvement beyond the standard of care. Further, Hung et al.<sup>104</sup> carried out a multicenter, prospective, open-label, randomized phase two trial in COVID-19 adult patients admitted to six hospitals in Hong Kong. Early triple antiviral therapy (combination of lopinavir 400 mg and ritonavir 100 mg every 12 h, ribavirin 400 mg every 12 h, and three doses of eight million international units of interferon  $\beta$ -1b on alternate days) was safe and superior to lopinavir–ritonavir alone (lopinavir 400 mg and ritonavir 100 mg every 12 h) in alleviating symptoms and shortening the time of viral elimination and length of hospitalization in patients with mild to moderate COVID-19<sup>104</sup>. Dual antiviral therapy with interferon  $\beta$ -1b as the backbone will be conducted in clinical studies in the future. Most recently, WHO reported the latest solidarity trial interim results of lopinavir, which, unlike the previously reported results, appeared to have little or no effect on hospitalized COVID-19 patients<sup>105</sup>.

The Luo group<sup>106</sup> screened the U.S. FDA-approved drug library and found that the anticoagulation agent dipyridamole [DIP, Fig. 5A-2 (42)] might bind to the SARS-CoV-2 protease 3CLpro, suppressing more than 50% of SARS-CoV-2 replication at a concentration of 100 nmol/L in Vero E6 cells (Table 2). Indeed, after two weeks of DIP adjunctive treatment, all eight severe patients showed remarkably positive outcomes.

Hattori et al.<sup>107</sup> reported that one indole-chloropyridinyl-ester derivative, GRL-0920 [Fig. 5A-2 (43)], targeting 3CLpro of SARS-CoV-2, exerted potent activity against SARS-CoV-2 ( $IC_{50} = 2.8 \mu\text{mol/L}$ ) in cell-based assays performed using Vero E6 cells without significant toxicity, as examined with immunocytochemistry (Table 2).

As mentioned above, although some SARS-CoV-2 3CLpro inhibitors have been reported, the previous literature on SARS-CoV-2 3CLpro inhibitors has not included data from the experiments using SARS-CoV-2-infected animal models. Qiao et al.<sup>108</sup> designed and synthesized 32 new bicyclic proline-containing 3CLpro inhibitors, all of which derived from boceprevir or telaprevir. All compounds inhibited the activity of SARS-CoV-2 3CLpro with  $IC_{50}$ s of 7.6–748.5 nmol/L *in vitro*. Two compounds, MI-09 and MI-30, [Fig. 5A-2 (44, 45)] showed excellent antiviral activity against SARS-CoV-2 with  $IC_{50}$ s of 0.86 and 0.54  $\mu\text{mol/L}$  (MOI of 0.1, Vero E6 cells), respectively in cell-based assays (Table 2). In a transgenic mouse model, MI-09 or MI-30 could significantly reduce lung viral load and lung lesions. Also,

MI-09 or MI-30 showed good pharmacokinetic properties and safety in rats.

### 5.2.2. Papain-like protease inhibitors

PLpro is the other crucial viral protease spurring the discovery of anti-SARS-CoV-2 drugs, and its crystal structure has recently been resolved (PDB code 6W9C). PLpro is also reported to drive virus evasion of host innate immune defenses by reversing host ubiquitination and ISGylation events<sup>109</sup>. Thus, PLpro inhibitors may not only directly inhibit SARS-CoV-2 replication, but also perform a complementary function by normalizing the body's immune response against virus invasion. Previous studies identified that thiopurine (6-mercaptopurine and 6-thioguanine, anti-tumor drugs) showed inhibitory activity against SARS-CoV and MERS-CoV PLpro<sup>110</sup>, so repurposing these candidates for treating COVID-19 seems to be a reasonable approach.

Some noncovalent small-molecule inhibitors, rac3j, rac3k and rac5c, against SARS-CoV PLpro<sup>111</sup> also target SARS-CoV-2 PLpro, preventing the self-processing of nsp 3 in cells and reducing SARS-CoV-2-induced CPE under high (33  $\mu\text{mol/L}$ ) concentrations. For rac5c, it is worth mentioning that treatment at 11  $\mu\text{mol/L}$  in 0.1% DMSO continued to show a clear reduction of CPE, indicating effective antiviral activity. For rac3j and rac3k, CPE reduction diminished at lower concentrations<sup>112</sup>.

Referring to the crystal structure of SARS-CoV-2 PLpro, Kouznetsova et al.<sup>113</sup> performed useful data mining of the conformation of FDA-approved drugs. 147 compounds were identified as potential inhibitors of SARS-CoV-2 PLpro. Among them, dasatinib [Fig. 5A-2 (46), Table 2] showed antiviral activity against SARS-CoV-2 in clinical cases<sup>114</sup>, but it was unclear whether dasatinib directly interacts with PLpro. A patient with chronic myeloid leukemia and COVID-19 was treated with dasatinib (100 mg/day) in combination with antibiotics for 11 days, resulting in the disappearance of fever. Two weeks later, two consecutive swab tests were negative for SARS-CoV-2 RNA. Dronedarone [Fig. 5A-2 (47)], which was reported by Jan et al.<sup>94</sup>, is effective in inhibiting the activity of PLpro. And dronedarone showed antiviral activity against CPE induced by SARS-CoV-2 infection with an  $IC_{50}$  of 4.5  $\mu\text{mol/L}$  ( $CC_{50}$  of 12.1  $\mu\text{mol/L}$ ) in Vero E6 cells (Table 2), which is an ion channel modulator.

Mirza et al.<sup>115</sup> reported compound Z93 as a potential human ubiquitin-specific protease 2 (USP2) inhibitor through integrated *in silico* efforts. USP2 inhibitors, such as thiopurine analogs, have been reported to inhibit SARS-CoV PLpro. However, based on the above results, it can only be speculated that Z93 might be a potential chemical lead targeting SARS-CoV-2 PLpro, thus warranting further evaluation *in vitro*. Additionally, the Pegan group<sup>109</sup> declared that naphthalene-based inhibitors [48 (6 in Ref. 109) and GRL-0617, Fig. 5A-2 (48, 49)] showed inhibitory activity against SARS-CoV-2 PLpro and antiviral activity with  $IC_{50}$ s of 21.0 and 27.6  $\mu\text{mol/L}$ , respectively (Table 2). Gao et al.<sup>116</sup> showed that GRL-0617 was effective in inhibiting SARS-CoV-2 PLpro activity with an  $IC_{50}$  of  $2.2 \pm 0.3 \mu\text{mol/L}$  and that its mechanism of action was not limited to occupying the substrate pockets, but rather extended to sealing the entrance to the substrate binding cleft, thereby preventing the binding of the substrate. Another team reported that GRL-0617 showed a promising inhibitory activity against SARS-CoV-2 PLpro *in vitro* with an  $IC_{50}$  of 2.1  $\mu\text{mol/L}$  and effective antiviral inhibition of SARS-CoV-2 in cell-based assays. No apparent cytotoxicity of GRL-

0617 on Vero E6 cells was observed with concentrations up to 100  $\mu\text{mol/L}$ <sup>117</sup>.

### 5.2.3. RNA-dependent RNA polymerase (RdRp) inhibitors

RdRp, a nsp, also known as nsp 12, catalyzes the synthesis of viral genome, which plays a central role in coronaviral replication. Thus, it is considered as an excellent drug target for antiviral inhibitors. The Rao group<sup>118</sup> solved a cryo-electron microscopy structure of full-length RdRp in complex with nsp 7 and nsp 8 at a resolution of 2.9 Å and speculated the binding mode of nucleotide analogs remdesivir and favipiravir to explain the mechanisms of inhibition. The elegant results provide novel insight and lay a solid foundation for structure-based antiviral inhibitor design.

Remdesivir [GS-5734, Fig. 5A-2 (50)], a nucleotide analogue, was originally developed for Ebola treatment<sup>119</sup>. Since its triphosphate form resembles adenosine triphosphate (ATP), it was used as a substrate for viral RdRp, and it performed broad-spectrum activity against coronaviruses<sup>120,121</sup>. Remdesivir was first suggested by Morse et al.<sup>6</sup> as a COVID-19 therapeutic for treatment of patients infected by SARS-CoV-2. Remdesivir ( $\text{IC}_{50} = 0.77 \mu\text{mol/L}$ ;  $\text{CC}_{50} > 100 \mu\text{mol/L}$ ;  $\text{SI} > 129.87$ ) potently blocked SARS-CoV-2 infection in Vero E6 cells at a MOI of 0.05 and showed high SI (Table 2)<sup>19</sup>. Recently, Beigel et al.<sup>122</sup> reported the results of the ACTT-1 clinical trial of remdesivir. The ACTT-1 clinical trial is a double-blind, randomized, placebo-controlled global phase III clinical trial. Remdesivir was superior to placebo in shortening recovery time and reducing lower respiratory tract infections in adult hospitalized patients with COVID-19<sup>122</sup>. On 1 May 2020, remdesivir was made available under the U.S. FDA Emergency Use Authorization (EUA) for the treatment of severely ill hospitalized patients with COVID-19. The research group also pointed out that combining remdesivir with other treatments or antiviral drugs to improve the prognosis of COVID-19 patients should be evaluated in the future<sup>122</sup>. Despite this, a randomized, double-blind, placebo-controlled study showed that 237 enrolled patients showed no association between remdesivir use and statistically significant clinical benefits<sup>123</sup>. This study had to be terminated early owing to the adverse events observed in patients. WHO published the mid-term results of the Solidarity Trial of Remdesivir using for COVID-19 patients on 15 October 2020. Unlike earlier expectations, remdesivir appeared to have little, or no, effect on hospitalized COVID-19 patients in terms of overall mortality, initiation of ventilation and duration of hospital stay<sup>124</sup>. Yin et al.<sup>126</sup> have reported that suramin, a 100-year-old drug, and its derivatives are at least 20-fold more potent than remdesivir in inhibiting SARS-CoV-2 infection by targeting RdRp. The crystal structure of RdRp in complex with suramin has revealed two binding sites in RdRp (Fig. 5C). As a non-nucleotide inhibitor, suramin could ultimately aid in structure-based drug development for COVID-19<sup>126</sup>.

Favipiravir [Fig. 5A-2 (51), Table 2,  $\text{IC}_{50} = 61.88 \mu\text{mol/L}$ ,  $\text{CC}_{50} > 400 \mu\text{mol/L}$ ,  $\text{SI} > 6.46$ ] had low anti-SARS-CoV-2 activity in cell culture assays<sup>19</sup>. However, favipiravir has been shown to completely protect mice against Ebola virus challenge and has an  $\text{IC}_{50}$  value of 67  $\mu\text{mol/L}$  in Vero E6 cells<sup>127</sup>, suggesting that further *in vivo* studies should be undertaken to assess the efficacy of this antiviral nucleoside in the treatment of COVID-19. In Shenzhen, a clinical trial of favipiravir on COVID-19 patients was conducted (ChiCTR2000029600), and it showed that 35 patients in the favipiravir arm had significantly shorter viral clearance duration in contrast with the control arm containing 45 patients<sup>128</sup>. In another multi-centric randomized study (ChiCTR200030254),

treatment with favipiravir of COVID-19 patients led to an improved recovery at the 7th day<sup>129</sup>.

$\beta$ -D-N4-Hydroxycytidine [EIDD-1931, Fig. 5A-2 (52)] is an orally available ribonucleoside analogue with broad-spectrum antiviral activity against RNA viruses, including influenza, Ebola, CoV, and Venezuelan equine encephalitis (VEE) virus<sup>130–133</sup>. Sheahan et al.<sup>120</sup> reported that EIDD-1931 showed antiviral activity against SARS-CoV-2 in Vero cells with an  $\text{IC}_{50}$  of 0.3  $\mu\text{mol/L}$  (Table 2). Both prophylactic and therapeutic administration of EIDD-2801, an orally available EIDD-1931-prodrug, in mice infected with SARS-CoV or MERS-CoV, could improve pulmonary function and reduce virus titer and body weight loss<sup>120</sup>. The mechanism of action of EIDD-2801 is different from that of remdesivir. Remdesivir is a chain terminator<sup>134</sup>, while EIDD-2801 causes mutagenesis in the viral RNA. In addition, EIDD-2801 is active against remdesivir-resistant mutants and has a higher genetic barrier to drug resistance than remdesivir<sup>120</sup>. For VEE and influenza viruses, compound EIDD-2801 inhibited RdRp to exert its antiviral functions, but the mechanism of action against coronaviruses was not well documented<sup>135</sup>.

### 5.2.4. Helicase inhibitors

Helicase, a motor protein, is responsible for separation and/or rearrangement of viral nucleic acid duplexes before transcription or replication<sup>136</sup>. The helicase known as nsp 13 consists of three major domains—a putative N-terminal metal-binding domain (MBD), a hinge domain, and a helicase domain. And the N-terminal forms a Zn-binding domain, while the C-terminal forms a helicase domain with a conserved motif and participates in both unravelling double-stranded (ds) DNA and capping of viral RNA. Studies have shown that nsp13-dependent disintegration was an essential process for the replication, transcription, and translation of SARS-CoV-2 genome<sup>137</sup>. Therefore, helicases are potential targets for antiviral therapies of COVID-19 and inhibitors of helicases, such as bananins, 5-hydroxychromone derivatives, ADKs, and SSYA10-001, and are expected to be used in the treatment of COVID-19<sup>138–141</sup>. In addition, clofazimine was shown to inhibit SARS-CoV-2 replication by interfering with the function of helicase<sup>69</sup>. The biggest challenge in targeting helicase is the relatively low selectivity of helicase inhibitors. Right now, no antiviral targeting helicase has moved beyond preclinical development.

### 5.2.5. 2'-O-Ribose methyltransferase (2'-O-MTase) inhibitors

The nsp 16, or 2'-O-MTase, is another crucial protein responsible for SARS-CoV replication<sup>142–144</sup> by catalyzing 5'-terminal caps structures (m7GpppN) of mRNA for methylation, thereby preventing recognition and activation of host immune responses<sup>144,145</sup>.

By using model docking and molecular dynamics simulation, Khan et al.<sup>144</sup> established dolutegravir [Fig. 5A-2 (53),  $\text{dtaG} = -9.4 \text{ kcal/mol}$ ] as an excellent lead candidate for the crucial protein 2'-O-Mtase. Dolutegravir, an integrase strand-transfer inhibitor, with inhibitory activity against human immunodeficiency virus type 1 (HIV-1) infection, could suppress SARS-CoV-2 replication with  $\text{IC}_{50}$  of 22.04  $\mu\text{mol/L}$  and  $\text{CC}_{50} > 40 \mu\text{mol/L}$  in Vero E6 cells (Table 2)<sup>146</sup>.

### 5.2.6. RNA-binding N-terminal domain inhibitors

N protein, usually located inside the virions, is an abundant coronavirus protein that binds with the viral genome to form the ribonucleoprotein. It plays a critical role in viral RNA

transcription and replication<sup>147</sup>, making it a potential antiviral drug target. Recent studies showed that N protein is a multi-functional protein responsible for binding to the viral RNA genome and packing it into a long helical nucleocapsid structure<sup>148</sup>. It is also reported to regulate host-pathogen interaction and induce protective immune responses<sup>149</sup>.

The Medhi group<sup>22</sup> identified two potential hit compounds, ZINC00003118440 and ZINC0000146942, both of which might bind the RNA-binding N-terminal domain of SARS-CoV-2 N protein, which were theophylline and pyrimidine derivatives, respectively. Thereafter, Kang et al.<sup>150</sup>, for the first time, resolved the X-ray crystal structure of SARS-CoV-2 N protein at a resolution of 2.7 Å, revealing the specific surface charge distributions that facilitates the drug discovery specific to ribonucleotide binding domain of SARS-CoV-2 N protein.

### 5.3. Others

Studies have shown that the genome sequence of SARS-CoV-2 is very similar to that of SARS-CoV. Several SARS-CoV-2 proteins with > 90% sequence similarity, such as S protein, 3CLpro, PLpro, RdRp and 2'-O-MTase, could be used as drug targets. Meanwhile, many small molecules have been described as potential drug candidates for treatment of COVID-19, but their targets have not been identified. Some of these small-molecule drugs, are summarized below.

#### 5.3.1. Broad-spectrum antiviral compounds

Early in the COVID-19 pandemic, some anti-flu drugs (for example, oseltamivir) were applied to treat COVID-19 patients<sup>151</sup>. Yamamoto et al.<sup>152</sup> reported that nine approved HIV-1 protease inhibitors exhibited antiviral activity against SARS-CoV-2 *in vitro*. Among these inhibitors, tipranavir [Fig. 6 (54)], IC<sub>50</sub> = 13.34 μmol/L, CC<sub>50</sub> = 76.80 μmol/L, SI = 5.76, ritonavir [Fig. 5A-2 (41)], IC<sub>50</sub> = 8.63 μmol/L, CC<sub>50</sub> = 74.11 μmol/L, SI = 8.59, saquinavir [Fig. 6 (55)], IC<sub>50</sub> = 8.83 μmol/L, CC<sub>50</sub> = 44.43 μmol/L, SI = 5.03, atazanavir [Fig. 6 (56)], IC<sub>50</sub> = 9.36 μmol/L, CC<sub>50</sub> > 81 μmol/L, SI > 8.65 and nelfinavir [Fig. 5A-2 (34)], IC<sub>50</sub> = 1.13 μmol/L, CC<sub>50</sub> = 24.32 μmol/L, SI = 21.52 all exhibited antiviral activity (Table 2). Notably, nelfinavir effectively inhibited SARS-CoV-2 replication at a low concentration and exhibited the high SI among of them<sup>152</sup>, indicated that nelfinavir is a potential drug

candidate for the treatment of COVID-19 and should therefore be evaluated in patients with SARS-CoV-2 infection.

#### 5.3.2. Screening of FDA-approved drugs for the prevention of SARS-CoV-2

Repurposing of approved drugs is a time-saving strategy for drug development. In this way, Touret et al.<sup>146</sup> screened the Prestwick Chemical Library composed of 1520 approved drugs in an SARS-CoV-2-infected cell-based assay. The results showed that 15 molecules exhibited inhibition of SARS-CoV-2 replication *in vitro*. Among of them, 11 compounds exhibited antiviral potency with  $2 < \text{IC}_{50} \leq 20 \mu\text{mol/L}$ . Two of them with the highest antiviral activity were obtained from azithromycin [Fig. 6 (57), IC<sub>50</sub> = 2.12 μmol/L, SI > 19] and hydroxychloroquine [Fig. 9 (76), IC<sub>50</sub> = 4.17 μmol/L, SI > 10] and were therefore selected for clinical trials (Table 2)<sup>153</sup>. Among of them, spiperone [Fig. 6 (58)], a dopaminergic D2 antagonist, which was already identified as an antiviral molecule against the human pathogenic polyomaviruses<sup>154</sup>, showed most potent antiviral activity against SARS-CoV-2 infection with an IC<sub>50</sub> of 2.49 μmol/L and SI value of 16 (Table 2). The next three most efficient drugs were opipramol dihydrochloride [Fig. 6 (59), IC<sub>50</sub> = 5.05 μmol/L, SI > 7.9], a tricyclic antidepressant, quinidine hydrochloride [Fig. 6 (60), IC<sub>50</sub> = 5.11 μmol/L, SI > 7.8], an antiarrhythmic drug, and alprostadil [Fig. 6 (61), IC<sub>50</sub> = 5.39 μmol/L, SI > 7.4], a prostaglandin known as a cardiovascular drug. The remaining nine drugs out of 15 showed  $1.0 < \text{SI} < 5.3$  (Table 2)<sup>146</sup>. Some of these candidates may provide information to guide downstream experiments in small animal models, discover more effective derivatives, or evaluate drug combinations *in vitro* with potential enhancement of efficacy.

Ivermectin [Fig. 6 (62)], an FDA-approved antiparasitic agent with a broad spectrum of activity, high efficacy and a broad safety profile, is reported to have potent antiviral activity against HIV-1 and dengue virus by inhibiting protein nuclear import<sup>155,156</sup>. Caly et al.<sup>157</sup> found that ivermectin could inhibit SARS-CoV-2 replication with an IC<sub>50</sub> of ~2 μmol/L *in vitro* (Table 2), demonstrating that it is worthy of further research to treat COVID-19.

The repurposed drug anakinra in a phase III randomized clinical trial was able to reduce the requirement of invasive mechanical ventilation and mortality rate in severe COVID-19 cases without serious side effects<sup>158</sup>.

Five FDA-approved drugs, including penciclovir [Fig. 6 (63)], were reevaluated for their effects on cytotoxicity, viral production,

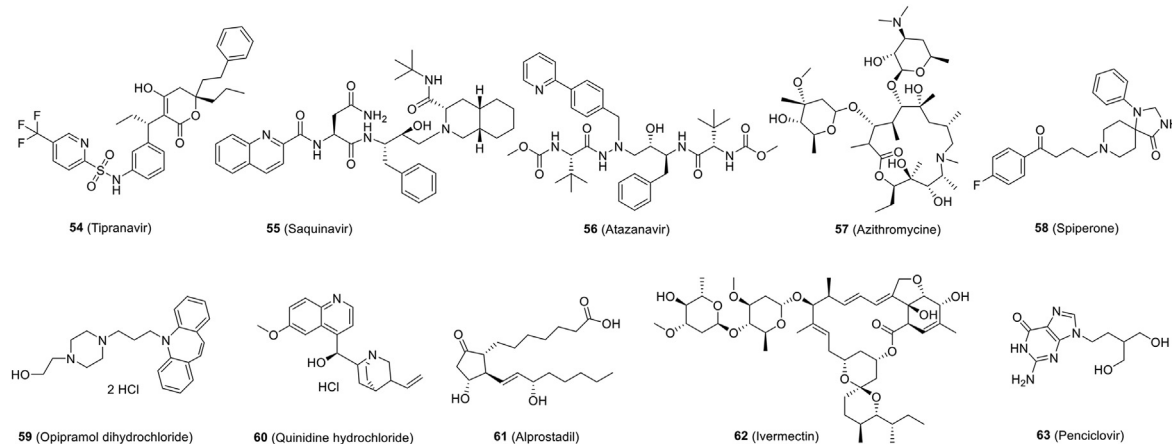


**Figure 6** Chemical structures of other small-molecule inhibitors against SARS-CoV-2.

and infection rates of SARS-CoV-2 by using standard methods<sup>19</sup>. The results showed that penciclovir inhibited viral infection with an IC<sub>50</sub> value of 95.96 μmol/L (Table 2), which was far from satisfactory compared to other compounds tested at the same time. However, some data indicated that compounds with high IC<sub>50</sub> values may have surprising antiviral activity *in vivo*<sup>127</sup>. Therefore, it is necessary to detect the antiviral activity of these compounds *in vivo*.

## 6. Small-molecule SARS-CoV-2 inhibitors targeting host proteins

Based on existing treatments, new SARS-CoV-2 mutations are likely to be resistant to drugs. Therefore, an initial suggestion is to use host-targeting therapeutic approach to reduce the aggressiveness and mortality resulted from SARS-CoV-2 infections.

### 6.1. Inhibitors targeting ACE2 to block the interaction between S protein and ACE2

Many studies have shown that host ACE2 is the specific receptor for SARS-CoV-2 S protein<sup>5,10</sup>. Inhibitors that block the binding between S protein and ACE2 have been considered to use for treatment of COVID-19 by preventing virus entry into the host cells. Candesartan and olmesartan [Fig. 7 (64, 65)], which are angiotensin II receptor blockers (ARBs), as reported, play a key role in virus entry<sup>23,159,160</sup>. Clinical trials will also be conducted on another ARB derivative, telmisartan [Fig. 7 (66), Clinical Trials gov, NCT04356495]<sup>161</sup>. In addition, blockers of angiotensin receptor one, such as losartan [Fig. 7 (67)], as inhibitors of the renin-angiotensin system, could be a useful therapeutic option in reducing lung inflammation and pneumonia in COVID-19 patients<sup>162,163</sup>. Currently on the clinical trial website, losartan is being used to study its effect on suppress the pathologic damage in inpatients and outpatients with COVID-19 and its safety to the COVID-19 patients with respiratory failure (Table 3)<sup>164,165</sup>.

An anthraquinone compound, emodin, which derived from genus *Rheum* and *Polygonum*, can interfere with the interactions between S protein and ACE2 by competing with ACE2 and inhibiting the 3a ion channel of coronavirus<sup>166,167</sup>. Promazine is an anti-psychotic drug that shares a similar structure with emodin and presents comparable inhibitory effect on the replication of

SARS-CoV with a similar mechanism of action<sup>168</sup>. Based on the similarity of S protein sequences between SARS-CoV-2 and SARS-CoV, we could conclude that emodin and promazine may inhibit SARS-CoV-2 infection by blocking the binding between S protein and ACE2, and both of them are considered as potential drugs for the treatment of COVID-19<sup>168–170</sup>.

Nicotianamine, a unique secondary metabolite in soybean, is a potent inhibitor of ACE2<sup>171</sup>, and it is considered as a potential drug candidate for the treatment of COVID-19<sup>172,173</sup>. Similarly, flavonoids were also a class of natural products which possess antioxidant, anti-inflammatory and antiviral functions. Lead flavonoids (*e.g.*, hesperidin, naringin, ECGC and quercetin) screened out by molecular docking might serve as cell entry inhibitors by targeting S protein or ACE2<sup>174</sup>.

### 6.2. TMPRSS2 inhibitors

SARS-CoV-2 attaches to the ACE2 receptors *via* S protein, which is subsequently cleaved by TMPRSS2, a host serine protease that has been exploited as therapeutic targets. Hoffmann and colleagues demonstrated that the TMPRSS2 inhibitors proved useful in blocking virus entry<sup>10</sup>.

Camostat mesylate [Fig. 8 (68)], a TMPRSS2 inhibitor in clinical, significantly reduced SARS-CoV-2 pseudovirus entry into Calu-3 cells with an IC<sub>50</sub> of ~1 μmol/L with no cytotoxic effects (CC<sub>50</sub> > 500 μmol/L, Table 3)<sup>10</sup>. Similarly, camostat mesylate was effective significantly in reducing Calu-3 authentic SARS-CoV-2 infection in Calu-3 cells and SARS-CoV-2 pseudovirus infection in primary human lung cells<sup>10</sup>. A randomized phase 2a clinical trial (Clinical Trials gov, NCT04321096) and double-blinded, randomized, placebo-controlled phase four trials in (Clinical Trials gov, NCT04338906) were performed to evaluate the activity of camostat mesylate as a treatment for SARS-CoV-2 infection. Bromhexine, a generic mucolytic, is a TMPRSS2 inhibitor<sup>175</sup>, which is currently being evaluated clinically as a treatment for COVID-19 (Clinical Trials gov, NCT04273763). In order to evaluate the impact of bromhexine on COVID-19 treatment, a larger phase one clinical trial with 140 participants (Clinical Trials gov, NCT04340349) was performed, including treatment with bromhexine alone or in combination with hydroxychloroquine sulfate. A broad-spectrum serine protease

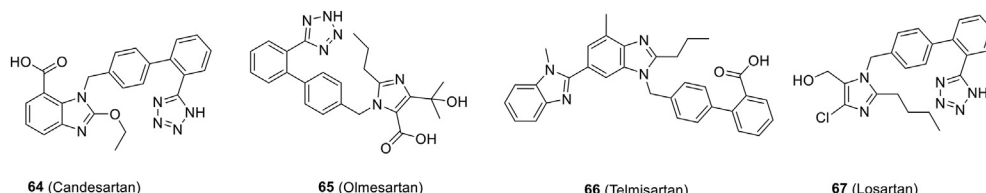


Figure 7 Chemical structures of small-molecule inhibitors targeting ACE2.

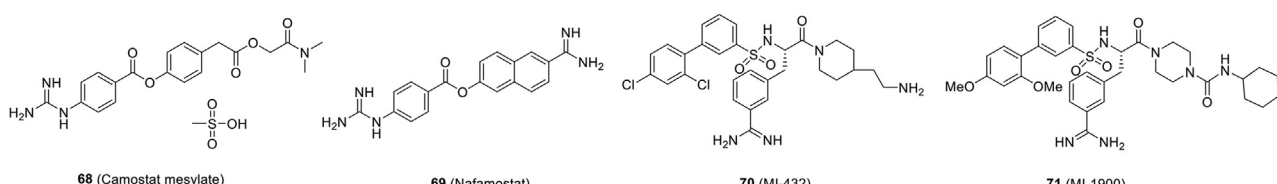


Figure 8 Chemical structures of small-molecule inhibitors targeting TMPRSS2.

inhibitor, nafamostat [Fig. 8 (69)], could inhibit the activity of TMPRSS2. Experiments have shown that nafamostat mesylate can inhibit SARS-CoV-2 infection to human lung cells<sup>176</sup>. Standard assays were also carried out by Wang et al.<sup>19</sup> to test the effects of nafamostat on the cytotoxicity, virus yield and infection rates of SARS-CoV-2, and the results demonstrate that the IC<sub>50</sub> value of nafamostat is 22.50 μmol/L with cytotoxicity CC<sub>50</sub> > 100 mmol/L (Table 3). In another article, nafamostat mesylate inhibited SARS-CoV-2 infection CPE in Calu-3 cells with an IC<sub>50</sub> of around 10 nmol/L<sup>177</sup>. Furthermore, Asakura and Ogawa<sup>178</sup> claimed that the combination of nafamostat and heparin may be effective against COVID-19 from the perspectives of antiviral and anti-DIC (disseminated intravascular coagulation) with enhanced fibrinolysis symptoms for COVID-19 patients. In addition, a randomized clinical trial was conducted to the evaluated ability of nafamostat to slow down lung disease for adult COVID-19 patients (Clinical Trials gov, NCT04352400).

MI-432<sup>179</sup> and MI-1900 [Fig. 8 (70, 71)] are two TMPRSS2 inhibitors, which are prospective peptide mimetic inhibitors<sup>180</sup>. The inhibitor MI-1900 is the less polar analog of MI-432. Recently, MI-432 showed inhibition against SARS-CoV-2 infection in Calu-3 cells, which reduced by 75-fold virus titer at a concentration of 10 μmol/L, and MI-1900 exhibited strong inhibition of SARS-CoV-2 replication at 50 μmol/L and reduced by 35- to 280-fold viral titers (Table 3)<sup>180</sup>.

### 6.3. Cathepsin B/L

In addition to TMPRSS2, cathepsin B and cathepsin L, being active in the early and late endosome, respectively, can also trigger viral S protein cleavage and promote viral fusion<sup>181,182</sup>.

P9, derived from mouse β-defensin-4, is a peptide that interfere cathepsin L activity, which showed antiviral activity against

SARS-CoV, MERS-CoV, and influenza viruses through the inhibition of endosomal acidification thus indirectly interfering cathepsin L activity<sup>183</sup>. The researchers optimized P9 by replacing arginine with the weakly positively charged amino acids (histidine and lysine) to generate P9R, which showed significantly higher potency against SARS-CoV-2 infection than P9, as determined by a plaque reduction assay in Vero E6 cells (0.9 vs. 2.4 μg/mL, Table 1). And the CC<sub>50</sub> of P9R was >300 μg/mL in MDCK, Vero E6 and A549 cells<sup>184</sup>. Further, the authors describe an eight-branched derivative, 8P9R, that showed more potent antiviral activity (IC<sub>50</sub> = 0.3 μg/mL) in high salt condition (PBS) than that of P9R in Vero E6 cells. The cytotoxicity assay indicated that CC<sub>50</sub> of 8P9R was higher than 200 μg/mL in Vero E6 cells (Table 1). The 8P9R can inhibit the two entry pathways of SARS-CoV-2 in cells including endocytic pathway and TMPRSS2-mediated surface pathway by aggregating viral particles. In addition, 8P9R, or the combination of repurposed drugs, arbidol, chloroquine and camostat could significantly suppress SARS-CoV-2 replication in hamsters and SARS-CoV in mice<sup>185</sup>.

Amantadine and chlorpromazine [Fig. 9 (72, 73)], which were previously used to abrogate viral entry via clathrin-mediated endocytosis<sup>24,186</sup>, proved to have no prominent antiviral efficacy against SARS-CoV-2 and only a partial inhibition at 100 μmol/L for amantadine in Vero E6 cells (Table 3)<sup>187</sup>. E64-d [Fig. 9 (74)], a broad cathepsin B/L inhibitor, showed inhibitory activity against SARS-CoV-2 pseudovirus infection with an IC<sub>50</sub> of ~4.487 μmol/L in Vero E6 cells (Table 3).

Chloroquine [Fig. 9 (75)] prevents viral infection by increasing the endosomal pH, which, in turn, inhibits hydrolytic activity of cathepsin L<sup>19</sup>. In *in vitro* experiments, chloroquine showed strong inhibitory activity against SARS-CoV-2 with an EC<sub>50</sub> of 1.13 μmol/L, CC<sub>50</sub> > 100 μmol/L and SI > 88.50 (Table 3) in Vero E6 cells (MOI = 0.05)<sup>19</sup>. Hydroxychloroquine [Fig. 9 (76)] is a

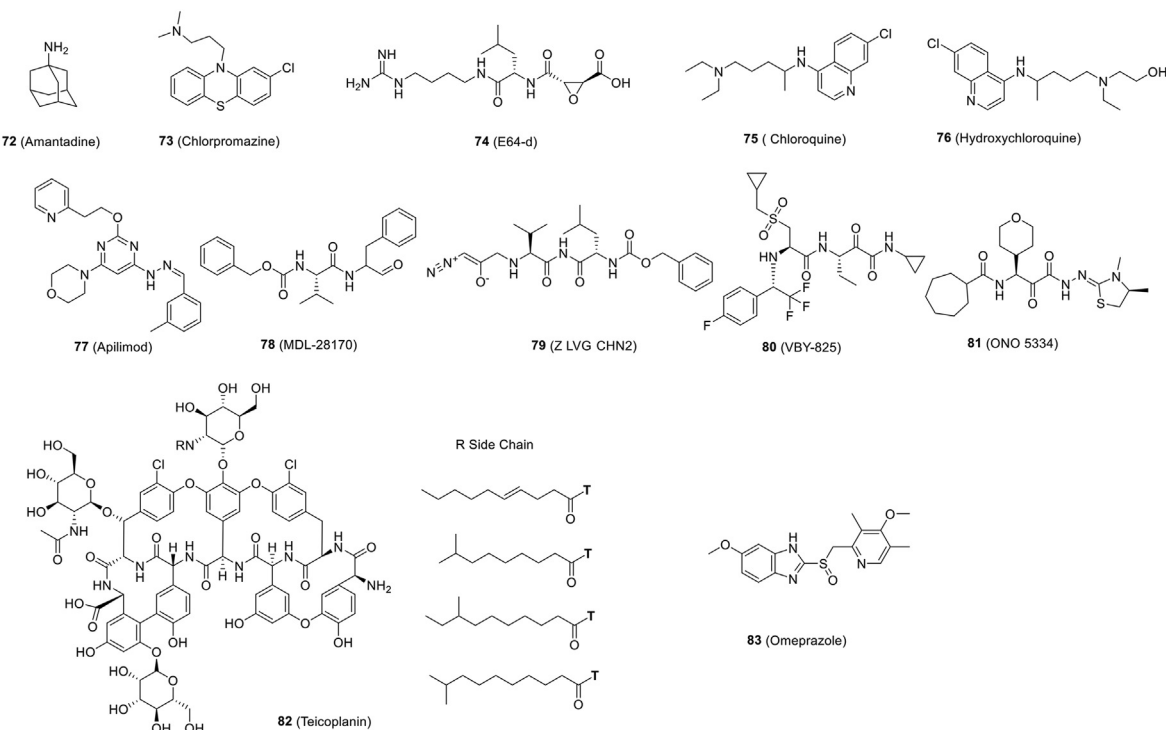


**Figure 9** Chemical structures of small-molecule inhibitors targeting cathepsin B/L.

derivative of chloroquine and is used to treat autoimmune diseases. The Chinese Clinical Trials Registry has documented several clinical trials using chloroquine or hydroxychloroquine for COVID-19<sup>188,189</sup>. Consequently, some research groups compared hydroxychloroquine with chloroquine for inhibitory against SARS-CoV-2 *in vitro*. The results showed that hydroxychloroquine had lower antiviral activity compared to chloroquine, at least at certain MOIs (Table 3)<sup>189</sup>. Although it was proven that chloroquine could inhibit SARS-CoV-2 infection in Vero cells, it does not block SARS-CoV-2 infection in the TMPRSS2-expressing Calu-3 cells<sup>190</sup>. The Maisonnasse group<sup>191</sup> tested different treatment strategies for hydroxychloroquine in rhesus macaques, including comparison with placebo treatment alone or in combination with azithromycin in macaques. Neither hydroxychloroquine nor the combination of hydroxychloroquine and azithromycin showed a significant effect on viral load in any of the analyzed tissues. The U.S. FDA has withdrawn its EUA status given to chloroquine and hydroxychloroquine in view of these recent developments. The latest clinical results of hydroxychloroquine were also published by WHO in the interim results of the Solidarity Trial of antiviral drugs for the treatment of COVID-19. The results showed that hydroxychloroquine cannot significantly reduce mortality of COVID-19 hospitalized patients. At the same time, it cannot reduce the rate of mechanical ventilation (intubation) and duration of hospital stay<sup>124</sup>.

To identify candidate therapeutics for COVID-19, Riva et al.<sup>68</sup> screened a drugs library consisting of approximately 12,000 clinical-stage or FDA-approved small molecules. They reported the identification of 21 molecules that inhibit SARS-CoV-2 infection in a dose-dependent manner. Five of the most potent compounds, apilimod [Fig. 9 (77)] and the cysteine protease inhibitors MDL-28170, Z LVG CHN2, VBY-825 and ONO 5334 [Fig. 9 (78–81)], were effective against SARS-CoV-2 infection with IC<sub>50</sub>s of 0.023, 0.22, 0.19, 0.3 and 0.41 μmol/L, respectively, in Vero E6 cells (Table 3). As reported, MDL-28170, a cathepsin B inhibitor, could impairs infection by SARS-CoV and Ebola virus<sup>192,193</sup>, ONO 5334 is a cathepsin K inhibitor<sup>194</sup>, and VBY-825 acts as a reversible cathepsin protease inhibitor<sup>195</sup>. Apilimod, a specific PIKfyve kinase inhibitor, was shown to be effective in inhibiting virus entry, which is in agreement with the report that PIKfyve is predominately presented in early endosomes and plays an important role in maintaining endomembrane homeostasis<sup>196</sup>. Another study reported that apilimod inhibits infection with authentic SARS-CoV-2 strain 2019-nCoV/USA-WA1/2020 virus in Vero E6 cells with an IC<sub>50</sub> of ~10 nmol/L (Table 3)<sup>197</sup>. Z LVG CHN2 probably acts as inhibitor of an endosomal protease<sup>198</sup>. Notably, MDL-28170, ONO 5334 and apilimod exhibited inhibitory activity against viral replication in human pneumocyte-like cells that derived from induced pluripotent stem cells, and apilimod displayed antiviral activity in a primary human lung explant model<sup>68</sup>.

Teicoplanin [Fig. 9 (82)], a currently used antibiotic in the treatment of Gram-positive bacterial infection, showed to be active against SARS-CoV, MERS-CoV and Ebola virus *in vitro*<sup>199,200</sup>. In the reports of Zhang et al.<sup>201</sup>, teicoplanin acts on the early step of coronavirus viral life cycle through directly inhibiting the enzymatic activity of cathepsin L. The concentration of teicoplanin required to inhibit 50% of SARS-CoV-2 pseudoviruses into the cytoplasm was only 1.66 μmol/L (Table 3) in HEK293T cells, which is much lower than the commonly used 8.78 μmol/L dose to inhibit Gram-positive bacteria<sup>201</sup>. Baron and

coworkers encourage further investigation of teicoplanin for the treatment of COVID-19<sup>199</sup>. Dalbavancin, a homolog of teicoplanin, also showed inhibitory activity against SARS-CoV-2 entry in a dose-dependent manner<sup>201</sup>.

Touret et al.<sup>146</sup> found that omeprazole [Fig. 9 (83)] can inhibit SARS-CoV-2 with IC<sub>50</sub> of 17.06 μmol/L and CC<sub>50</sub> > 40 μmol/L in Vero E6 cells (Table 3). Omeprazole, a proton pump inhibitor used as an antiulcer agent, has been demonstrated to increase the pH of endosomal/Golgi pathway either by inhibiting ATPase proton pomp, or by buffering the pH. This endosomal pH modification will limit the processing of S protein by endosomal proteases, thereby blocking the entry of viruses mediated by the membrane fusion process<sup>146</sup>.

The 3CLpro calpain inhibitors II/XII are also reported to be active against human cathepsin L<sup>88</sup>. Calpain inhibitors II/XII inhibit the activity of cathepsin L with IC<sub>50</sub>s of 0.41 and 1.62 nmol/L, respectively<sup>88</sup>. One of the advantages of calpain inhibitors II and XII, as dual inhibitors, is their ability to target the viral protease 3CLpro and the human protease cathepsin L, thus showing better drug effects at lower doses. Another advantage is that they can inhibit drug resistance.

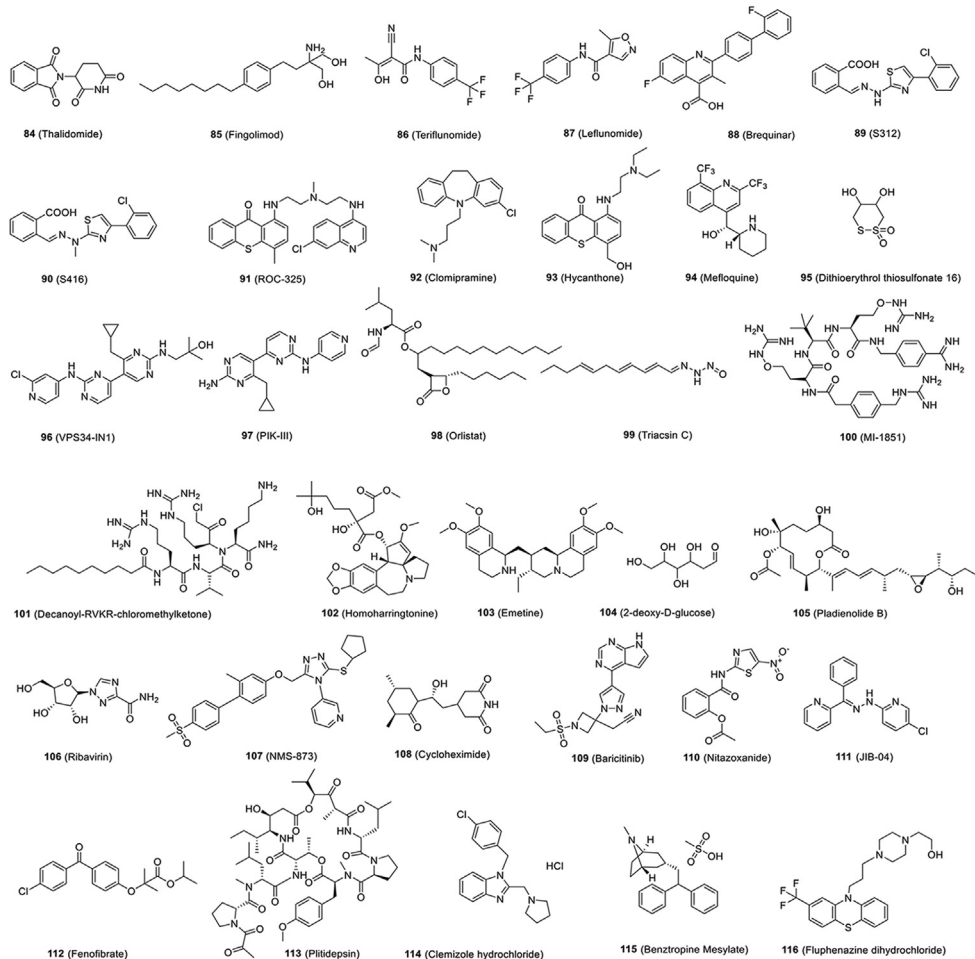
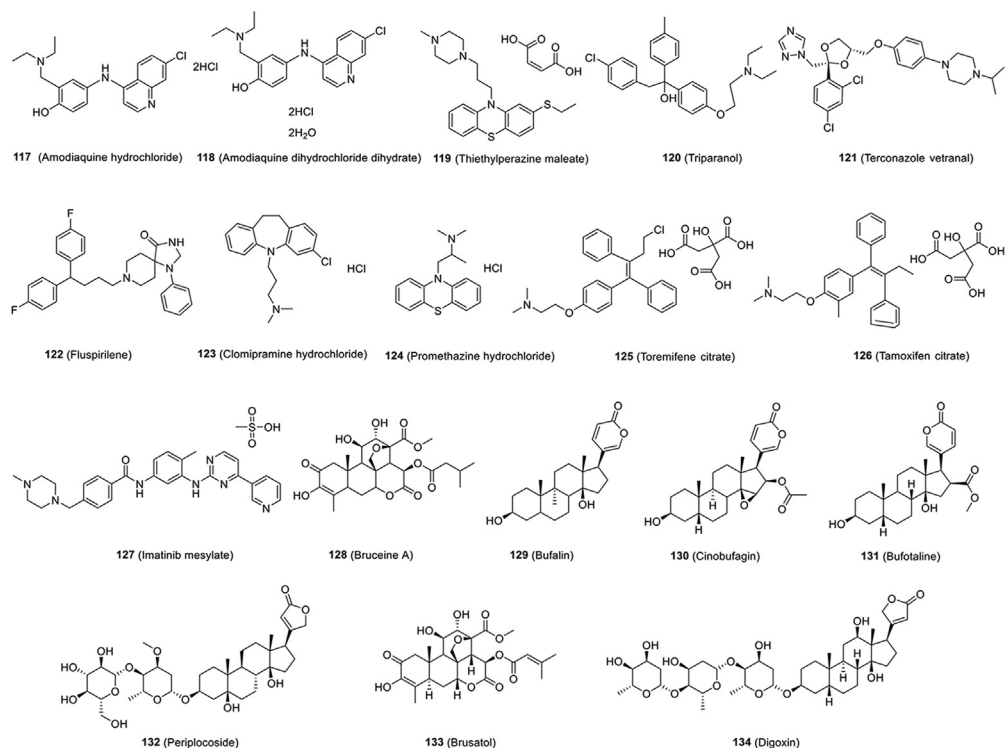
Cathepsin B/L are crucial elements of the lysosomal pathway, and disruption of these host cell proteases offers potential for COVID-19 therapies. Smieszek et al.<sup>202</sup> conducted a HTS to identify compounds that could downregulate the expression of cathepsin L/cathepsin B. Amantadine (10 μmol/L) can downregulate the expression of the cathepsin L gene, which appears to further disrupt the lysosomal pathway. Based on this, researchers believe that amantadine can reduce the viral load in SARS-CoV-2-positive patients and that it may be used as an effective treatment to reduce virus replication and infectivity, which may lead to better clinical outcomes.

#### 6.4. Others

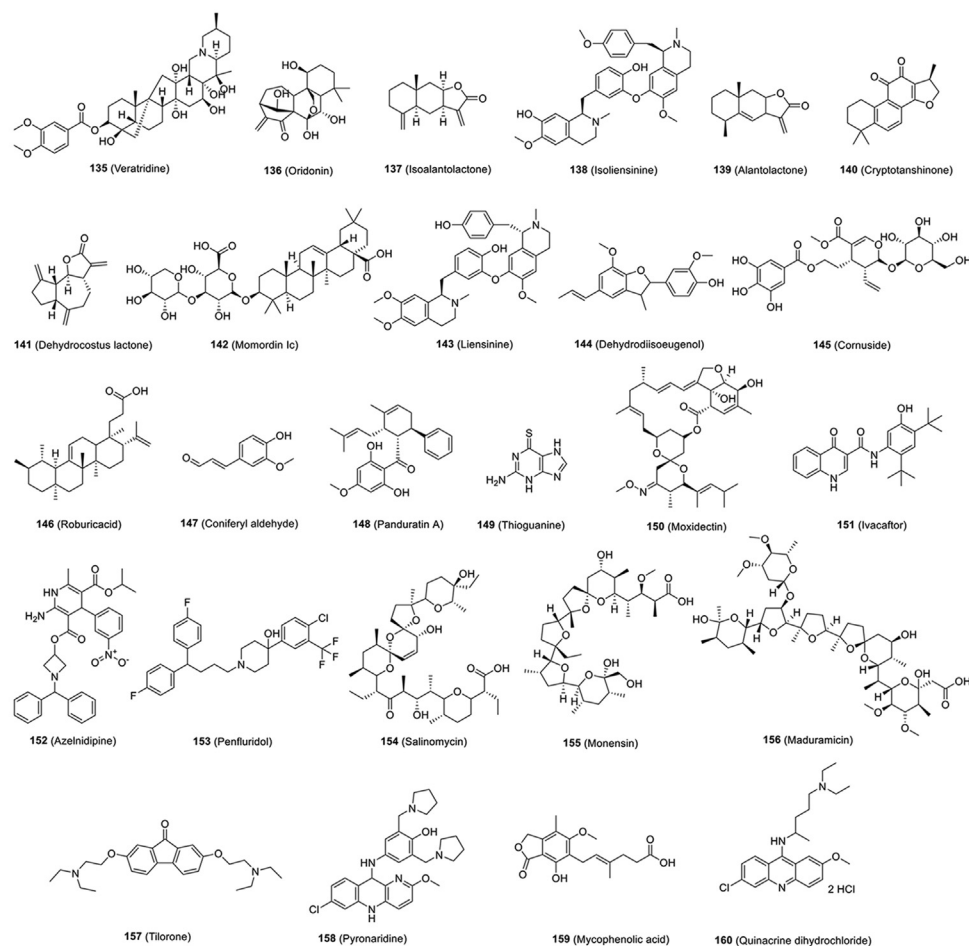
Innate immune response plays roles in combating coronavirus infection, while interferon can enhance the immune responses<sup>25</sup>. In human cells, blockage of the signal pathway required for viral replication is expected to exhibit some antiviral effect.

In patients infected with SARS-CoV-2, histological examination showed a strong cytokine storm and inflammatory response, and with the release of large amounts of interleukin (IL)-6, excessive inflammation and further lung damage resulted<sup>26,203</sup>. Thalidomide [Fig. 10A (84)] has anti-inflammatory activity owing to its ability to accelerate the degradation of messenger RNA in blood cells, thereby reducing tumor necrosis factor-α. In addition, thalidomide can increase the secretion of interleukins, such as IL-12, and activate natural killer cells<sup>204</sup>. Thalidomide was one of many drugs redirected after the COVID-19 outbreak and used in clinical trials to treat COVID-19 patients (Table 3)<sup>205</sup>. It is a treatment for cancer and inflammatory diseases, but it is currently being used in two phase two clinical trials in combination with low-dose hormone therapy and adjuvant therapy for COVID-19.

Multiple sclerosis (MS) is an immune-mediated neurological disease that requires long-term immunotherapy and has been shown to increase the risk of SARS-CoV-2 infection<sup>206</sup>. Fingolimod [Fig. 10A (85)], a sphingosine-1-phosphate receptor immunomodulator, which is effective in the treatment of MS and is currently being tested as a treatment for COVID-19-associated acute respiratory distress syndrome (Table 3)<sup>205,207</sup>. A patient with MS infected with SARS-CoV-2 was treated with fingolimod and had a favorable outcome<sup>206</sup>.

**A****B**

**Figure 10** Chemical structures of other small-molecule inhibitors targeting host.

**C****Figure 10** (continued)

In one study, Hu et al.<sup>208</sup> evaluated leflunomide for COVID-19 treatment with a small cohort of patients, while the active metabolite of leflunomide, teriflunomide [Fig. 10A (86)], as an approved DHODH inhibitor, has been approved for treating autoimmune diseases<sup>209</sup>. They also proved that teriflunomide conferred a profound antiviral efficacy of  $IC_{50} = 6 \mu\text{mol/L}$  in SARS-CoV-2-infected cells at MOI of 0.03 (Table 3). Clinical data show that patients treated with leflunomide had shorter viral shedding time (median of 5 days) than that of the controls (median of 11 days). The C-reactive protein levels of patients given leflunomide also decreased significantly, indicating that immunopathological inflammation was well controlled. In leflunomide-treated patients, no obvious adverse reactions were observed<sup>208</sup>. This small-scale preliminary study on the compassionate use of leflunomide provides data basis for leflunomide as a potential therapeutic for COVID-19 in the future.

By virtual screening, Xiong et al.<sup>210</sup> identified two potent human DHODH inhibitors with the same novel scaffold, S312 and S416, which is obviously different from those of leflunomide/teriflunomide<sup>208</sup> or brequinar<sup>211</sup>. All compounds of teriflunomide, leflunomide, brequinar, S312, and S416 [Fig. 10A (86–90)] showed inhibitory effects against SARS-CoV-2 (at MOI = 0.05), with  $IC_{50}$ s of 26.06, 41.49, 0.123, 1.56 and 0.017  $\mu\text{mol/L}$  and  $CC_{50}$ s of 850.5, 879.0, 231.3, 158.2 and 178.6  $\mu\text{mol/L}$ , respectively<sup>210</sup> (Table 3). These results indicate that both S312/S416 and

leflunomide/teriflunomide, which have dual actions of antiviral and immunoregulation, may have the clinical potential to cure SARS-CoV-2.

Chloroquine and hydroxychloroquine, which are widely studied as clinical drugs for COVID-19, have a variety of cellular effects, including alkalizing lysosomes and blocking autophagy. Therefore, Gorshkov et al.<sup>212</sup> evaluated additional lysosomotropic compounds to identify drugs that inhibit SARS-CoV-2. Six compounds (ROC-325, clomipramine, hycanthone, chloroquine, hydroxychloroquine and mefloquine) [Fig. 10A (91–93), Fig. 9 (75, 76), Fig. 10A (94)] showed inhibition of SARS-CoV-2 infection in Vero E6 cells with  $IC_{50}$ s ranging from 2.0 to 13  $\mu\text{mol/L}$  (Table 3) and SIs ranging from 1.5- to > 10-fold. In the EpiAirway 3D tissue model, these compounds exhibited a variety of functions, including prevention of lysosome function and autophagy and the entry of pseudotyped particles, increase of the pH of the lysosome, and reduction of (ROC-325) viral titers.

In order to enter and infect cells, viruses use a series of strategies to take advantage of the cellular and biochemical properties of cell membranes. As demonstrated, one of the entry mechanisms used by HIV was thiol-mediated uptake<sup>213</sup>. Cheng et al.<sup>214</sup> systematically screened many effective inhibitors using fluorescent cyclic oligochalcogenides that enter cells by thiol-mediated uptake. Preliminary results on SARS-CoV-2 pseudovirus infection

showed that the most potent activities were found for dithioerythritol thiosulfonate 16 [Fig. 10A (95)] with an IC<sub>50</sub> of around 50 μmol/L, while toxicity was detected only at 500 μmol/L<sup>214</sup>. This study revealed that thiol-mediated uptake may be an interesting research direction for the development of future anti-SARS-CoV-2 drugs.

Halfon et al.<sup>215</sup> reported that GNS561 showed most potent anti-viral effect against two SARS-CoV-2 strains (IC<sub>50</sub> = 0.006 μmol/L for USA-WA1/2020 and IC<sub>50</sub> = 0.03 μmol/L for IHU MI6; MOI = 0.1) compared to chloroquine and remdesivir (Table 3). GNS561, located in LAMP2-positive lysosomes, together with SARS-CoV-2, blocked autophagy by increasing the size of LC3-II spots and increasing the volume of autophagic vacuoles in the cytoplasm with the presence of multilamellar bodies characteristic of a complexed autophagy<sup>215</sup>.

VPS34 is a multifunctional protein involved in autophagy, endocytosis and other processes. Two well-characterized VPS34 inhibitors, VPS34-IN1 [Fig. 10A (96)]<sup>216</sup> and PIK-III [Fig. 10A (97)]<sup>217</sup>, showed anti-SARS-CoV-2 effects at a MOI of 0.01 with IC<sub>50</sub>s of 0.29 and 0.202 μmol/L in Vero E6 cells, respectively. However, both VPS34-IN1 and PIK-III exhibited strong cytotoxicity at 50 and 16.67 μmol/L in Vero E6 cells, respectively (Table 3)<sup>218</sup>. Orlistat and triacsin C [Fig. 10A (98, 99)] inhibit fatty acid metabolism, which have exhibited antiviral activity<sup>219,220</sup>. Both compounds also exhibited antiviral activity against SARS-CoV-2 with IC<sub>50</sub>s of 422.3 and 19.5 μmol/L in Vero E6 cells, respectively (Table 3) and did not induce obvious cytotoxicity, even at the high concentrations of 50 and 500 μmol/L, respectively. Time-of-addition studies show that these four inhibitors act at the post-entry step in the virus life cycle. Next, the researchers explored if these inhibitors were effective in Calu-3 by directly measuring production of infectious SARS-CoV-2 and cytotoxicity. IC<sub>50</sub>s of 0.55 μmol/L (VPS34-IN1), 0.12 μmol/L (PIK-III), 21.25 μmol/L (orlistat), and 0.04 μmol/L (triacsin C), and CC<sub>50</sub>s of > 50 μmol/L (VPS34-IN1), > 50 μmol/L (PIK-III), > 1 mmol/L (orlistat), and > 50 μmol/L (triacsin C) were reported at the same time (Table 3)<sup>218</sup>.

MI-1851 [Fig. 10A (100)], a furin inhibitor, efficiently inhibited SARS-CoV-2 multiplication in Calu-3 cells, which produced a 30- to 190-fold reduction in virus titers at 10 μmol/L (Table 3). Combining various TMPRSS2 inhibitors (MI-432 or MI-1900) with furin inhibitor MI-1851 exhibited more potent antiviral activity against SARS-CoV-2 than any TMPRSS2 or furin inhibitor in an equimolar amount<sup>180</sup>. In addition, decanoyl-RVKR-chloromethylketone, a peptidomimetic furin inhibitor [Fig. 10A (101)] was shown to block SARS-CoV-2 S processing and inhibit SARS-CoV-2 infection with an IC<sub>50</sub> of 0.057 μmol/L by plaque reduction assay<sup>221</sup> (Table 3).

Homoharringtonine and emetine [Fig. 10A (102, 103)] showed antiviral activity against SARS-CoV-2 with IC<sub>50</sub>s of 2.55 and 0.46 μmol/L in Vero E6 cells, respectively (Table 3)<sup>99</sup>. Homoharringtonine has been reported to have antitumor activity by inhibiting protein transcription via its binding the site for ribosomal A<sup>222,223</sup>. Homoharringtonine has shown effective antiviral activity against herpes virus, coronavirus, rhabdoviruses and other viruses<sup>222,224,225</sup>. Emetine is a protein synthesis inhibitor, inhibits malaria through binding to the ribosomal E site of *Plasmodium falciparum*<sup>226,227</sup>. However, potential cardiotoxicity has limited its clinical use in recent years.

Bojkova et al.<sup>228</sup> have identified SARS-CoV-2-modulated host cell pathways. Inhibition of these pathways could suppress SARS-CoV infection in human cells. A human cell-culture model

infected with a clinical isolate of SARS-CoV-2 was established to analyze the infection profile of SARS-CoV-2 by translatome and proteome proteomics. Their results showed that SARS-CoV-2 reshaped the central cellular pathways, such as translation, splicing, carbon metabolism, protein homeostasis and nucleic acid metabolism. Small-molecule inhibitors that target these pathways prevent the virus from replicating in cells. Indeed, inhibition of glycolysis by 2-deoxy-D-glucose [2-DG, Fig. 10A (104)], an inhibitor of hexokinase (*i.e.*, glycolysis), was previously shown to suppress rhinovirus infection in mice<sup>229</sup>. Blocking glycolysis with nontoxic concentrations of 2-DG inhibited SARS-CoV-2 replication in Caco-2 cells (Table 3)<sup>228</sup>. Pladienolide B [Fig. 10A (105)], a spliceosome inhibitor, targets the splicing factor SF3B1, which inhibited SARS-CoV-2 replication with an IC<sub>50</sub> of 0.007 μmol/L that were not toxic to human Caco-2 cells (Table 3)<sup>228</sup>. Next, the team performed gene ontology analysis and identified a major cluster of metabolic pathways consisting of diverse nucleic acid metabolism sub-pathways upon SARS-CoV-2 infection. The researchers further confirmed that the replication of coronavirus depends on availability of cellular nucleotide pools<sup>230</sup>. Compounds interfering with nucleic acid metabolism, such as ribavirin [Fig. 10A (106)], could inhibit SARS-CoV-2 replication at low micromolar (IC<sub>50</sub> = 0.07 μmol/L) and clinically achievable concentrations (Table 3)<sup>228,231</sup>. A clinical trial for ribavirin was recently initiated (Clinical Trials gov; NCT04356677). At the same time, NMS-873 [Fig. 10A (107)], a small-molecule inhibitor of ATP P97, could effectively inhibit SARS-CoV-2 replication at low nanomolar concentrations (IC<sub>50</sub> = 0.025 μmol/L, Table 3)<sup>140,228</sup>, revealing that these two types of inhibitors can be used as potential treatment options for SARS-CoV-2. Cycloheximide [Fig. 10A (108)], an inhibitor of translation elongation, significantly inhibited SARS-CoV-2 replication with an IC<sub>50</sub> of 0.17 μmol/L that are not toxic to human Caco-2 cells (Table 3)<sup>228</sup>.

AP-2-associated protein kinase 1 (AAK1) is a host kinase that regulates clathrin-mediated endocytosis<sup>232</sup>. Baricitinib [Fig. 10A (109)], a janus kinase inhibitor, is an AAK1-binding drug, which was supposed as a suitable drug candidate for COVID-19 because it can inhibit viral assembly by preventing AAK1-mediated endocytosis<sup>232</sup>. According to the EU Clinical Trials Register phases two and 3 (2020-001854-23), as well as phase-4 (2020-001354-22), clinical trials are now using baricitinib on COVID-19 patients (Table 3).

Nitazoxanide [Fig. 10A (110)] is an FDA-approved antibiotic for the treatment of diarrhea caused by *Giardia parvum* and *Giardia lamblia* and has broad-spectrum antiviral activity<sup>233</sup>. Nitazoxanide, which targets host-regulated processes involved in viral replication<sup>233</sup>, has shown *in vitro* activity against MERS-CoV and other animal coronaviruses<sup>234,235</sup>. The recent experimental result showed that nitazoxanide also had inhibitory activity against SARS-CoV-2 *in vitro* (IC<sub>50</sub> = 2.12 μmol/L; CC<sub>50</sub> > 35.53 μmol/L; SI > 16.76) (Table 3)<sup>19</sup>. In another study, nitazoxanide and JIB-04 [Fig. 10A (111)] had IC<sub>50</sub> values of 4.90 μmol/L and 695 nmol/L in Vero E6 cells (Table 3), respectively. JIB-04 is a pan-Jumonji histone demethylase inhibitor<sup>236</sup>. Neither drug induced cytotoxicity at 300 μmol/L and thus had excellent selectivity index (SI > 150)<sup>237</sup>. A recent review evaluated nine clinical trials of nitazoxanide for assessing the safety, cost and potential use of this drug for COVID-19<sup>238</sup>.

Rodon et al.<sup>187</sup> screened drugs that can combat SARS-CoV-2-induced CPE and virus replication *in vitro* from existing drugs approved for use in humans. Among of them, Fenofibrate [Fig. 10A (112)] is clinically used to treat dyslipidemia *via* activation

of PPAR $\alpha$ , and it also inhibited the CPE exerted by SARS-CoV-2 on Vero E6 cells at 20  $\mu\text{mol/L}$  (Table 3). Plitidepsin [Fig. 10A (113)], the most potent one, targets eukaryotic elongation factor 1A2 and has been previously used for the treatment of multiple myeloma<sup>187</sup>. White and colleagues also reported that plitidepsin exhibits antiviral activity against SARS-CoV-2<sup>239</sup>. Based on immunofluorescence technology, they tested the inhibitory effects of plitidepsin on SARS-CoV-2 replication in Vero E6 cells, hACE2-293 T cells and human lung cells with IC<sub>50</sub>s of 0.70, 0.73 and 1.62 nmol/L with limited toxicity in cell culture (Table 3). Meanwhile, they demonstrated the *in vivo* antiviral activity of plitidepsin in two SARS-CoV-2 infected mouse models with reduced viral replication in the lungs. Plitidepsin has also successfully completed a phase 1/2 clinical study for the treatment of COVID-19 (Clinical Trials gov, NCT04382066).

Nitric oxide (NO) is a gas with various biological activities produced by arginine through NO synthase. NO inhalation is beneficial for most patients with severe ARDS<sup>240</sup>. Inhalation of NO triggers the relaxation of smooth muscles in pulmonary blood vessels, leading to increased blood flow and adequate ventilation in the lungs<sup>241</sup>. NO showed inhibition of the synthesis of viral RNA and proteins<sup>242</sup>. Therefore, NO inhalation may be an effective method for the treatment of patients with severe COVID-19<sup>169,241</sup>.

Clemizole hydrochloride [Fig. 10A (114)], a potent inhibitor of transient receptor potential channel TRPC<sub>5</sub> and an orally bioavailable histamine H1 antagonist with potential antitumor and anti-allergic activities<sup>243</sup>, could prevent SARS-CoV-2 replication with an IC<sub>50</sub> of 23.94  $\mu\text{mol/L}$  and CC<sub>50</sub> > 40  $\mu\text{mol/L}$  in Vero E6 cells (Table 3)<sup>146</sup>.

Benztropine Mesylate [Fig. 10A (115)], an anticholinergic that works by blocking a certain natural substance (acetylcholine) is used to treat symptoms of Parkinson's disease or involuntary movement. It could inhibit SARS-CoV-2 replication with an IC<sub>50</sub> of 13.8  $\mu\text{mol/L}$  (MOI = 0.004) or 17.79  $\mu\text{mol/L}$  (MOI = 0.01) and CC<sub>50</sub> of >> 50  $\mu\text{mol/L}$  in Vero E6 cells by CellTiter-Glo assays (Table 3)<sup>244</sup>.

The Weston group presented data on the antiviral activity of several FDA-approved drugs against SARS-CoV-2, including mefloquine hydrochloride [Fig. 10A (94)], fluphenazine dihydrochloride, amodiaquine hydrochloride, amodiaquine dihydrochloride dihydrate, thiethylperazine maleate, triparanol, terconazole vetranal, fluspironilene, clomipramine hydrochloride, promethazine hydrochloride, toremifene citrate, tamoxifen citrate and imatinib mesylate [Fig. 10A and B (116–127)], and the IC<sub>50</sub> values of these drugs are at non-cytotoxic concentrations<sup>244</sup>. The IC<sub>50</sub>s at MOI = 0.01 and CC<sub>50</sub>s in Vero E6 cells of these drugs are shown in Table 3. Also, another team reported that toremifene and tamoxifen, as selective estrogen receptor modulators (SERMs), can affect ACE2 expression and offer a potential therapeutic approach for SARS-CoV-2<sup>170,245</sup>.

Zhang et al.<sup>246</sup> established a CPE-based HTS assay in Vero-E6 cells that are permissive to SARS-CoV-2 infection to screen for inhibitors aiming for the entire viral life cycle. They screened a library collection of natural compounds containing 1058 compounds to identify potential inhibitors of SARS-CoV-2 in cell culture. After the primary screening, 30 hits with > 50% protection from CPE were identified. Among them, 17 drugs are newly discovered inhibitors of SARS-CoV-2. They next evaluated the effects of 17 newly discovered anti-SARS-CoV-2 compounds (bruceine A, cinobufagin, bufotaline, periplocoside, brusatol, veratridine, oridonin, isoalantolactone, isoliensinine, alantolactone,

dehydrcostus lactone, momordinic, liensinine, dehydrodiisoeugenol, cornuside, roburicacid, coniferylaldehyde) and three previously reported coronaviruses inhibitors (bufalin, digoxin, and cryptotanshinone) [Fig. 10B (128–147)] by measuring the alterations of viral genome levels. All tested compounds showed inhibitory effects on virus propagation in a dose-dependent manner with the IC<sub>50</sub> values ranging from 0.011 to 11.03  $\mu\text{mol/L}$  (Table 3). According to the results of CCK-8 assay, the CC<sub>50</sub> values of these compounds were also calculated (Table 3).

Kanjanasirirat et al.<sup>247</sup> have used fluorescence-based SARS-CoV-2 nucleoprotein detection and plaque reduction assays to screen for antiviral candidates. Among 122 Thai natural products, they found that panduratin A [Fig. 10B (148)] could significantly inhibit SARS-CoV-2 infection in Vero E6 cells with IC<sub>50</sub> of 0.81  $\mu\text{mol/L}$  (CC<sub>50</sub> = 14.71  $\mu\text{mol/L}$ , Table 3). Their study also reported that treatment with panduratin A was able to inhibit viral infectivity in human airway epithelial cells.

Using cell-based infection assays, Jan et al.<sup>94</sup> have screened more than 3000 agents that have been applied in humans and animals, including 2855 small molecules and 190 traditional herbal medicines. They have identified 15 active small molecules in concentrations ranging from 0.1 nmol/L to 50  $\mu\text{mol/L}$  (Table 3), including nelfinavir [Fig. 5A-2 (34)], boceprevir [Fig. 5A-1 (28)], thioguanine [Fig. 10B (149)], cepharanthine [Fig. 4 (4)], emetine [Fig. 10A (103)], ivermectin [Fig. 6 (62)], moxidectin [Fig. 10B (150)], mefloquine [Fig. 10A (94)], ivacaftor, azelnidipine, penfluridol [Fig. 10B (151–153)], dronedarone [Fig. 5A-2 (44)], salinomycin, monensin and maduramicin [Fig. 10B (154–156)]. Mefloquine identified protected hamster disease models against challenge with SARS-CoV-2.

Puhl et al.<sup>248</sup> found that some drugs shown to have *in vitro* activity against Ebola also showed activity against SARS-CoV-2. Therefore, they tested three small-molecule drugs active against Ebola virus in various cell lines (VeroE6, Vero 76, Caco-2, Calu-3, A549-ACE2, HUH-7 and monocytes) infected with SARS-CoV-2<sup>248</sup>. The compilation of these results suggests that there is considerable variability in antiviral activity observed in different cell lines. They found that tilorone and pyronaridine [Fig. 10B (157, 158)] inhibited virus replication with IC<sub>50</sub>s of 180 and 198 nmol/L in A549-ACE2 cells, respectively (Table 3).

Hopefully, clofazimine was verified to inhibit SARS-CoV-2 by its interference with viral membrane fusion and the function of helicase, as well as upregulated gene expression of innate immune-related pathways in cells<sup>69</sup>.

## 7. Conclusions and perspectives

Despite tremendous global efforts, COVID-19 remains a serious concern. Although many clinical trials of the repurposed drugs, immune-based therapies and investigational antivirals have been conducted, there is still no highly effective therapeutic for treatment of COVID-19 available. The mutation and pandemic of SARS-CoV-2 make vaccine and drug discovery more uncertain. Accordingly, developing specific or broad-spectrum inhibitors for SARS-CoV-2 virus entry, replication or prevention is urgently needed.

Continuous worldwide surveillance of the SARS-CoV-2 genome and continued efforts for quick screening of small-molecule databases will allow us to produce effective lead compounds or drug candidates, facilitating further *in vitro*, *in vivo* and clinical trials with which to determine their efficacy in the management of COVID-19. Computer-based drug design can

accelerate the drug development process, but new interventions are still likely to require months to years to develop. Considering the case fatality rate of COVID-19, the quick screening of therapeutic agents for the repurposing of FDA-approved and clinical trial drugs may be a more practical approach. Repurposing old drugs for new indications may potentially lower development costs and shorten development timelines. Indeed, several clinical drugs and drug combinations are under repositioning in the treatment of COVID-19 patients. However, none of the clinical trials has resulted in completely satisfactory results, except for experiments still ongoing without final results.

In the long-term perspective, much basic work needs to be done in terms of generating effective small-molecule drugs. Like SARS-CoV and MERS-CoV, SARS-CoV-2 genome encodes nsps (3CLpro, PLpro, helicase and RdRp), structural proteins (S glycoprotein) and accessory proteins. S proteins and nsps described above are identified as attractive targets for antiviral agent development. So far, hundreds of active compounds have been screened for inhibitors against SARS-CoV-2 infection; however, many of these studies have not been rigorously conducted. Thus, it is essential for researchers to fully assess promiscuous compounds, avoiding the false positive activity readouts. In many cases, hit compounds containing Michael receptor, phenolic and quinone substructures or other unstable chemical bonds are actually nondruggable, now recognized as pan assay interference compounds (PAINS). Furthermore, protein structural analyses suggest that active sites in viral proteins are probably conserved among SARS-CoV, MERS-CoV and SARS-CoV-2. Therefore, we have enough relevant experience to design coronavirus inhibitors. Continuous efforts toward the accurate crystal structure of verified drug targets, preclinical evaluation of drug candidates, gathering of clinical evidence, as well as artificial intelligence, are all necessary for the successful identification of anti-SARS-CoV-2 drugs. Furthermore, host-targeted agents able to stimulate innate antiviral responses, or modulate virus–host interactions, are also options for COVID-19 treatment. With the ongoing efforts to prevent gradually increasing cases around the globe, the outbreak of COVID-19 has highlighted the importance for the development of broad-spectrum antiviral agents to combat future coronaviruses.

### Acknowledgments

This work was supported by grants from the National Natural Science Foundation of China (81974302 and 82041025), the Program for “333 Talents Project” of Hebei Province (A202002003, China), and Science and Technology Project of Hebei Education Department (QN2021071, China).

### Author contributions

Shibo Jiang and Fei Yu designed the work. Fei Yu, Yaning Gao, Rong Xiang, Zhengsen Yu, Yang Wang, and Lili Wang collected data and wrote the manuscript. Shanshan Huo, Yanbai Li, Ruiying Liang and Qinghong Hao designed and regenerated the conceptual pictures. Shibo Jiang, Fei Yu and Tianlei Ying revised the manuscript. All of the authors have read and approved the final manuscript.

### Conflicts of interest

The authors have no conflicts of interest to declare.

### References

- Zhu N, Zhang D, Wang W, Li X, Yang B, Song J, et al. A novel coronavirus from patients with pneumonia in China, 2019. *N Engl J Med* 2020;382:727–33.
- Wu F, Zhao S, Yu B, Chen YM, Wang W, Song ZG, et al. Author correction: a new coronavirus associated with human respiratory disease in China. *Nature* 2020;580:e7.
- Jiang S, Shi Z, Shu Y, Song J, Gao GF, Tan W, et al. A distinct name is needed for the new coronavirus. *Lancet* 2020;395:949.
- Kim JM, Chung YS, Jo HJ, Lee NJ, Kim MS, Woo SH, et al. Identification of coronavirus isolated from a patient in Korea with COVID-19. *Osong Public Health Res Perspect* 2020;11:3–7.
- Zhou P, Yang XL, Wang XG, Hu B, Zhang L, Zhang W, et al. A pneumonia outbreak associated with a new coronavirus of probable bat origin. *Nature* 2020;579:270–3.
- Morse JS, Lalonde T, Xu S, Liu WR. Learning from the past: possible urgent prevention and treatment options for severe acute respiratory infections caused by 2019-nCoV. *Chembiochem* 2020;21:730–8.
- Coronaviridae Study Group of the International Committee on Taxonomy of V. The species severe acute respiratory syndrome-related coronavirus: classifying 2019-nCoV and naming it SARS-CoV-2. *Nat Microbiol* 2020;5:536–44.
- Kim D, Lee JY, Yang JS, Kim JW, Kim VN, Chang H. The architecture of SARS-CoV-2 transcriptome. *Cell* 2020;181:914–21.e10.
- Chan JF, Kok KH, Zhu Z, Chu H, To KK, Yuan S, et al. Genomic characterization of the 2019 novel human-pathogenic coronavirus isolated from a patient with atypical pneumonia after visiting Wuhan. *Emerg Microb Infect* 2020;9:221–36.
- Hoffmann M, Kleine-Weber H, Schroeder S, Kruger N, Herrler T, Erichsen S, et al. SARS-CoV-2 cell entry depends on ACE2 and TMPRSS2 and is blocked by a clinically proven protease inhibitor. *Cell* 2020;181:271–80.e8.
- Clausen TM, Sandoval DR, Spliid CB, Pihl J, Perrett HR, Painter CD, et al. SARS-CoV-2 infection depends on cellular heparan sulfate and ACE2. *Cell* 2020;183:1043–57.e15.
- Ou X, Liu Y, Lei X, Li P, Mi D, Ren L, et al. Characterization of spike glycoprotein of SARS-CoV-2 on virus entry and its immune cross-reactivity with SARS-CoV. *Nat Commun* 2020;11:1620.
- Fehr AR, Perlman S. Coronaviruses: an overview of their replication and pathogenesis. *Methods Mol Biol* 2015;1282:1–23.
- Graham RL, Sparks JS, Eckerle LD, Sims AC, Denison MR. SARS coronavirus replicase proteins in pathogenesis. *Virus Res* 2008;133:88–100.
- Masters PS. The molecular biology of coronaviruses. *Adv Virus Res* 2006;66:193–292.
- Stertz S, Reichelt M, Spiegel M, Kuri T, Martinez-Sobrido L, Garcia-Sastre A, et al. The intracellular sites of early replication and budding of SARS-coronavirus. *Virology* 2007;361:304–15.
- Lin MH, Moses DC, Hsieh CH, Cheng SC, Chen YH, Sun CY, et al. Disulfiram can inhibit MERS and SARS coronavirus papain-like proteases via different modes. *Antivir Res* 2018;150:155–63.
- Sheahan TP, Sims AC, Leist SR, Schafer A, Won J, Brown AJ, et al. Comparative therapeutic efficacy of remdesivir and combination lopinavir, ritonavir, and interferon beta against MERS-CoV. *Nat Commun* 2020;11:222.
- Wang M, Cao R, Zhang L, Yang X, Liu J, Xu M, et al. Remdesivir and chloroquine effectively inhibit the recently emerged novel coronavirus (2019-nCoV) in vitro. *Cell Res* 2020;30:269–71.
- Zaher NH, Mostafa MI, Altaher AY. Design, synthesis and molecular docking of novel triazole derivatives as potential CoV helicase inhibitors. *Acta Pharm* 2020;70:145–59.
- O’Keefe BR, Giomarelli B, Barnard DL, Shenoy SR, Chan PK, McMahon JB, et al. Broad-spectrum *in vitro* activity and *in vivo* efficacy of the antiviral protein griffithsin against emerging viruses of the family Coronaviridae. *J Virol* 2010;84:2511–21.

22. Sarma P, Shekhar N, Prajapat M, Avti P, Kaur H, Kumar S, et al. *In-silico* homology assisted identification of inhibitor of RNA binding against 2019-nCoV N-protein (N terminal domain). *J Biomol Struct Dyn* 2020;39:1–9.
23. Lan J, Ge J, Yu J, Shan S, Zhou H, Fan S, et al. Structure of the SARS-CoV-2 spike receptor-binding domain bound to the ACE2 receptor. *Nature* 2020;581:215–20.
24. Phonphok Y, Rosenthal KS. Stabilization of clathrin coated vesicles by amantadine, tromantadine and other hydrophobic amines. *FEBS Lett* 1991;281:188–90.
25. Omrani AS, Saad MM, Baig K, Bahloul A, Abdul-Matin M, Alaidaroos AY, et al. Ribavirin and interferon alfa-2a for severe middle east respiratory syndrome coronavirus infection: a retrospective cohort study. *Lancet Infect Dis* 2014;14:1090–5.
26. Xu X, Han M, Li T, Sun W, Wang D, Fu B, et al. Effective treatment of severe COVID-19 patients with tocilizumab. *Proc Natl Acad Sci U S A* 2020;117:10970–5.
27. Han Y, Duan X, Yang L, Nilsson-Payant BE, Wang P, Duan F, et al. Identification of SARS-CoV-2 inhibitors using lung and colonic organoids. *Nature* 2021;589:270–5.
28. Ni L, Zhou L, Zhou M, Zhao J, Wang DW. Combination of western medicine and Chinese traditional patent medicine in treating a family case of COVID-19. *Front Med* 2020;14:210–4.
29. Li R, Hou Y, Huang J, Pan W, Ma Q, Shi Y, et al. Lianhua-qingwen exerts anti-viral and anti-inflammatory activity against novel coronavirus (SARS-CoV-2). *Pharmacol Res* 2020;156:104761.
30. Gordon DE, Jang GM, Bouhaddou M, Xu J, Obernier K, White KM, et al. A SARS-CoV-2 protein interaction map reveals targets for drug repurposing. *Nature* 2020;583:459–68.
31. Wrapp D, Wang N, Corbett KS, Goldsmith JA, Hsieh CL, Abiona O, et al. Cryo-EM structure of the 2019-nCoV spike in the prefusion conformation. *Science* 2020;367:1260–3.
32. Walls AC, Park YJ, Tortorici MA, Wall A, McGuire AT, Veesler D. Structure, function, and antigenicity of the SARS-CoV-2 spike glycoprotein. *Cell* 2020;181:281–92.e6.
33. Wan Y, Shang J, Graham R, Baric RS, Li F. Receptor recognition by the novel coronavirus from Wuhan: an analysis based on decade-long structural studies of SARS coronavirus. *J Virol* 2020;94:e00127-20.
34. Walls AC, Tortorici MA, Snijder J, Xiong X, Bosch BJ, Rey FA, et al. Tectonic conformational changes of a coronavirus spike glycoprotein promote membrane fusion. *Proc Natl Acad Sci U S A* 2017;114:11157–62.
35. Liu S, Xiao G, Chen Y, He Y, Niu J, Escalante CR, et al. Interaction between heptad repeat 1 and 2 regions in spike protein of SARS-associated coronavirus: implications for virus fusogenic mechanism and identification of fusion inhibitors. *Lancet* 2004;363:938–47.
36. Bosch BJ, van der Zee R, de Haan CA, Rottier PJ. The coronavirus spike protein is a class I virus fusion protein: structural and functional characterization of the fusion core complex. *J Virol* 2003;77:8801–11.
37. He Y. Synthesized peptide inhibitors of HIV-1 gp41-dependent membrane fusion. *Curr Pharmaceut Des* 2013;19:1800–9.
38. Lu L, Liu Q, Zhu Y, Chan KH, Qin L, Li Y, et al. Structure-based discovery of middle east respiratory syndrome coronavirus fusion inhibitor. *Nat Commun* 2014;5:3067.
39. Wang C, Xia S, Zhang P, Zhang T, Wang W, Tian Y, et al. Discovery of hydrocarbon-stapled short alpha-helical peptides as promising middle east respiratory syndrome coronavirus (MERS-CoV) fusion inhibitors. *J Med Chem* 2018;61:2018–26.
40. Bosch BJ, Martina BE, Van Der Zee R, Lepault J, Hajema BJ, Versluis C, et al. Severe acute respiratory syndrome coronavirus (SARS-CoV) infection inhibition using spike protein heptad repeat-derived peptides. *Proc Natl Acad Sci U S A* 2004;101:8455–60.
41. Ujike M, Nishikawa H, Otaka A, Yamamoto N, Yamamoto N, Matsuoka M, et al. Heptad repeat-derived peptides block protease-mediated direct entry from the cell surface of severe acute respiratory syndrome coronavirus but not entry via the endosomal pathway. *J Virol* 2008;82:588–92.
42. Liu JJ, Kao CL, Hsieh SC, Wey MT, Kan LS, Wang WK. Identification of a minimal peptide derived from heptad repeat (HR) 2 of spike protein of SARS-CoV and combination of HR1-derived peptides as fusion inhibitors. *Antivir Res* 2009;81:82–7.
43. Aydin H, Al-Khooly D, Lee JE. Influence of hydrophobic and electrostatic residues on SARS-coronavirus S2 protein stability: insights into mechanisms of general viral fusion and inhibitor design. *Protein Sci* 2014;23:603–17.
44. Xia S, Yan L, Xu W, Agrawal AS, Algaissi A, Tseng CK, et al. A pan-coronavirus fusion inhibitor targeting the HR1 domain of human coronavirus spike. *Sci Adv* 2019;5:eaav4580.
45. Xia S, Liu M, Wang C, Xu W, Lan Q, Feng S, et al. Inhibition of SARS-CoV-2 (previously 2019-nCoV) infection by a highly potent pan-coronavirus fusion inhibitor targeting its spike protein that harbors a high capacity to mediate membrane fusion. *Cell Res* 2020;30:343–55.
46. Zhu Y, Chong H, Yu D, Guo Y, Zhou Y, He Y. Design and characterization of cholesterylated peptide HIV-1/2 fusion inhibitors with extremely potent and long-lasting antiviral activity. *J Virol* 2019;93:e02312–8.
47. Chong H, Xue J, Zhu Y, Cong Z, Chen T, Wei Q, et al. Monotherapy with a low-dose lipopeptide HIV fusion inhibitor maintains long-term viral suppression in rhesus macaques. *PLoS Pathog* 2019;15:e1007552.
48. Zhu Y, Zhang X, Ding X, Chong H, Cui S, He J, et al. Exceptional potency and structural basis of a T1249-derived lipopeptide fusion inhibitor against HIV-1, HIV-2, and simian immunodeficiency virus. *J Biol Chem* 2018;293:5323–34.
49. Zhu Y, Yu D, Yan H, Chong H, He Y. Design of potent membrane fusion inhibitors against SARS-CoV-2, an emerging coronavirus with high fusogenic activity. *J Virol* 2020;94:e00635-20.
50. Xia S, Zhu Y, Liu M, Lan Q, Xu W, Wu Y, et al. Fusion mechanism of 2019-nCoV and fusion inhibitors targeting HR1 domain in spike protein. *Cell Mol Immunol* 2020;17:765–7.
51. de Vries RD, Schmitz KS, Bovier FT, Predella C, Khao J, Noack D, et al. Intranasal fusion inhibitory lipopeptide prevents direct-contact SARS-CoV-2 transmission in ferrets. *Science* 2021;371:1379–82.
52. Zhang G, Pomplun S, Loftis R, Tan X, Loas A, Pentelute BL. Investigation of ACE2 N-terminal fragments binding to SARS-CoV-2 Spike RBD. *bioRxiv* 2020. Available from: <https://www.biorxiv.org/content/10.1101/2020.03.19.999318v2>.
53. Cao L, Goreshnik I, Coventry B, Case JB, Miller L, Kozodoy L, et al. *De novo* design of picomolar SARS-CoV-2 miniprotein inhibitors. *Science* 2020;370:426–31.
54. Beddingfield BJ, Iwanaga N, Chapagain P, Zheng W, Roy J, Hu TY, et al. The integrin binding peptide, ATN-161, as a novel therapy for SARS-CoV-2 infection. *JACC Basic Transl Sci* 2021;6:1–8.
55. De Clercq E. New developments in anti-HIV chemotherapy. *Biochim Biophys Acta* 2002;1587:258–75.
56. Han Y, Kral P. Computational design of ACE2-based peptide inhibitors of SARS-CoV-2. *ACS Nano* 2020;14:5143–7.
57. Watson A, Ferreira L, Hwang P, Xu J, Stroud R. Peptide antidotes to SARS-CoV-2 (COVID-19). *bioRxiv* 2020. Available from: <https://www.biorxiv.org/content/10.1101/2020.08.06.238915v2>.
58. Yang C, Pan X, Xu X, Cheng C, Huang Y, Li L, et al. Salvianolic acid C potently inhibits SARS-CoV-2 infection by blocking the formation of six-helix bundle core of spike protein. *Signal Transduct Target Ther* 2020;5:220.
59. Vankadari N. Arbidol: a potential antiviral drug for the treatment of SARS-CoV-2 by blocking trimerization of the spike glycoprotein. *Int J Antimicrob Agents* 2020;56:105998.
60. Wang X, Cao R, Zhang H, Liu J, Xu M, Hu H, et al. The anti-influenza virus drug, arbidol is an efficient inhibitor of SARS-CoV-2 *in vitro*. *Cell Discov* 2020;6:28.
61. Deng L, Li C, Zeng Q, Liu X, Li X, Zhang H, et al. Arbidol combined with LPV/r versus LPV/r alone against corona virus disease 2019: a retrospective cohort study. *J Infect* 2020;81:e1–5.

62. Lian N, Xie H, Lin S, Huang J, Zhao J, Lin Q. Umifenovir treatment is not associated with improved outcomes in patients with coronavirus disease 2019: a retrospective study. *Clin Microbiol Infect* 2020; **26**:917–21.
63. Zhang JN, Wang WJ, Peng B, Peng W, Zhang YS, Wang YL, et al. Potential of arbidol for post-exposure prophylaxis of COVID-19 transmission: a preliminary report of a retrospective cohort study. *Curr Med Sci* 2020; **40**:480–5.
64. Li Y, Xie Z, Lin W, Cai W, Wen C, Guan Y, et al. Efficacy and safety of lopinavir/ritonavir or arbidol in adult patients with mild/moderate COVID-19: an exploratory randomized controlled trial. *Med (N Y)* 2020; **1**:105–13. e4.
65. Bojadzic D, Alcazar O, Chen J, Chuang ST, Condor CJM, Shehadeh LA, et al. Small-molecule inhibitors of the coronavirus spike: ACE2 protein–protein interaction as blockers of viral attachment and entry for SARS-CoV-2. *ACS Infect Dis* 2021; **7**:1519–34.
66. Chen CZ, Xu M, Pradhan M, Gorshkov K, Petersen JD, Straus MR, et al. Identifying SARS-CoV-2 entry inhibitors through drug repurposing screens of SARS-S and MERS-S pseudotyped particles. *ACS Pharmacol Transl Sci* 2020; **3**:1165–75.
67. Gopal M, Padayatchi N, Metcalfe JZ, O'Donnell MR. Systematic review of clofazimine for the treatment of drug-resistant tuberculosis. *Int J Tubercul Lung Dis* 2013; **17**:1001–7.
68. Riva L, Yuan S, Yin X, Martin-Sancho L, Matsunaga N, Pache L, et al. Discovery of SARS-CoV-2 antiviral drugs through large-scale compound repurposing. *Nature* 2020; **586**:113–9.
69. Yuan S, Yin X, Meng X, Chan JF, Ye ZW, Riva L, et al. Clofazimine broadly inhibits coronaviruses including SARS-CoV-2. *Nature* 2021; **593**:418–23.
70. Chen Y, Liu Q, Guo D. Emerging coronaviruses: genome structure, replication, and pathogenesis. *J Med Virol* 2020; **92**:418–23.
71. Liu S, Zheng Q, Wang Z. Potential covalent drugs targeting the main protease of the SARS-CoV-2 coronavirus. *Bioinformatics* 2020; **36**:3295–8.
72. Chen Y, Yang WH, Huang LM, Wang YC, Yang CS, Yi LL, Hou MH, et al. Inhibition of severe acute respiratory syndrome coronavirus 2 main protease by tafenoquine *in vitro*. *bioRxiv* 2020. Available from: <https://www.biorxiv.org/content/10.1101/2020.08.14.250258v1>.
73. Dow GS, Lutnick A, Fenner J, Wesche D, Yeo KR, Rayner C. Tafenoquine inhibits replication of SARS-CoV-2 at pharmacologically relevant concentrations *in vitro*. *bioRxiv* 2020. Available from: <https://www.biorxiv.org/content/10.1101/2020.07.12.199059v1>.
74. Rathnayake AD, Zheng J, Kim Y, Perera KD, Mackin S, Meyerholz DK, et al. 3C-like protease inhibitors block coronavirus replication *in vitro* and improve survival in MERS-CoV-infected mice. *Sci Transl Med* 2020; **12**:eabc5332.
75. Su H, Yao S, Zhao W, Li M, Liu J, Shang W, et al. Discovery of baicalin and baicalein as novel, natural product inhibitors of SARS-CoV-2 3CL protease *in vitro*. *bioRxiv* 2020. Available from: <https://www.biorxiv.org/content/10.1101/2020.04.13.038687v1>.
76. Huang S, Liu Y, Zhang Y, Zhang R, Zhu C, Fan L, et al. Baicalein inhibits SARS-CoV-2/VSV replication with interfering mitochondrial oxidative phosphorylation in a mPTP dependent manner. *Signal Transduct Target Ther* 2020; **5**:266.
77. Liu H, Ye F, Sun Q, Liang H, Li C, Li S, et al. Scutellaria baicalensis extract and baicalein inhibit replication of SARS-CoV-2 and its 3C-like protease *in vitro*. *J Enzym Inhib Med Chem* 2021; **36**:497–503.
78. Drayman N, Jones KA, Azizi SA, Froggatt HM, Tan K, Maltseva NI, et al. Drug repurposing screen identifies masitinib as a 3CLpro inhibitor that blocks replication of SARS-CoV-2 *in vitro*. *bioRxiv* 2020. Available from: <https://www.biorxiv.org/content/10.1101/2020.08.31.274639v1>.
79. Jin Z, Du X, Xu Y, Deng Y, Liu M, Zhao Y, et al. Structure of M(pro) from SARS-CoV-2 and discovery of its inhibitors. *Nature* 2020; **582**:289–93.
80. Ma C, Hu Y, Townsend JA, Lagarias PI, Marty MT, Kolocouris A, et al. Ebselen, disulfiram, carmofur, PX-12, tideglusib, and shikonin are nonspecific promiscuous SARS-CoV-2 main protease inhibitors. *ACS Pharmacol Transl Sci* 2020; **3**:1265–77.
81. Jin Z, Zhao Y, Sun Y, Zhang B, Wang H, Wu Y, et al. Structural basis for the inhibition of SARS-CoV-2 main protease by antineoplastic drug carmofur. *Nat Struct Mol Biol* 2020; **27**:529–32.
82. Dai W, Zhang B, Jiang XM, Su H, Li J, Zhao Y, et al. Structure-based design of antiviral drug candidates targeting the SARS-CoV-2 main protease. *Science* 2020; **368**:1331–5.
83. Zhang L, Lin D, Sun X, Curth U, Drosten C, Sauerhering L, et al. Crystal structure of SARS-CoV-2 main protease provides a basis for design of improved alpha-ketoamide inhibitors. *Science* 2020; **368**:409–12.
84. Vuong W, Khan MB, Fischer C, Arutyunova E, Lamer T, Shields J, et al. Feline coronavirus drug inhibits the main protease of SARS-CoV-2 and blocks virus replication. *Nat Commun* 2020; **11**:4282.
85. Iketani S, Forouhar F, Liu H, Hong SJ, Lin FY, Nair MS, et al. Lead compounds for the development of SARS-CoV-2 3CL protease inhibitors. *Nat Commun* 2021; **12**:2016.
86. Ma C, Sacco MD, Hurst B, Townsend JA, Hu Y, Szeto T, et al. Boceprevir, GC-376, and calpain inhibitors II, XII inhibit SARS-CoV-2 viral replication by targeting the viral main protease. *Cell Res* 2020; **30**:678–92.
87. Fu L, Ye F, Feng Y, Yu F, Wang Q, Wu Y, et al. Both Boceprevir and GC376 efficaciously inhibit SARS-CoV-2 by targeting its main protease. *Nat Commun* 2020; **11**:4417.
88. Sacco MD, Ma C, Lagarias P, Gao A, Townsend JA, Meng X, et al. Structure and inhibition of the SARS-CoV-2 main protease reveal strategy for developing dual inhibitors against M(pro) and cathepsin L. *Sci Adv* 2020; **6**:eabe0751.
89. Hu Y, Ma C, Szeto T, Hurst B, Tarbet B, Wang J, Boceprevir, calpain inhibitors II and XII, and GC-376 have broad-spectrum antiviral activity against coronaviruses. *ACS Infect Dis* 2021; **7**:586–97.
90. Caceres CJ, Cardenas-Garcia S, Carnaccini S, Seibert B, Rajao DS, Wang J, et al. Efficacy of GC-376 against SARS-CoV-2 virus infection in the K18 hACE2 transgenic mouse model. *Sci Rep* 2021; **11**:9609.
91. Shi Y, Shuai L, Wen Z, Wang C, Yan Y, Jiao Z, et al. The preclinical inhibitor GS441524 in combination with GC376 efficaciously inhibited the proliferation of SARS-CoV-2 in the mouse respiratory tract. *Emerg Microb Infect* 2021; **10**:481–92.
92. Vatansever EC, Yang KS, Drelich AK, Kratch KC, Cho CC, Kempaiah KR, et al. Bepridil is potent against SARS-CoV-2 *in vitro*. *Proc Natl Acad Sci U S A* 2021; **118**:e2012201118.
93. Yang KS, Ma XR, Ma Y, Alugubelli YR, Scott DA, Vatansever EC, et al. A quick route to multiple highly potent SARS-CoV-2 main protease inhibitors. *ChemMedChem* 2021; **16**:942–8.
94. Jan JT, Cheng TR, Juang YP, Ma HH, Wu YT, Yang WB, et al. Identification of existing pharmaceuticals and herbal medicines as inhibitors of SARS-CoV-2 infection. *Proc Natl Acad Sci U S A* 2021; **118**:e2021579118.
95. Zhu W, Xu M, Chen CZ, Guo H, Shen M, Hu X, et al. Identification of SARS-CoV-2 3CL protease inhibitors by a quantitative high-throughput screening. *ACS Pharmacol Transl Sci* 2020; **3**:1008–16.
96. Salgado-Benvindo C, Thaler M, Tas A, Ogando NS, Bredenbeek PJ, Ninaber DK, et al. Suramin inhibits SARS-CoV-2 infection in cell culture by interfering with early steps of the replication cycle. *Antimicrob Agents Chemother* 2020; **64**:e00900–20.
97. Chu CM, Cheng VC, Hung IF, Wong MM, Chan KH, Chan KS, et al. Role of lopinavir/ritonavir in the treatment of SARS: initial virological and clinical findings. *Thorax* 2004; **59**:252–6.
98. Chan JF, Yao Y, Yeung ML, Deng W, Bao L, Jia L, et al. Treatment with lopinavir/ritonavir or interferon-beta1b improves outcome of MERS-CoV infection in a nonhuman primate model of common marmoset. *J Infect Dis* 2015; **212**:1904–13.
99. Choy KT, Wong AY, Kaewpreedee P, Sia SF, Chen D, Hui KPY, et al. Remdesivir, lopinavir, emetine, and homoharringtonine inhibit SARS-CoV-2 replication *in vitro*. *Antivir Res* 2020; **178**:104786.

100. Nukoolkarn V, Lee VS, Malaisree M, Aruksakulwong O, Hannongbua S. Molecular dynamic simulations analysis of ritonavir and lopinavir as SARS-CoV 3CL(pro) inhibitors. *J Theor Biol* 2008; **254**:861–7.
101. Wu CY, Jan JT, Ma SH, Kuo CJ, Juan HF, Cheng YS, et al. Small molecules targeting severe acute respiratory syndrome human coronaviruses. *Proc Natl Acad Sci U S A* 2004; **101**:10012–7.
102. Lim J, Jeon S, Shin HY, Kim MJ, Seong YM, Lee WJ, et al. Case of the index patient who caused tertiary transmission of COVID-19 infection in Korea: the application of lopinavir/ritonavir for the treatment of COVID-19 infected pneumonia monitored by quantitative RT-PCR. *J Kor Med Sci* 2020; **35**:e79.
103. Cao B, Wang Y, Wen D, Liu W, Wang J, Fan G, et al. A trial of lopinavir-ritonavir in adults hospitalized with severe COVID-19. *N Engl J Med* 2020; **382**:1787–99.
104. Hung IF, Lung KC, Tso EY, Liu R, Chung TW, Chu MY, et al. Triple combination of interferon beta-1b, lopinavir-ritonavir, and ribavirin in the treatment of patients admitted to hospital with COVID-19: an open-label, randomised, phase 2 trial. *Lancet* 2020; **395**:1695–704.
105. WHO R&D Blueprint. *Informal consultation on prioritization of candidate therapeutic agents for use in novel coronavirus 2019 infection*. World Health Organization; 2020. Available from: <https://www.who.int/teams/blueprint/covid-19>.
106. Liu X, Li Z, Liu S, Sun J, Chen Z, Jiang M, et al. Potential therapeutic effects of dipyridamole in the severely ill patients with COVID-19. *Acta Pharm Sin B* 2020; **10**:1205–15.
107. Hattori SI, Higashi-Kuwata N, Raghavaiah J, Das D, Bulut H, Davis DA, et al. GRL-0920, an indole chloropyridinyl ester, completely blocks SARS-CoV-2 infection. *mBio* 2020; **11**:e01833-20.
108. Qiao J, Li YS, Zeng R, Liu FL, Luo RH, Huang C, et al. SARS-CoV-2 M(pro) inhibitors with antiviral activity in a transgenic mouse model. *Science* 2021; **371**:1374–8.
109. Freitas BT, Durie IA, Murray J, Longo JE, Miller HC, Crich D, et al. Characterization and noncovalent inhibition of the deubiquitinase and deISGylase activity of SARS-CoV-2 papain-like protease. *ACS Infect Dis* 2020; **6**:2099–109.
110. Chen X, Chou CY, Chang GG. Thiopurine analogue inhibitors of severe acute respiratory syndrome-coronavirus papain-like protease, a deubiquitinating and deISGylating enzyme. *Antivir Chem Chemother* 2009; **19**:151–6.
111. Baez-Santos YM, Barraza SJ, Wilson MW, Agius MP, Mielech AM, Davis NM, et al. X-ray structural and biological evaluation of a series of potent and highly selective inhibitors of human coronavirus papain-like proteases. *J Med Chem* 2014; **57**:2393–412.
112. Klemm T, Ebert G, Calleja DJ, Allison CC, Richardson LW, Bernardini JP, et al. Mechanism and inhibition of the papain-like protease, PLpro, of SARS-CoV-2. *EMBO J* 2020; **39**:e106275.
113. Kouzenetsova VL, Zhang A, Tatineni M, Miller MA, Tsigelnik IF. Potential COVID-19 papain-like protease PL(pro) inhibitors: repurposing FDA-approved drugs. *PeerJ* 2020; **8**:e9965.
114. Abruzzese E, Luciano L, D'Agostino F, Trawinska MM, Pane F, De Fabritis P. SARS-CoV-2 (COVID-19) and chronic myeloid leukemia (CML): a case report and review of ABL kinase involvement in viral infection. *Mediterr J Hematol Infect Dis* 2020; **12**:e2020031.
115. Mirza MU, Ahmad S, Abdullah I, Froeyen M. Identification of novel human USP2 inhibitor and its putative role in treatment of COVID-19 by inhibiting SARS-CoV-2 papain-like (PLpro) protease. *Comput Biol Chem* 2020; **89**:107376.
116. Gao X, Qin B, Chen P, Zhu K, Hou P, Wojdyla JA, et al. Crystal structure of SARS-CoV-2 papain-like protease. *Acta Pharm Sin B* 2021; **11**:237–45.
117. Fu Z, Huang B, Tang J, Liu S, Liu M, Ye Y, et al. The complex structure of GRL0617 and SARS-CoV-2 PLpro reveals a hot spot for antiviral drug discovery. *Nat Commun* 2021; **12**:488.
118. Gao Y, Yan L, Huang Y, Liu F, Zhao Y, Cao L, et al. Structure of the RNA-dependent RNA polymerase from COVID-19 virus. *Science* 2020; **368**:779–82.
119. Eastman RT, Roth JS, Brimacombe KR, Simeonov A, Shen M, Patnaik S, et al. Remdesivir: a review of its discovery and development leading to emergency use authorization for treatment of COVID-19. *ACS Cent Sci* 2020; **6**:672–83.
120. Sheahan TP, Sims AC, Zhou S, Graham RL, Pruijssers AJ, Agostini ML, et al. An orally bioavailable broad-spectrum antiviral inhibits SARS-CoV-2 in human airway epithelial cell cultures and multiple coronaviruses in mice. *Sci Transl Med* 2020; **12**:eabb5883.
121. Agostini ML, Andres EL, Sims AC, Graham RL, Sheahan TP, Lu X, et al. Coronavirus susceptibility to the antiviral remdesivir (GS-5734) is mediated by the viral polymerase and the proofreading exoribonuclease. *mBio* 2018; **9**:e00221-18.
122. Beigel JH, Tomashek KM, Dodd LE, Mehta AK, Zingman BS, Kalil AC, et al. Remdesivir for the treatment of COVID-19—final report. *N Engl J Med* 2020; **383**:1813–26.
123. Wang Y, Zhang D, Du G, Du R, Zhao J, Jin Y, et al. Remdesivir in adults with severe COVID-19: a randomised, double-blind, placebo-controlled, multicentre trial. *Lancet* 2020; **395**:1569–78.
124. Pan H, Peto R, Henao-Restrepo AM, Preziosi MP, Sathyamoorthy V, Abdoor Karim Q, et al. Repurposed antiviral drugs for COVID-19—interim WHO solidarity trial results. *N Engl J Med* 2021; **384**:497–511.
125. Elfiky AA. Ribavirin, Remdesivir, Sofosbuvir, Galidesivir, and tenofovir against SARS-CoV-2 RNA dependent RNA polymerase (RdRp): a molecular docking study. *Life Sci* 2020; **253**:117592.
126. Yin W, Luan X, Li Z, Zhou Z, Wang Q, Gao M, et al. Structural basis for inhibition of the SARS-CoV-2 RNA polymerase by suramin. *Nat Struct Mol Biol* 2021; **28**:319–25.
127. Oestereich L, Ludtke A, Wurr S, Rieger T, Munoz-Fontela C, Gunther S. Successful treatment of advanced Ebola virus infection with T-705 (favipiravir) in a small animal model. *Antivir Res* 2014; **105**:17–21.
128. Coomes EA, Haghbayan H. Favipiravir, an antiviral for COVID-19? *J Antimicrob Chemother* 2020; **75**:2013–4.
129. Du YX, Chen XP. Favipiravir: pharmacokinetics and concerns about clinical trials for 2019-nCoV infection. *Clin Pharmacol Ther* 2020; **108**:242–7.
130. Reynard O, Nguyen XN, Alazard-Dany N, Barateau V, Cimarelli A, Volchkov VE. Identification of a new ribonucleoside inhibitor of Ebola virus replication. *Viruses* 2015; **7**:6233–40.
131. Urakova N, Kuznetsova V, Crossman DK, Sokratian A, Guthrie DB, Kolykhakov AA, et al.  $\beta$ -D- $N^4$ -Hydroxycytidine is a potent anti-alphavirus compound that induces a high level of mutations in the viral genome. *J Virol* 2018; **92**:e01965-17.
132. Toots M, Yoon JJ, Cox RM, Hart M, Sticher ZM, Makhsoos N, et al. Characterization of orally efficacious influenza drug with high resistance barrier in ferrets and human airway epithelia. *Sci Transl Med* 2019; **11**:eaax5866.
133. Agostini ML, Pruijssers AJ, Chappell JD, Gribble J, Lu X, Andres EL, et al. Small-molecule antiviral  $\beta$ -D- $N^4$ -hydroxycytidine inhibits a proofreading-intact coronavirus with a high genetic barrier to resistance. *J Virol* 2019; **93**:e01348-19.
134. Gordon CJ, Tchesnokov EP, Feng JY, Porter DP, Gotte M. The antiviral compound remdesivir potently inhibits RNA-dependent RNA polymerase from middle east respiratory syndrome coronavirus. *J Biol Chem* 2020; **295**:4773–9.
135. Mestres J. The target landscape of  $N^4$ -hydroxycytidine based on its chemical neighborhood. *bioRxiv* 2020. Available from: <https://www.biorxiv.org/content/10.1101/2020.03.30.016485v1>.
136. Kwong AD, Rao BG, Jeang KT. Viral and cellular RNA helicases as antiviral targets. *Nat Rev Drug Discov* 2005; **4**:845–53.
137. Frick DN, Lam AM. Understanding helicases as a means of virus control. *Curr Pharmaceut Des* 2006; **12**:1315–38.
138. Tanner JA, Zheng BJ, Zhou J, Watt RM, Jiang JQ, Wong KL, et al. The adamantane-derived bananins are potent inhibitors of the helicase activities and replication of SARS coronavirus. *Chem Biol* 2005; **12**:303–11.

139. Kim MK, Yu MS, Park HR, Kim KB, Lee C, Cho SY, et al. 2,6-Bis-arylmethoxy-5-hydroxychromones with antiviral activity against both hepatitis C virus (HCV) and SARS-associated coronavirus (SCV). *Eur J Med Chem* 2011;46:5698–704.
140. Lee C, Lee JM, Lee NR, Jin BS, Jang KJ, Kim DE, et al. Aryl diketocacids (ADK) selectively inhibit duplex DNA-unwinding activity of SARS coronavirus NTPase/helicase. *Bioorg Med Chem Lett* 2009;19:1636–8.
141. Adedeji AO, Singh K, Calcaterra NE, DeDiego ML, Enjuanes L, Weiss S, et al. Severe acute respiratory syndrome coronavirus replication inhibitor that interferes with the nucleic acid unwinding of the viral helicase. *Antimicrob Agents Chemother* 2012;56: 4718–28.
142. Decroly E, Debarnot C, Ferron F, Bouvet M, Coutard B, Imbert I, et al. Crystal structure and functional analysis of the SARS-coronavirus RNA cap 2'-O-methyltransferase nsp 10/nsp 16 complex. *PLoS Pathog* 2011;7:e1002059.
143. Menachery VD, Debbink K, Baric RS. Coronavirus non-structural protein 16: evasion, attenuation, and possible treatments. *Virus Res* 2014;194:191–9.
144. Khan RJ, Jha RK, Amera GM, Jain M, Singh E, Pathak A, et al. Targeting SARS-CoV-2: a systematic drug repurposing approach to identify promising inhibitors against 3C-like proteinase and 2'-O-ribose methyltransferase. *J Biomol Struct Dyn* 2020;39:2679–92.
145. Encinar JA, Menendez JA. Potential drugs targeting early innate immune evasion of SARS-coronavirus 2 via 2'-O-methylation of viral RNA. *Viruses* 2020;12:525.
146. Touret F, Gilles M, Barral K, Nougairede A, van Helden J, Decroly E, et al. *In vitro* screening of a FDA approved chemical library reveals potential inhibitors of SARS-CoV-2 replication. *Sci Rep* 2020;10:13093.
147. Cong Y, Ulasli M, Schepers H, Mauthe M, V'Kovski P, Kriengburg F, et al. Nucleocapsid protein recruitment to replication-transcription complexes plays a crucial role in coronaviral life cycle. *J Virol* 2020;94:e01925-19.
148. McBride R, van Zyl M, Fielding BC. The coronavirus nucleocapsid is a multifunctional protein. *Viruses* 2014;6:2991–3018.
149. Ahmed SF, Quadeer AA, McKay MR. Preliminary identification of potential vaccine targets for the COVID-19 coronavirus (SARS-CoV-2) based on SARS-CoV immunological studies. *Viruses* 2020; 12:254.
150. Kang S, Yang M, Hong Z, Zhang L, Huang Z, Chen X, et al. Crystal structure of SARS-CoV-2 nucleocapsid protein RNA binding domain reveals potential unique drug targeting sites. *Acta Pharm Sin B* 2020; 10:1228–38.
151. Huang C, Wang Y, Li X, Ren L, Zhao J, Hu Y, et al. Clinical features of patients infected with 2019 novel coronavirus in Wuhan, China. *Lancet* 2020;395:497–506.
152. Yamamoto N, Matsuyama S, Hoshino T, Yamamoto N. Nelfinavir inhibits replication of severe acute respiratory syndrome coronavirus 2 *in vitro*. *bioRxiv* 2020. Available from: <https://www.biorxiv.org/content/10.1101/2020.04.06.206476v1>.
153. Brown SM, Peltan ID, Webb B, Kumar N, Starr N, Grissom C, et al. Hydroxychloroquine versus azithromycin for hospitalized patients with suspected or confirmed COVID-19 (AHAPS). protocol for a pragmatic, open-label, active comparator trial. *Ann Am Thorac Soc* 2020;17:1008–15.
154. Goodwin EC, Atwood WJ, DiMaio D. High-throughput cell-based screen for chemicals that inhibit infection by simian virus 40 and human polyomaviruses. *J Virol* 2009;83:5630–9.
155. Gonzalez CA, Sahagun PAM, Diez Liebana MJ, Fernandez MN, Sierra VM, Garcia VJJ. The pharmacokinetics and interactions of ivermectin in humans—a mini-review. *AAPS J* 2008;10:42–6.
156. Wagstaff KM, Sivakumaran H, Heaton SM, Harrich D, Jans DA. Ivermectin is a specific inhibitor of importin alpha/beta-mediated nuclear import able to inhibit replication of HIV-1 and dengue virus. *Biochem J* 2012;443:851–6.
157. Caly L, Druce JD, Catton MG, Jans DA, Wagstaff KM. The FDA-approved drug ivermectin inhibits the replication of SARS-CoV-2 *in vitro*. *Antivir Res* 2020;178:104787.
158. Huet T, Beaussier H, Voisin O, Jouveshomme S, Dauriat G, Lazareth I, et al. Anakinra for severe forms of COVID-19: a cohort study. *Lancet Rheumatol* 2020;2:e393–400.
159. Kuster GM, Pfister O, Burkard T, Zhou Q, Twerenbold R, Haaf P, et al. SARS-CoV2: should inhibitors of the renin-angiotensin system be withdrawn in patients with COVID-19? *Eur Heart J* 2020;41:1801–3.
160. Callera GE, Antunes TT, Correa JW, Moorman D, Gutson A, He Y, et al. Differential renal effects of candesartan at high and ultra-high doses in diabetic mice—potential role of the ACE2/AT2R/Mas axis. *Biosci Rep* 2016;36:e00398.
161. Deppe S, Boger RH, Weiss J, Benndorf RA. Telmisartan: a review of its pharmacodynamic and pharmacokinetic properties. *Expert Opin Drug Metabol Toxicol* 2010;6:863–71.
162. Gurwitz D. Angiotensin receptor blockers as tentative SARS-CoV-2 therapeutics. *Drug Dev Res* 2020;81:537–40.
163. Sun ML, Yang JM, Sun YP, Su GH. Inhibitors of RAS might be a good choice for the therapy of COVID-19 pneumonia. *Zhonghua Jiehe He Huxi Zazhi* 2020;43:E014.
164. Speth RC. Response to recent commentaries regarding the involvement of angiotensin-converting enzyme 2 (ACE2) and renin-angiotensin system blockers in SARS-CoV-2 infections. *Drug Dev Res* 2020;81:643–6.
165. Talreja H, Tan J, Dawes M, Supershad S, Rabindranath K, Fisher J, et al. A consensus statement on the use of angiotensin receptor blockers and angiotensin converting enzyme inhibitors in relation to COVID-19 (corona virus disease 2019). *N Z Med J* 2020;133:85–7.
166. Schwarz S, Wang K, Yu W, Sun B, Schwarz W. Emodin inhibits current through SARS-associated coronavirus 3a protein. *Antivir Res* 2011;90:64–9.
167. Ho TY, Wu SL, Chen JC, Li CC, Hsiang CY. Emodin blocks the SARS coronavirus spike protein and angiotensin-converting enzyme 2 interaction. *Antivir Res* 2007;74:92–101.
168. Sanklecha V. Novel coronavirus COVID-19 and its diagnosis and treatments. *Int J* 2020;8:39–43.
169. Zhang L, Liu Y. Potential interventions for novel coronavirus in China: a systematic review. *J Med Virol* 2020;92:479–90.
170. Zhou Y, Hou Y, Shen J, Huang Y, Martin W, Cheng F. Network-based drug repurposing for novel coronavirus 2019-nCoV/SARS-CoV-2. *Cell Discov* 2020;6:14.
171. Takahashi S, Yoshiya T, Yoshizawa-Kumagaye K, Sugiyama T. Nicotianamine is a novel angiotensin-converting enzyme 2 inhibitor in soybean. *Biomed Res* 2015;36:219–24.
172. Chen H, Du Q. Preprints. Potential natural compounds for preventing SARS-CoV-2 (2019-nCoV) infection. *Preprints*. 2020. Available from: <https://www.preprints.org/manuscript/202001.0358/v2#>.
173. Yang Y, Islam MS, Wang J, Li Y, Chen X. Traditional Chinese medicine in the treatment of patients infected with 2019-new coronavirus (SARS-CoV-2): a review and perspective. *Int J Biol Sci* 2020; 16:1708–17.
174. Bhowmik D, Nandi R, Prakash A, Kumar D. Evaluation of flavonoids as 2019-nCoV cell entry inhibitor through molecular docking and pharmacological analysis. *Helix* 2021;7:e06515.
175. Lucas JM, Heinlein C, Kim T, Hernandez SA, Malik MS, True LD, et al. The androgen-regulated protease TMPRSS2 activates a proteolytic cascade involving components of the tumor microenvironment and promotes prostate cancer metastasis. *Cancer Discov* 2014; 4:1310–25.
176. Hoffmann M, Schroeder S, Kleine-Weber H, Muller MA, Drosten C, Pohlmann S. Nafamostat mesylate blocks activation of SARS-CoV-2: new treatment option for COVID-19. *Antimicrob Agents Chemother* 2020;64:e00754-20.
177. Yamamoto M, Kiso M, Sakai-Tagawa Y, Iwatsuki-Horimoto K, Imai M, Takeda M, et al. The anticoagulant nafamostat potently inhibits SARS-CoV-2 S protein-mediated fusion in a cell fusion

- assay system and viral infection *in vitro* in a cell-type-dependent manner. *Viruses* 2020;12:629.
178. Asakura H, Ogawa H. Potential of heparin and nafamostat combination therapy for COVID-19. *J Thromb Haemostasis* 2020;18:1521–2.
  179. Hammami M, Rühmann E, Maurer E, Heine A, Güttschow M, Klebe G, et al. New 3-amidinophenylalanine-derived inhibitors of matriptase. *MedChemComm* 2012;3:807–13.
  180. Bestle D, Heindl MR, Limburg H, Van Lam van T, Pilgram O, Moulton H, et al. TMPRSS2 and furin are both essential for proteolytic activation of SARS-CoV-2 in human airway cells. *Life Sci Alliance* 2020;3:e202000786.
  181. Qiu Z, Hingley ST, Simmons G, Yu C, Das Sarma J, Bates P, et al. Endosomal proteolysis by cathepsins is necessary for murine coronavirus mouse hepatitis virus type 2 spike-mediated entry. *J Virol* 2006;80:5768–76.
  182. Regan AD, Shryabman R, Cohen RD, Whittaker GR. Differential role for low pH and cathepsin-mediated cleavage of the viral spike protein during entry of serotype II feline coronaviruses. *Vet Microbiol* 2008;132:235–48.
  183. Zhao H, Zhou J, Zhang K, Chu H, Liu D, Poon VK, et al. A novel peptide with potent and broad-spectrum antiviral activities against multiple respiratory viruses. *Sci Rep* 2016;6:22008.
  184. Zhao H, To KK, Sze KH, Yung TT, Bian M, Lam H, et al. A broad-spectrum virus- and host-targeting peptide against respiratory viruses including influenza virus and SARS-CoV-2. *Nat Commun* 2020;11:4252.
  185. Zhao H, To KK, Lam H, Zhou X, Chan JF, Peng Z, et al. Cross-linking peptide and repurposed drugs inhibit both entry pathways of SARS-CoV-2. *Nat Commun* 2021;12:1517.
  186. Wang LH, Rothberg KG, Anderson RG. Mis-assembly of clathrin lattices on endosomes reveals a regulatory switch for coated pit formation. *J Cell Biol* 1993;123:1107–17.
  187. Rodon J, Munoz-Basagoiti J, Perez-Zsolt D, Noguera-Julian M, Paredes R, Mateu L, et al. Identification of plitidepsin as potent inhibitor of SARS-CoV-2-induced cytopathic effect after a drug repurposing screen. *Front Pharmacol* 2021;12:646676.
  188. Liu J, Cao R, Xu M, Wang X, Zhang H, Hu H, et al. Hydroxychloroquine, a less toxic derivative of chloroquine, is effective in inhibiting SARS-CoV-2 infection *in vitro*. *Cell Discov* 2020;6:16.
  189. Gao J, Tian Z, Yang X. Breakthrough: chloroquine phosphate has shown apparent efficacy in treatment of COVID-19 associated pneumonia in clinical studies. *Biosci Trends* 2020;14:72–3.
  190. Hoffmann M, Mosbauer K, Hofmann-Winkler H, Kaul A, Kleine-Weber H, Kruger N, et al. Chloroquine does not inhibit infection of human lung cells with SARS-CoV-2. *Nature* 2020;585:588–90.
  191. Maisonnasse P, Guedj J, Contreras V, Behillil S, Solas C, Marlin R, et al. Hydroxychloroquine use against SARS-CoV-2 infection in non-human primates. *Nature* 2020;585:584–7.
  192. Schneider M, Ackermann K, Stuart M, Wex C, Protzer U, Schatzl HM, et al. Severe acute respiratory syndrome coronavirus replication is severely impaired by MG132 due to proteasome-independent inhibition of M-calpain. *J Virol* 2012;86:10112–22.
  193. Zhou Y, Simmons G. Development of novel entry inhibitors targeting emerging viruses. *Expert Rev Anti Infect Ther* 2012;10:1129–38.
  194. Yamada H, Mori H, Nakanishi Y, Nishikawa S, Hashimoto Y, Ochi Y, et al. Effects of the cathepsin K inhibitor ONO-5334 and concomitant use of ONO-5334 with methotrexate on collagen-induced arthritis in cynomolgus monkeys. *Int J Rheumatol* 2019;2019:5710340.
  195. Elie BT, Gocheva V, Shree T, Dalrymple SA, Holsinger LJ, Joyce JA. Identification and pre-clinical testing of a reversible cathepsin protease inhibitor reveals anti-tumor efficacy in a pancreatic cancer model. *Biochimie* 2010;92:1618–24.
  196. Rutherford AC, Traer C, Wassmer T, Pattini K, Bujny MV, Carlton JG, et al. The mammalian phosphatidylinositol 3-phosphate 5-kinase (PIKfyve) regulates endosome-to-TGN retrograde transport. *J Cell Sci* 2006;119:3944–57.
  197. Kang YL, Chou YY, Rothlauf PW, Liu Z, Soh TK, Cureton D, et al. Inhibition of PIKfyve kinase prevents infection by Zaire ebolavirus and SARS-CoV-2. *Proc Natl Acad Sci U S A* 2020;117:20803–13.
  198. Bjorck L, Grubb A, Kjellen L. Cystatin C, a human proteinase inhibitor, blocks replication of herpes simplex virus. *J Virol* 1990;64:941–3.
  199. Baron SA, Devaux C, Colson P, Raoult D, Rolain JM. Teicoplanin: an alternative drug for the treatment of COVID-19? *Int J Antimicrob Agents* 2020;55:105944.
  200. Colson P, Raoult D. Fighting viruses with antibiotics: an overlooked path. *Int J Antimicrob Agents* 2016;48:349–52.
  201. Zhang J, Ma X, Yu F, Liu J, Zou F, Pan T, et al. Teicoplanin potently blocks the cell entry of 2019-nCoV. *bioRxiv* 2020. Available from: <https://www.biorxiv.org/content/10.1101/2020.02.05.935387v1>.
  202. Smieszek SP, Przychodzen BP, Polymeropoulos MH. Amantadine disrupts lysosomal gene expression: a hypothesis for COVID19 treatment. *Int J Antimicrob Agents* 2020;55:106004.
  203. Barlow A, Landolf KM, Barlow B, Yeung SYA, Heavner JJ, Claassen CW, et al. Review of emerging pharmacotherapy for the treatment of coronavirus disease 2019. *Pharmacotherapy* 2020;40:416–37.
  204. Newfield C. New medical indications for thalidomide and its derivatives. *The Science Journal of the Lander College of Arts and Sciences* 2018;12:3.
  205. Rosa SGV, Santos WC. Clinical trials on drug repositioning for COVID-19 treatment. *Rev Panam Salud Pública* 2020;44:e40.
  206. Foerch C, Friedauer L, Bauer B, Wolf T, Adam EH. Severe COVID-19 infection in a patient with multiple sclerosis treated with fingolimod. *Mult Scler Relat Disord* 2020;42:102180.
  207. Giovannoni G, Hawkes C, Lechner-Scott J, Levy M, Waubant E, Gold J. The COVID-19 pandemic and the use of MS disease-modifying therapies. *Mult Scler Relat Disord* 2020;39:102073.
  208. Hu K, Wang M, Zhao Y, Zhang Y, Wang T, Zheng Z, et al. A small-scale medication of leflunomide as a treatment of COVID-19 in an open-label blank-controlled clinical trial. *Virol Sin* 2020;35:725–33.
  209. Fragozo YD, Brooks JB. Leflunomide and teriflunomide: altering the metabolism of pyrimidines for the treatment of autoimmune diseases. *Expert Rev Clin Pharmacol* 2015;8:315–20.
  210. Xiong R, Zhang L, Li S, Sun Y, Ding M, Wang Y, et al. Novel and potent inhibitors targeting DHODH are broad-spectrum antivirals against RNA viruses including newly-emerged coronavirus SARS-CoV-2. *Protein Cell* 2020;11:723–39.
  211. Chen SF, Perrella FW, Behrens DL, Papp LM. Inhibition of dihydroorotate dehydrogenase activity by brequinar sodium. *Cancer Res* 1992;52:3521–7.
  212. Gorshkov K, Chen CZ, Bostwick R, Rasmussen L, Tran BN, Cheng YS, et al. The SARS-CoV-2 cytopathic effect is blocked by lysosome alkalinizing small molecules. *ACS Infect Dis* 2020;7:1389–408.
  213. Ryser HJ, Fluckiger R. Progress in targeting HIV-1 entry. *Drug Discov Today* 2005;10:1085–94.
  214. Cheng Y, Pham AT, Kato T, Lim B, Moreau D, López-Andarias J, et al. Inhibitors of thiol-mediated uptake. *Chem Sci* 2021;12:626–31.
  215. Halfon P, Bestion E, Zandi K, Andreani J, Baudoin JP, Scola BL, et al. GNS561 exhibits potent *in vitro* antiviral activity against SARS-CoV-2 through autophagy inhibition. *bioRxiv* 2020. Available from: <https://www.biorxiv.org/content/10.1101/2020.10.06.327635v1>.
  216. Bago R, Malik N, Munson MJ, Prescott AR, Davies P, Sommer E, et al. Characterization of VPS34-IN1, a selective inhibitor of Vps34, reveals that the phosphatidylinositol 3-phosphate-binding SGK3 protein kinase is a downstream target of class III phosphoinositide 3-kinase. *Biochem J* 2014;463:413–27.
  217. Dowdle WE, Nyfeler B, Nagel J, Elling RA, Liu S, Triantafellow E, et al. Selective VPS34 inhibitor blocks autophagy and uncovers a role for NCOA4 in ferritin degradation and iron homeostasis *in vivo*. *Nat Cell Biol* 2014;16:1069–79.

218. Silvas JA, Jureka AS, Nicolini AM, Chvatal SA, Basler CF. Inhibitors of VPS34 and lipid metabolism suppress SARS-CoV-2 replication. *bioRxiv* 2020. Available from: <https://www.biorxiv.org/content/10.1101/2020.07.18.210211v1>.
219. Ammer E, Nietzsche S, Rien C, Kuhnl A, Mader T, Heller R, et al. The anti-obesity drug orlistat reveals anti-viral activity. *Med Microbiol Immunol* 2015; **204**:635–45.
220. Nasheri N, Joyce M, Rouleau Y, Yang P, Yao S, Tyrrell DL, et al. Modulation of fatty acid synthase enzyme activity and expression during hepatitis C virus replication. *Chem Biol* 2013; **20**:570–82.
221. Cheng YW, Chao TL, Li CL, Chiu MF, Kao HC, Wang SH, et al. Furin inhibitors block SARS-CoV-2 spike protein cleavage to suppress virus production and cytopathic effects. *Cell Rep* 2020; **33**: 108254.
222. Dong HJ, Wang ZH, Meng W, Li CC, Hu YX, Zhou L, et al. The natural compound homoharringtonine presents broad antiviral activity *in vitro* and *in vivo*. *Viruses* 2018; **10**:601.
223. Lu S, Wang J. Homoharringtonine and omacetaxine for myeloid hematological malignancies. *J Hematol Oncol* 2014; **7**:2.
224. Dyall J, Coleman CM, Hart BJ, Venkataraman T, Holbrook MR, Kindrachuk J, et al. Repurposing of clinically developed drugs for treatment of Middle East respiratory syndrome coronavirus infection. *Antimicrob Agents Chemother* 2014; **58**:4885–93.
225. Andersen PI, Krpina K, Ianevski A, Shtaida N, Jo E, Yang J, et al. Novel antiviral activities of obatoclax, emetine, niclosamide, brequinol, and homoharringtonine. *Viruses* 2019; **11**:964.
226. Grollman AP. Structural basis for inhibition of protein synthesis by emetine and cycloheximide based on an analogy between ipecac alkaloids and glutarimide antibiotics. *Proc Natl Acad Sci U S A* 1966; **56**:1867–74.
227. Wong W, Bai XC, Brown A, Fernandez IS, Hanssen E, Condron M, et al. Cryo-EM structure of the plasmodium falciparum 80S ribosome bound to the anti-protozoan drug emetine. *Elife* 2014; **3**:e03080.
228. Bojkova D, Klann K, Koch B, Widera M, Krause D, Ciesek S, et al. Proteomics of SARS-CoV-2-infected host cells reveals therapy targets. *Nature* 2020; **583**:469–72.
229. Gualdoni GA, Mayer KA, Kapsch AM, Kreuzberg K, Puck A, Kienzl P, et al. Rhinovirus induces an anabolic reprogramming in host cell metabolism essential for viral replication. *Proc Natl Acad Sci U S A* 2018; **115**:E7158–65.
230. Pruijssers AJ, Denison MR. Nucleoside analogues for the treatment of coronavirus infections. *Curr Opin Virol* 2019; **35**:57–62.
231. Wu LS, Rower JE, Burton Jr JR, Anderson PL, Hammond KP, Baouchi-Mokrane F, et al. Population pharmacokinetic modeling of plasma and intracellular ribavirin concentrations in patients with chronic hepatitis C virus infection. *Antimicrob Agents Chemother* 2015; **59**:2179–88.
232. Richardson P, Griffin I, Tucker C, Smith D, Oechsle O, Phelan A, et al. Baricitinib as potential treatment for 2019-nCoV acute respiratory disease. *Lancet* 2020; **395**:e30–1.
233. Rossignol JF. Nitazoxanide: a first-in-class broad-spectrum antiviral agent. *Antivir Res* 2014; **110**:94–103.
234. Rossignol JF. Nitazoxanide, a new drug candidate for the treatment of middle east respiratory syndrome coronavirus. *J Infect Public Health* 2016; **9**:227–30.
235. Cao J, Forrest JC, Zhang X. A screen of the NIH clinical collection small molecule library identifies potential anti-coronavirus drugs. *Antivir Res* 2015; **114**:1–10.
236. Wang L, Chang J, Varghese D, Dellinger M, Kumar S, Best AM, et al. A small molecule modulates Jumonji histone demethylase activity and selectively inhibits cancer growth. *Nat Commun* 2013; **4**:2035.
237. Son J, Huang S, Zeng Q, Bricker TL, Case JB, Zhou J, et al. Nitazoxanide and JIB-04 have broad-spectrum antiviral activity and inhibit SARS-CoV-2 replication in cell culture and coronavirus pathogenesis in a pig model. *bioRxiv* 2020. Available from: <https://www.biorxiv.org/content/10.1101/2020.09.24.312165v1>.
238. Pepperrell T, Pilkington V, Owen A, Wang J, Hill AM. Review of safety and minimum pricing of nitazoxanide for potential treatment of COVID-19. *J Virus Erad* 2020; **6**:52–60.
239. White KM, Rosales R, Yildiz S, Kehrer T, Miorin L, Moreno E, et al. Plitidespin has potent preclinical efficacy against SARS-CoV-2 by targeting the host protein eEF1A. *Science* 2021; **371**: 926–31.
240. Rossaint R, Gerlach H, Schmidt-Ruhnke H, Pappert D, Lewandowski K, Steudel W, et al. Efficacy of inhaled nitric oxide in patients with severe ARDS. *Chest* 1995; **107**:1107–15.
241. Berhes M, Fabian A, Laszlo I, Vegh T, Molnar C, Fulesdi B, et al. Organ replacement therapy and life-supporting treatment modalities in critically ill COVID-19 patients. *Orv Hetil* 2020; **161**:704–9.
242. Hui DS. An overview on severe acute respiratory syndrome (SARS). *Monaldi Arch Chest Dis* 2005; **63**:149–57.
243. Richter JM, Schaefer M, Hill K. Clemizole hydrochloride is a novel and potent inhibitor of transient receptor potential channel TRPC5. *Mol Pharmacol* 2014; **86**:514–21.
244. Weston S, Coleman CM, Haupt R, Logue J, Matthews K, Li Y, et al. Broad anti-coronavirus activity of food and drug administration-approved drugs against SARS-CoV-2 *in vitro* and SARS-CoV *in vivo*. *J Virol* 2020; **94**:e01218–20.
245. Lu L, Su S, Yang H, Jiang S. Antivirals with common targets against highly pathogenic viruses. *Cell* 2021; **184**:1604–20.
246. Zhang ZR, Zhang YN, Li XD, Zhang HQ, Xiao SQ, Deng F, et al. A cell-based large-scale screening of natural compounds for inhibitors of SARS-CoV-2. *Signal Transduct Target Ther* 2020; **5**:218.
247. Kanjanasirirat P, Suksatu A, Manopwisedjaroen S, Munyoo B, Tuchinda P, Jearawuttanakul K, et al. High-content screening of Thai medicinal plants reveals Boesenbergia rotunda extract and its component panduratin A as anti-SARS-CoV-2 agents. *Sci Rep* 2020; **10**:19963.
248. Puhl AC, Fritch EJ, Lane TR, Tse LV, Yount BL, Sacramento CQ, et al. Repurposing the ebola and marburg virus inhibitors tilorone, quinacrine, and pyronaridine: *in vitro* activity against SARS-CoV-2 and potential mechanisms. *ACS Omega* 2021; **6**:7454–68.